

Pocket

The Genesis of Archean Pyroclastic Rocks of the Manigotagan  
River Formation, Southeastern Manitoba

by

David Michael Seneshen

A thesis  
presented to the University of Manitoba  
in fulfillment of the  
thesis requirement for the degree of  
Masters of Science  
in  
Geology

Winnipeg, Manitoba

(c) David Michael Seneshen, 1990



National Library  
of Canada

Bibliothèque nationale  
du Canada

Canadian Theses Service    Service des thèses canadiennes

Ottawa, Canada  
K1A 0N4

The author has granted an irrevocable non-exclusive licence allowing the National Library of Canada to reproduce, loan, distribute or sell copies of his/her thesis by any means and in any form or format, making this thesis available to interested persons.

The author retains ownership of the copyright in his/her thesis. Neither the thesis nor substantial extracts from it may be printed or otherwise reproduced without his/her permission.

L'auteur a accordé une licence irrévocable et non exclusive permettant à la Bibliothèque nationale du Canada de reproduire, prêter, distribuer ou vendre des copies de sa thèse de quelque manière et sous quelque forme que ce soit pour mettre des exemplaires de cette thèse à la disposition des personnes intéressées.

L'auteur conserve la propriété du droit d'auteur qui protège sa thèse. Ni la thèse ni des extraits substantiels de celle-ci ne doivent être imprimés ou autrement reproduits sans son autorisation.

ISBN 0-315-63264-X

THE GENESIS OF ARCHEAN PYROCLASTIC ROCKS OF THE  
MANIGOTAGAN RIVER FORMATION, SOUTHEASTERN MANITOBA

BY

DAVID MICHAEL SENESHEN

A thesis submitted to the Faculty of Graduate Studies of  
the University of Manitoba in partial fulfillment of the requirements  
of the degree of

MASTER OF SCIENCE

© 1990

Permission has been granted to the LIBRARY OF THE UNIVER-  
SITY OF MANITOBA to lend or sell copies of this thesis. to  
the NATIONAL LIBRARY OF CANADA to microfilm this  
thesis and to lend or sell copies of the film, and UNIVERSITY  
MICROFILMS to publish an abstract of this thesis.

The author reserves other publication rights, and neither the  
thesis nor extensive extracts from it may be printed or other-  
wise reproduced without the author's written permission.

I hereby declare that I am the sole author of this thesis.

I authorize the University of Manitoba to lend this thesis to other institutions or individuals for the purpose of scholarly research.

David Michael Seneshen

I further authorize the University of Manitoba to reproduce this thesis by photocopying or by other means, in total or in part, at the request of other institutions or individuals for the purpose of scholarly research.

David Michael Seneshen

The University of Manitoba requires the signatures of all persons using or photocopying this thesis. Please sign below, and give address and date.

## ABSTRACT

The 50 to 500+ m thick, Manigotagan River Formation is a subvertically dipping, overturned, homoclinal sequence that is a transition zone between the underlying volcanic Narrows Formation and overlying sedimentary Edmunds Lake Formation. The formation consists of seven members that, in ascending order, are: felsic ignimbrites, mafic to intermediate tephra-fall deposits, felsic to intermediate mass-flow deposits and minor mafic lava flows, intermediate peperite, mafic lava flows, felsic turbidites, and felsic ignimbrites. This study focuses on the genesis of the ignimbrites and tephra-fall deposits within a 1.2 km long segment of the formation.

The ignimbrites range in thickness from 6 to 50 m and extend beyond the study area. They are composed of variable proportions of recognizable juvenile and cognate particles in a fine-grained granoblastic aggregate inferred to be recrystallized vitric ash. The ignimbrites are composite sheets composed of 5 to at least 12 flow units, most of which comprise a lower, non-stratified, graded or ungraded lapilli-tuff division and upper bedded or massive, normally graded or apparently ungraded, upper tuff division; less commonly they consist of only a lapilli-tuff division. The

ignimbrites were apparently emplaced subaqueously following subaerial eruptions. The lapilli-tuff divisions were emplaced by high density turbidity flows possibly transformed from pyroclastic flows that entered the sea. Fine ash was probably produced by a combination of processes including (1) separation of fines above a collapsing eruption column, (2) elutriation of fines from fluidized pyroclastic flows, (3) littoral explosions, and (4) wave winnowing of the proximal parts of the lapilli-tuff division. Low density turbidity flows, triggered by earthquakes and/or wave activity, transported and deposited the fine ash over the preceding lapilli-tuff divisions to form the upper tuff divisions. A unique feature of the ignimbrites is the coexistence of plagioclase-phyric pumice and pyrogenic quartz crystals in flow units. The source of the pumice remains speculative, but it may have been eroded from an earlier plinian air-fall deposit by pyroclastic flows.

Tephra-fall deposits range in thickness from 17 to 91 m and also extend beyond the study area. The tephra-fall member consists of three, compositionally distinct, laterally continuous, blanket-like units that, in ascending order, are: (1) lower mafic to intermediate lapilli-tuff and tuff, (2) mafic lapilli-tuff and tuff, and (3) upper mafic to intermediate lapilli-tuff and tuff. The units are composed of lapilli- to block-sized, vesicular to non-

vesicular, felsic and mafic fragments, rare crystal particles, and 35 to 97% fine-grained matrix. The units consist of relatively thin, alternating, ungraded, poorly sorted, matrix-supported, fragment-rich and fragment-poor beds with gradational bed contacts. In the central mafic lapilli-tuff and tuff unit, fragments show variable degrees of post-depositional, heat-induced alteration indicating that the fragments were still hot when they were incorporated in the deposit. The lapilli-tuff and tuff comprising Member 2 were apparently emplaced subaqueously as tephra-fall following shallow water, or possibly, subaerial, flank fissure-type, phreatomagmatic eruptions.



## ACKNOWLEDGEMENTS

Funding for this study was provided by the Geological Services Branch, Manitoba Department of Energy and Mines, as part of a regional mapping project in the southeastern part of the Rice Lake Greenstone Belt and by an NSERC grant awarded to Dr. L.D. Ayres. I would like to thank Dr. W. Weber of the Geological Services Branch for initiating this project and for providing stimulating discussions about the geology of the Rice Lake Greenstone Belt.

I thank Dr. L.D. Ayres for supervising this study and for providing constructive comments on previous drafts of this thesis. His undying quest for a better understanding of geological processes has instilled in me the importance of careful observation and proper data documentation.

I thank Dave Owens for assisting in mapping of the Stormy Lake Area and for providing stimulating geological discussions. Rob Gaba, Peter Stewart, and Dr. P. Theyer of the Geological Services Branch also provided valuable insight into the geological complexities of the Stormy Lake Area. I also extend thanks to Ken Korman, Jordan Weiss, Jackie Ruitter, and Susan Lambert for providing excellent assistance in the field and to Dr. A.C. Turnock for the use of his rock saw.

## TABLE OF CONTENTS

<b>ABSTRACT</b>		<b>iv</b>
<b>ACKNOWLEDGEMENTS</b>		<b>vii</b>
<u>Chapter</u>		<u>page</u>
<b>I.</b>	<b>INTRODUCTION</b>	<b>1</b>
	Archean and Cenozoic Volcanoes	4
	Problems in Archean Stratigraphic Analysis	5
	Volcanic Facies and Provenance	6
	Present Study	8
	Previous Work	9
	Methods of Study	11
	Terminology and Classification Schemes	12
<b>II.</b>	<b>GEOLOGICAL SETTING OF THE STUDY AREA</b>	<b>17</b>
	Stratigraphy of the Stormy Lake Area	18
	Structural Geology	22
	Metamorphism	22
<b>III.</b>	<b>STRATIGRAPHIC FRAMEWORK OF THE MANIGOTAGAN RIVER FORMATION</b>	<b>24</b>
<b>IV.</b>	<b>RECOGNITION OF JUVENILE COMPONENTS IN PRECAMBRIAN PYROCLASTIC ROCKS</b>	<b>29</b>
<b>V.</b>	<b>SUBAQUEOUS PYROCLASTIC FLOW DEPOSITS</b>	<b>32</b>
	Components of Ignimbrites in the Manigotagan River Formation	34
	Dacite Fragments	34
	Pumice	37
	Vitric Felsic Fragments	41
	Minor Fragment Types	44
	Crystal Particles	47
	Vitric Ash	52
	Description of Upper Ignimbrite (Member 7)	56
	Lower Lapilli-tuff Division	59
	Upper Tuff Division	62
	Description of the Lower Ignimbrite (Member 1)	68
	Lower Lapilli-tuff Division	69
	Upper Tuff Division	72

<b>VI.</b>	<b>SUBAQUEOUS TEPHRA-FALL DEPOSITS . . . . .</b>	<b>75</b>
	Mafic to Intermediate Lapilli-Tuff and Tuff . . . . .	76
	Components Comprising the Lapilli-Tuff and Tuff . . . . .	76
	Bedding Characteristics . . . . .	83
	Minor Volcanic Conglomerate and Sandstone . . . . .	84
	Mafic Lapilli-Tuff and Tuff . . . . .	90
	Components Comprising the Lapilli-Tuff and Tuff . . . . .	91
	Rimmed, Vesicular, Microlitic Mafic Fragments (Type 1) . . . . .	92
	Partly-Rimmed, Vesicular, Microlitic Mafic Fragments (Type 2) . . . . .	99
	Non-Vesicular, Microlitic Mafic Fragments (Type 3) . . . . .	103
	Crystal Particles . . . . .	103
	Granoblastic Matrix . . . . .	104
	Bedding Characteristics . . . . .	106
	Mafic to Intermediate Lapilli-Tuff and Tuff . . . . .	111
	Components Comprising the Lapilli-Tuff and Tuff . . . . .	113
	Bedding Characteristics . . . . .	115
<b>VII.</b>	<b>DISCUSSION . . . . .</b>	<b>118</b>
	Introduction . . . . .	118
	Subaqueous Pyroclastic Flow Deposits . . . . .	119
	Comparison With Ignimbrites In The Literature . . . . .	119
	Environment of Eruption and Deposition . . . . .	120
	Emplacement of the Ignimbrites . . . . .	123
	Emplacement of the Lapilli-Tuff Division . . . . .	125
	Emplacement of the Upper Tuff Division . . . . .	129
	Significance of Lateral Variations . . . . .	134
	Source of Components Comprising the Ignimbrites . . . . .	135
	Composite Model for the Emplacement of the Ignimbrites . . . . .	142
	Subaqueous Tephra-Fall Deposits . . . . .	149
	Environment of Eruption and Deposition . . . . .	149
	Evidence of Hot Particles . . . . .	150
	Emplacement of Lapilli-Tuff and Tuff of Member 2 . . . . .	152
	Subaqueous Mass Flow Deposits . . . . .	153
	Subaqueous Tephra-Fall Deposits . . . . .	154
	Emplacement of Volcanic Conglomerate and Sandstone . . . . .	155
	Eruption Type . . . . .	157

VIII. CONCLUSIONS . . . . .	160
BIBLIOGRAPHY . . . . .	164

## LIST OF FIGURES

<u>Figure</u>	<u>page</u>
1. Distribution of greenstone belts in the Superior Province of the Canadian Shield . . . . .	2
2. Lithological map showing location of the Stormy Lake Map Area and the Study Area . . . . .	10
3. Distribution of major lithologies in the Stormy Lake Area with major fold axes and location of Study Area . . . . .	19
4. Photomicrographs (plane light and x-polars) showing an elongate, plagioclase-phyric dacite fragment . . . . .	36
5. Vertical separation of pumice and vitric felsic fragments in flow unit 3b of upper ignimbrite member . . . . .	38
6. Photomicrograph of a partly collapsed pumice fragment in which original vesicularity is still preserved . . . . .	40
7. Photograph of lapilli-tuff from the upper ignimbrite (Member 7) . . . . .	42
8. Photomicrograph of a subrounded, plagioclase-phyric, vitric felsic fragment . . . . .	43
9. Thin section drawing of fragments in lapilli-tuff from the upper ignimbrite (Member 7) . . . . .	45
10. Photomicrograph of a subangular, mafic scoria fragment in which original vesicularity is preserved . . . . .	46
11. Photomicrograph of a subhedral, apparently, unbroken plagioclase crystal from the upper ignimbrite . . . . .	48
12. Photomicrograph of an apparently broken, anhedral microcline crystal from the upper ignimbrite . . . . .	50

13.	Photomicrograph of a subrounded vitric felsic fragment from the upper ignimbrite . . . . .	53
14.	Photomicrograph showing lenticular vitric felsic fragments and crystals from the lower ignimbrite . . . . .	55
15.	Stratigraphic sections (7-1, 7-2) through the upper ignimbrite . . . . .	57
16.	Photograph of a pumice-rich bed in flow unit 4a of the upper ignimbrite . . . . .	66
17.	Photograph showing faintly bedded pumiceous tuff in flow unit 3a of the upper ignimbrite . . . . .	67
18.	Partial stratigraphic sections (1-1, 1-2) through the lower ignimbrite . . . . .	70
19.	Photograph depicting a scoured contact at the base of flow unit 2a in the lower ignimbrite . . . . .	71
20.	Photograph of normally graded beds in the upper tuff division of flow unit 1a of the lower ignimbrite . . . . .	74
21.	Stratigraphic section 2a-1 through lower, mafic to intermediate lapilli-tuff and tuff unit (2a) . . . . .	77
22.	Photograph of a subangular, vesicular, felsic volcanic fragment in lower unit (2a) of Member 2 . . . . .	82
23.	Photomicrograph of a partly hexagonal, embayed quartz crystal in volcanic sandstone of Unit 2a . . . . .	86
24.	Photograph showing a scoured contact at the base of the upper felsic sequence in unit 2a . . . . .	88
25.	Photograph showing an irregular contact at the base of the lower mafic sequence in unit 2a . . . . .	89
26.	Thin section drawing of a type 1 mafic fragment from mafic lapilli-tuff of unit 2b . . . . .	93
27.	Photomicrograph of the core of a type 1 mafic fragment from mafic lapilli-tuff of unit 2b . . . . .	94
28.	Photomicrograph of a polycrystalline albite amygdule in a type 1 fragment from unit 2b . . . . .	95

29.	Photomicrograph of a polycrystalline quartz/albite amygdule in a type 1 fragment from unit 2b . . . . .	96
30.	Photomicrograph of a type 1 mafic fragment from mafic lapilli-tuff of unit 2b . . . . .	98
31.	Distribution of polycrystalline plagioclase amygdules in the matrix of mafic lapilli-tuff (unit 2b) . . . . .	102
32.	Photomicrograph of an actinolite pseudomorph after an original clinopyroxene crystal (unit 2b) . . . . .	105
33.	Stratigraphic section 2b-1 through mafic lapilli-tuff and tuff of unit 2b . . . . .	107
34.	Photograph of bedding in mafic lapilli-tuff and tuff of unit 2b . . . . .	110
35.	Photograph of isolated, volcanic bomb in mafic lapilli-tuff of unit 2b . . . . .	112
36.	Stratigraphic section 2c-1 through mafic to intermediate lapilli-tuff of Unit 2c . . . . .	116
37.	Composite model for the generation and emplacement of the Manigotagan River Formation ignimbrites . . . . .	144
37.	Composite model for the generation and emplacement of the Manigotagan River Formation ignimbrites . . . . .	147
<b>Plate 1.</b>	<b>Geological map (1:1000) of the Manigotagan River Formation . . . . .</b>	<b>Back pocket</b>

## LIST OF TABLES

<u>Table</u>	<u>page</u>
1. Grain size limits for pyroclastic components . . . .	13
2. Non-genetic classification of volcanoclastic rocks . . . . .	15
3. Summary of formations in the Stormy Lake Area . . .	20
4. Summary of members in the Manigotagan River Formation . . . . .	25
5. Megascopic features of the upper and lower ignimbrites (Members 7 and 1) . . . . .	33
6. Compositional and textural features of fragments in ignimbrites of Members 1 and 7 . . . . .	35
7. Internal characteristics of the lower lapilli- tuff division . . . . .	60
8. Internal characteristics of the upper tuff division . . . . .	63
9. Compositional and textural features of fragments from lapilli-tuff and tuff of Member 2 . . . . .	78
10. Internal characteristics of tephra-fall and channel-fill deposits of Member 2 . . . . .	80



## Chapter I

### INTRODUCTION

Archean greenstone belts are a major component of the Canadian shield (Fig. 1). They occur as linear or arcuate belts of deformed and metamorphosed, volcanic and sedimentary rocks that are commonly disrupted by felsic to mafic plutons and are typically enclosed by granitoid rocks. The volcanic and sedimentary rocks are thought to represent the products of Archean shield and stratovolcanoes which were subsequently deformed and metamorphosed (Ayles and Thurston, 1985; Glikson, 1976).

In many Archean greenstone belts, thick, tholeiitic basalt and komatiitic lava flow sequences are succeeded upwards by thick, calc-alkaline, andesitic to rhyolitic, lava flow and pyroclastic sequences. The lower mafic sequences are thought to represent subaqueous shield volcanoes that built upwards into felsic to intermediate stratovolcanoes, now represented by the calc-alkaline sequences, with eventual emergence to form islands (Ayles and Thurston, 1985). These island volcanoes, with unvegetated slopes, would have been highly unstable and would have been rapidly eroded producing flanking, subaqueous, volcanoclastic aprons comprised largely of

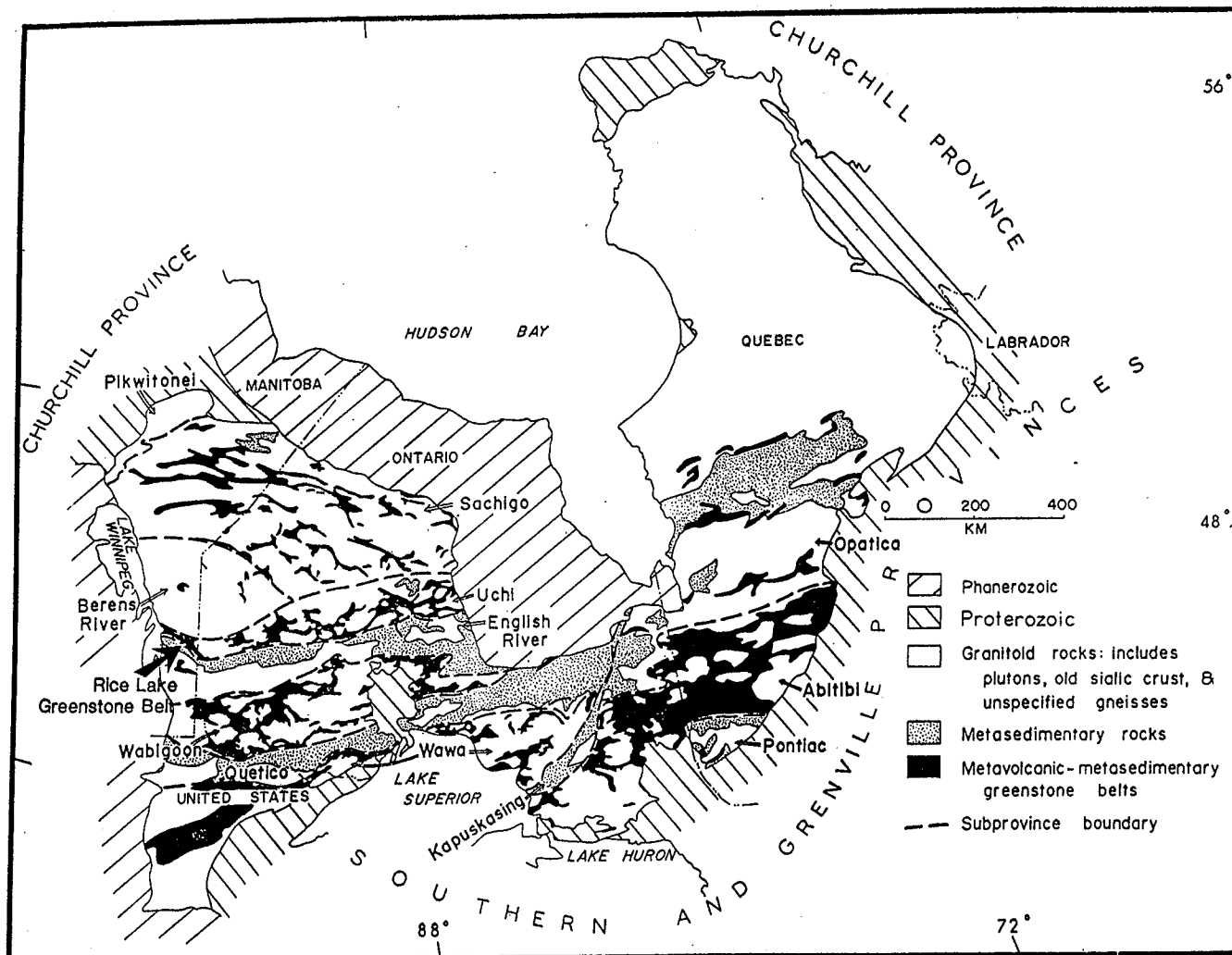


Figure 1: Distribution of greenstone belts in the Superior Province of the Canadian Shield with location of the Rice Lake Greenstone Belt (modified after Ayres and Thurston, 1985).

pyroclastic debris (Ojakangas, 1985; Ayres, 1982; Sigurdsson, 1982; Car, 1980). Lava flows and primary pyroclastic rocks interlayered with such volcanoclastic aprons record the late stages of volcanism from emergent stratovolcanoes. Volcanic and sedimentary rocks comprising the Manigotagan River Formation, in the southeast part of the Archean (Turek et al., 1985) Rice Lake greenstone belt, are representative of such late stage volcanism and sedimentation and are a narrow transition zone between an underlying, dominantly volcanic environment and an overlying, dominantly sedimentary environment.

This study focuses on a 1.2-km long segment of the 50- to 450-m thick Manigotagan River Formation which represents a subvertical section through the subaqueous flank of an Archean stratovolcano. The study was undertaken with the following three objectives in mind:

1. interpretation of volcanic eruption types and depositional processes,
2. interpretation of environments of volcanism and deposition, and
3. reconstruction of part of an Archean stratovolcano.

## 1.1 ARCHEAN AND CENOZOIC VOLCANOES

Recent work on volcanoclastic sequences in modern island arc settings (Vessel and Davies, 1981; Sigurdsson et al., 1980; Carey and Sigurdsson, 1980; Sparks et al., 1980; Kuenzi et al., 1979; Brazier et al., 1982; Sparks et al., 1983) has provided new insight into the composition and structure of volcanoclastic aprons. This data is useful in interpreting the depositional history of volcanoclastic sequences in Archean greenstone belts.

Although major differences between Archean and Cenozoic volcanoes have been documented (Ayres and Thurston, 1985; Goodwin and Smith, 1980), the volcanoes of both ages produced the same succession of mafic to felsic volcanic sequences. Archean and Cenozoic volcanic processes may have been quite similar, although the relative proportions of eruption types were probably different, as exemplified by volumetric and compositional differences between Archean and Cenozoic volcanic successions (Ayres, 1982). Erosion rates must have been higher in the Archean because of the absence of terrestrial vegetation, but, in general, erosional and depositional processes on Archean and Cenozoic island volcanoes were probably similar because of the observed similarity of sedimentary structures and inferred depositional environments in Archean and Cenozoic volcanoclastic sequences.

Consequently, the study of Archean and Cenozoic volcanoclastic sequences should complement each other. In Archean greenstone belts, the flanking volcanoclastic aprons of stratovolcanoes are more deeply dissected than those in Cenozoic volcanoes. The present outcrop surface in many Archean greenstone belts is a subvertical, two-dimensional section representing an upright or overturned limb of a syncline or anticline. In addition to outcrop sections, drill core may be available to correlate units in the subsurface.

#### 1.1.1 Problems in Archean Stratigraphic Analysis

Although subvertical sections are exposed in many Archean greenstone belts, stratigraphic analysis is hampered by metamorphism, tectonism, and, in parts of some belts, where only single fold limbs are exposed, the absence of an exposed third dimension. Metamorphism changes the original mineralogy and texture of volcanic and sedimentary rocks. In such rocks, the modification of primary fragment shapes and delicate internal textures hinders interpretations of provenance and volcanic eruption types.

Tectonism hampers stratigraphic analysis in two ways. Firstly, compression and tension differentially thicken or thin lithologies of contrasting competency, thereby modifying original thickness and shape (Car, 1980) which are critical parameters for genetic interpretations.

Furthermore, according to Ojakangas (1985), primary structures, which are prerequisites for interpretation of depositional processes, may be obscured by secondary cleavage development. Secondly, post-depositional faults cause omission, repetition or offset of units in a stratigraphic sequence. Thus, vertical and lateral facies analysis, which is critical in reconstruction of an ancient volcano, is difficult.

To facilitate reconstruction of the volcano, transport directions must be determined, but these are difficult to assess because of the two-dimensional nature of the subvertical section exposed by the erosional surface. The present erosional surface is some random section through the interior of a volcano or adjacent sedimentary basin. As noted by Car (1980), true transport directions are given only by relatively rare sections through the apex of the volcano. Most random sections will be through the flank of the volcano at various distances from the apex, and examination of such sections will give only apparent paleo-transport directions.

### 1.1.2 Volcanic Facies and Provenance

In analysis of Archean volcanoclastic sequences, the following points must be addressed:

1. the proximity of the sequence to a volcanic vent,

2. the number of volcanoes that contributed material to the sequence, and
3. the nature of the provenance of the sedimentary rocks.

Proximity to source is reflected by the facies classification used herein (Fisher and Schmincke, 1984, p. 356-359). Three facies can be defined:

1. near-source facies consisting of lava flows and pyroclastic material derived from direct volcanism or secondary erosional processes acting on the steep flanks of the volcano,
2. an intermediate-source facies characterized by lava flows, pyroclastic flow and fall deposits and reworked pyroclastic deposits, and
3. a distal-source facies consisting mostly of volcanic epiclastic rocks and local air-fall ash layers.

The number of volcanoes that contributed material to a sequence can only be deduced by extensive vertical and lateral facies analysis. Such an analysis is beyond the scope of this thesis which deals only with a limited portion of a volcanoclastic sequence.

The provenance can be resolved through detailed field, petrographic, and chemical analyses. Archean sedimentary rocks elsewhere were derived from a variety of sources including: ultramafic volcanic (Lajoie and Ludden, 1984),

mafic volcanic (Dunlop and Buick, 1981; Padgham, 1980), felsic volcanic (Ayres, 1983; Wood, 1980; Barley et al., 1979); granitoid (Lajoie and Ludden, 1984; Eriksson, 1978; Henderson, 1972), and sedimentary (Meyn and Palonen, 1980; Donaldson and Jackson, 1965). Through resolution of the provenance of the sedimentary rocks, speculations can be made about the paleo-environment.

## 1.2 PRESENT STUDY

This study was initiated and sponsored by the Geological Services Branch of the Manitoba Department of Energy and Mines. The Manigotagan River Formation was chosen for detailed study because:

1. it is largely a fragmental sequence and is thus more informative for reconstruction of ancient processes than some of the other formations,
2. it shows rapid internal variability in composition and texture,
3. it is a laterally extensive, stratigraphic sequence with well preserved primary textures and structures, and
4. outcrop exposures are excellent as a result of a recent forest fire.

The study area comprises 0.5 km<sup>2</sup> and is in the southeast part of the Rice Lake greenstone belt, in the Superior



Province of the Canadian Shield, about 160 km northeast of Winnipeg (Figs. 1, 2). The study area straddles provincial Highway 304 and outcrops are readily accessible. In this area, both the sedimentologic and volcanologic aspects of the Manigotagan River Formation were studied in detail, but only the volcanologic aspects are incorporated in this thesis.

### 1.2.1 Previous Work

The earliest reconnaissance work in the southeast part of the Rice Lake greenstone belt (Long Lake-Gem Lake areas) was done by Moore (1914), DeLury (1921, 1937), Cooke (1922), and Wright (1923, 1925, 1927, 1932). This was followed by detailed mapping (1:12000) in the Halfway Lake-Beresford Lake area by Stockwell and Lord (1939) and further regional mapping (1:63360) of Beresford Lake and Gem Lake by Stockwell (1945a, 1945b). Subsequently, Russel (1952) published a detailed geological map and report of the Lily Lake-Kickley Lake area, and Weber (1971) remapped the Long Lake-Gem Lake area at 1:63360, publishing a descriptive and interpretive report in Project Pioneer (McRitchie and Weber, 1971). Other pertinent reports published in Project Pioneer include: volcanological (Church and Wilson, 1971), sedimentological (Campbell, 1971), and structural (Zwanzig, 1971) studies in the southeast part of the Rice Lake greenstone belt. The Stormy Lake area was recently remapped

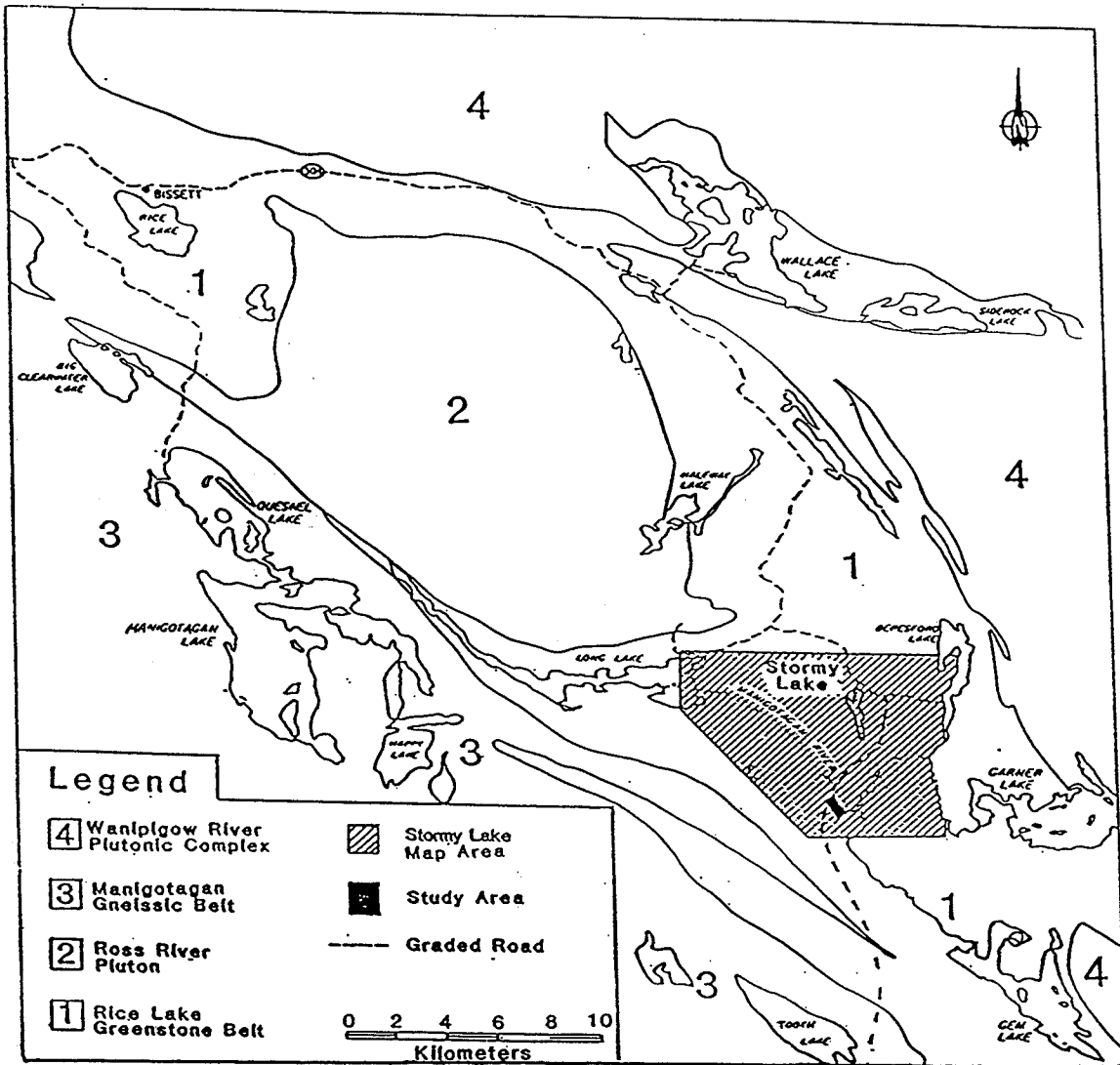


Figure 2: Lithological map showing location of the Stormy Lake Map Area and the Study Area (modified after Seneshen and Owens, 1985).

at 1:10000 (Fig. 2) to better resolve stratigraphic and structural complexities and to evaluate the economic potential for gold mineralization (Seneshen and Owens, 1985).

### 1.2.2 Methods of Study

The better exposed parts of the Manigotagan River Formation were mapped at 1:10000 during June and July of 1986. An additional two weeks were spent in the field during the latter part of June, 1987.

Although exposure in the map-area is good as a consequence of the recent forest fire, many outcrops were covered by a thin veneer of soil and ash. This veneer was removed by sweeping, and subsequent washing by rainfall left clean exposures. In addition to mapping, 21 detailed stratigraphic sections were measured on well exposed outcrops. Data that were collected from outcrops included structural measurements (bedding, foliation, etc.), contact relationships, top directions, bed thicknesses, grading characteristics, qualitative and quantitative clast abundances and sizes, clast shapes, channel dimensions, lava flow thicknesses, vesicularity, pillow sizes, pillow shapes, and other data that would facilitate interpretation.

A total of 367 rock samples were obtained from the study area, 42 of which were cut out of the outcrop with a rock

saw. All samples were slabbed and 330 thin sections were prepared. A total of 23 rock slabs were etched in hydrofluoric acid to enhance primary textures. Modal analyses were done on 21 thin sections of volcanic sandstone; approximately 1100 points were counted in each thin section. Four samples of felsic tuff were analysed by X-ray diffraction to confirm the presence or absence of microcline. Although data were collected from all 7 members of the Manigotagan River Formation, only data collected from pyroclastic Members (1, 2, and 7) will be incorporated in this thesis which is focused on the documentation and genesis of primary pyroclastic rocks.

### 1.2.3 Terminology and Classification Schemes

The Manigotagan River Formation consists of varying proportions of primary and reworked pyroclastic rocks and lava flows. All lithologies comprising the formation have been metamorphosed, but the prefix "meta" will be omitted from rock names.

Primary pyroclastic rocks are those that were transported and emplaced directly by pyroclastic flow, surge, or fall processes without reworking after deposition. The components of primary pyroclastic rocks in the Manigotagan River Formation have been named according to Fisher and Schmincke (1984) and include juvenile, cognate, and accidental components. The size classification of pyroclastic

Table 1 Grain size limits for pyroclastic components (after Fisher, 1961).

Grain Size (mm)		Pyroclastic Fragments
256	Coarse Fine	Blocks and Bombs
64		
		Lapilli
2		
1/16	Coarse	Ash
1/256	Fine	

components (Table 1) is that of Fisher (1961). Pyroclastic rocks have been named in two ways: (1) according to proportion and size of components Fisher (1966, as modified by Fisher and Schmincke, 1984), and (2) according to genesis (Wright et al., 1980). In this thesis, the term ignimbrite refers to all pyroclastic flow deposits as defined by Wright et al. (1980).

Reworked pyroclastic rocks are those that have been transported, largely by sediment gravity flows, but have retained diagnostic features indicative of an original pyroclastic origin. Reworked pyroclastic rocks of the Manigotagan River Formation are here named volcanic conglomerate, volcanic sandstone, volcanic siltstone, and volcanic mudstone (Table 2) according to Fisher (1961, as modified by Cas and Wright, 1987). Reworked pyroclastic rocks comprise a major part of the Manigotagan River Formation, but only those that comprise a minor part of Member 2 will be included in this thesis.

Lava flows, which include both pillowed and massive types, are a relatively minor component of the Manigotagan River Formation. Some massive and pillowed flows were partly brecciated by autoclastic processes (Parsons, 1969) involving friction and thermal quench mechanisms. This thesis focuses mainly on pyroclastic flow and fall deposits, and, thus, the lava flows will not be incorporated.

**Table 2 Non-genetic classification of volcanoclastic rocks  
 {modified from Fisher (1961) by Cas and Wright (1987)}.**

---

Volcanic breccia	
closed framework	
open framework	
non-cohesive, granular matrix	
cohesive mud-sized matrix	
Volcanic Conglomerate	
closed framework	
open framework	
non-cohesive, granular matrix	
cohesive mud-sized matrix	
2 mm _____	2 mm
Volcanic Sandstone	
0.0625 mm _____	0.0625 mm
Volcanic Mudstone	
volcanic siltstone	
volcanic claystone	if sufficiently well sorted and volcanic origin is clear

---

Because this study focuses on physical volcanology, units comprising the Manigotagan River Formation were not chemically analysed. The derivation of primary magma compositions would be hampered by the high carbonate contents of many units, but Weber (1971) has presented chemical analyses of felsic to intermediate volcanic rocks from nearby areas. Chemically defined dacite and rhyolite fragments in these areas are texturally and mineralogically similar to some fragments identified in the Manigotagan River Formation, and, thus, the same compositional terms will be used. For lithologies that do not have chemically defined, nearby equivalents, the terms felsic, intermediate, and mafic will be used as compositional modifiers. Here, the terms felsic, intermediate, and mafic are implied to be the compositional equivalents of rhyolite to dacite, andesite, and basalt respectively.



## Chapter II

### GEOLOGICAL SETTING OF THE STUDY AREA

The southeasterly-trending Rice Lake greenstone belt is composed of metamorphosed volcanic and sedimentary rocks that have been deformed into steeply plunging, overturned, synclines and anticlines (Weber, 1971). The belt is about 85 km long with a maximum width of about 15 km; metamorphic grade ranges from middle greenschist to amphibolite facies. Volcanic rocks, which comprise a major part of the belt, range from felsic to mafic in composition. The belt has been disrupted regionally and locally by mafic to felsic intrusions and is bordered on the northeast by the Wanipigow River Plutonic Complex and on the southwest by the Manigotagan Gneissic Belt (Fig. 2). Volcanic and plutonic rocks from the belt yield U-Pb zircon ages of about 2730 Ma (Turek et al., 1985).

Most of the volcanic and sedimentary rocks of the Rice Lake greenstone belt were placed in the Rice Lake Group by Weber (1971). The Rice Lake Group, in ascending order, consists of: (1) the Bidou Lake Subgroup, (2) the Gem Lake Subgroup, and (3) the Edmunds Lake Formation. With the exception of an unnamed basalt and the Stovel Lake Formation, all other formations of the Bidou Lake Subgroup

are exposed in the Stormy Lake area, in the southeast part of the belt (Fig. 3). Other formations exposed in the Stormy Lake Area include the Rathall Lake Formation (here named the Manigotagan River Formation) of the Gem Lake Subgroup and the Edmunds Lake Formation. The reasons for renaming the Rathall Lake Formation will be presented in a subsequent section.

## 2.1 STRATIGRAPHY OF THE STORMY LAKE AREA

In the Stormy Lake area, seven formations have been mapped (Fig. 3), each of which records a separate event of volcanism and/or sedimentation (Table 3). Within this area, there is an upward transition from mainly mafic volcanic rocks in the northeast, through felsic volcanic rocks in the central area, to dominantly volcanic epiclastic rocks in the southwest and southeast. This transition probably represents the upward construction of a subaqueous mafic shield volcano into an emergent stratovolcano with subsequent erosional destruction forming a volcanoclastic apron around the volcano.

The vent region cannot be defined precisely at present, but may be in the Gem Lake area, 10 km southeast of Stormy Lake. Here, Weber (1971) mapped a 1.4 km long by 1 km wide, subcircular structure consisting largely of flow-layered rhyolite flows and coarse rhyolite breccia. Although the shape of this structure is peculiar in the present

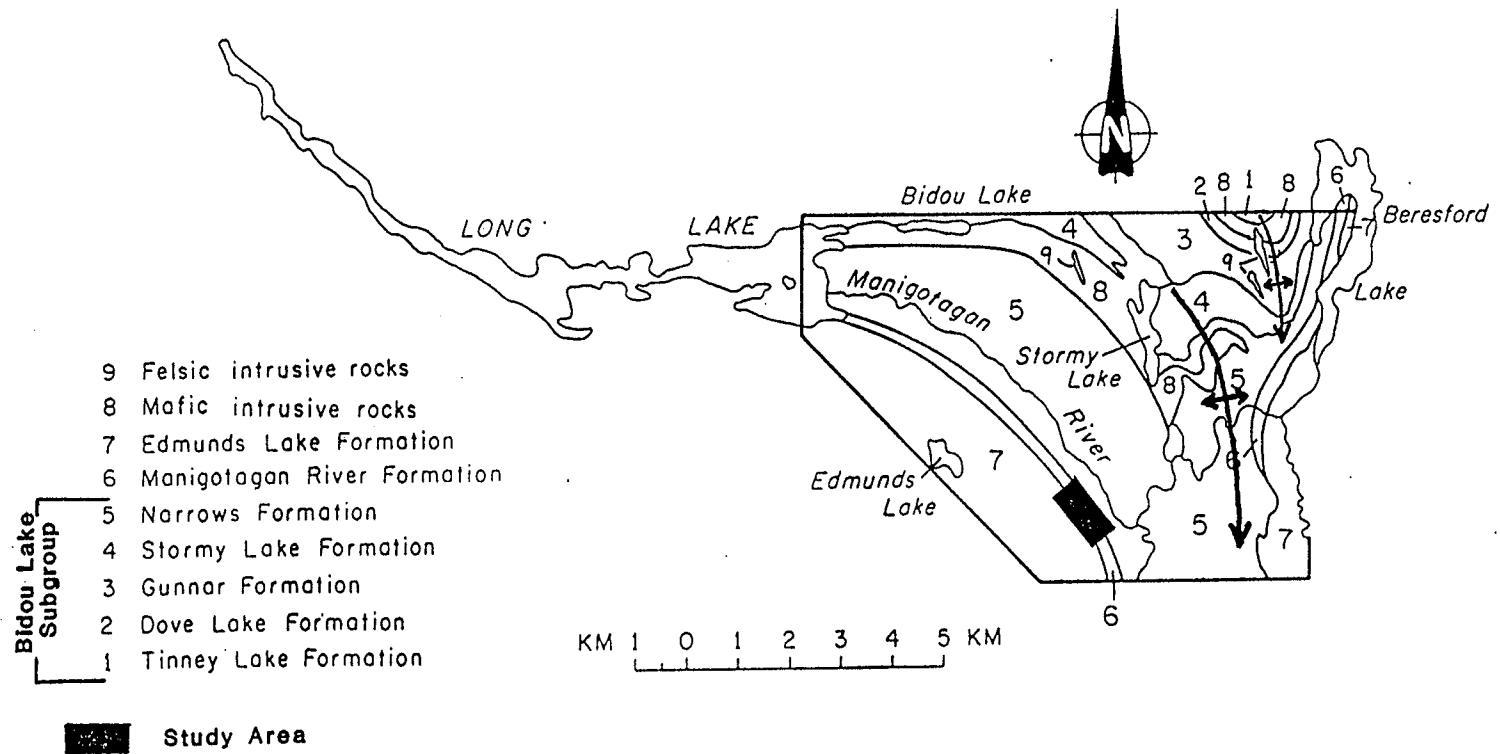


Figure 3: Distribution of major lithologies in the Stormy Lake Area with major fold axes and location of Study Area (after Seneshen and Owens, 1985).

Table 3 Summary of formations in the Stormy Lake Area.

Formation	Formation Thickness (m)	Contacts		Lithology
		Upper	Lower	
Edmunds Lake Formation	600-1400	unknown	unknown	Laterally continuous volcanic sandstone, siltstone, and mudstone beds; minor volcanic conglomerate and oxide-facies iron formation lenses
Manigotagan River Formation	50-500	unknown	gradational or sharp where truncated by gabbro	Mainly felsic to intermediate reworked pyroclastic rocks with subordinate mafic to felsic primary pyroclastic rocks and minor mafic lava flows
Narrows Formation	150-2800	gradational or sharp where truncated by gabbro	gradational	Interbedded felsic to intermediate tuff-breccia, lapilli-tuff, and crystal tuff
Stormy Lake Formation	100-500	gradational	sharp	Interbedded volcanic conglomerate and sandstone with subordinate mafic lava flows and oxide-facies iron formation
Gunnar Formation	200-1600	sharp	sharp	Poorly amygdaloidal, interlayered massive and pillowed to locally brecciated mafic lava flows with local interlayered cherty siltstone
Dove Lake Formation	40-260	sharp	sharp, truncated by gabbro	Interbedded volcanic sandstone and siltstone with subordinate mafic to intermediate tuff-breccia
Tinney Lake Formation	430 *	sharp, truncated by gabbro	unknown	Poorly amygdaloidal, massive and pillowed to locally brecciated mafic lava flows

\* this is a minimum thickness

subvertical plane of exposure, the rhyolite flows and coarse breccias may be a vent complex, and possibly the source of the Narrows Formation and felsic volcanic units in the overlying Manigotagan River Formation.

The Manigotagan River Formation, the focus of this study, is a transition zone between the volcanic Narrows Formation and the overlying sedimentary Edmunds Lake Formation. It was previously named the Rathall Lake Formation (Campbell, 1971; Weber, 1971), but, in the Stormy Lake Area, it was redesignated as the Manigotagan River Formation by Seneshen and Owens (1985) to emphasize the presence of previously unrecognized volcanic units. In this formation, volcanic boulder conglomerate and greywacke were noted by Weber (1971) and Campbell (1971), but other lithologies such as pyroclastic flow deposits and lava flows were not recognized due to poor exposure.

A variety of mafic to felsic intrusions have been documented in the Stormy Lake area (Seneshen and Owens, 1985). Multiphase gabbro sills and dikes occur in every formation but are especially abundant in the Stormy Lake Formation (Owens, 1986). Discordant felsic dikes are the youngest rocks and include both quartz-feldspar porphyry and aplite phases. They occur in the Gunnar and Dove Lake Formations and in earlier gabbro sills (Fig. 3).

## 2.2 STRUCTURAL GEOLOGY

In the Stormy Lake area, the axial trace of a major, southeasterly plunging anticlinorium bends westward, possibly due to cross-folding (Fig. 3). The study area is on the southwest limb of the anticlinorium and represents a southwest-facing, slightly overturned, homoclinal sequence (Fig. 3). Top indicators that were used in determination of facing direction include scours, graded bedding, load structures, and pillows. All top indicators yielded a consistent facing direction.

Major faults with large displacements were not observed in the Stormy Lake area, but small faults locally offset gabbro intrusions by as much as 10 m. The best examples of such faults were observed immediately south of Stormy Lake. In the section exposed in the study area, the subvertical lithologic units are warped to the northwest (Plate 1), but can be traced laterally for the entire length of the map-area, a distance of 1.2 km, without major offset.

## 2.3 METAMORPHISM

In the study area, metamorphic grade is middle greenschist facies. Chlorite and/or actinolite have replaced original mafic minerals, and albite and sericite have replaced original plagioclase. Accessory metamorphic minerals include carbonate, epidote, biotite, magnetite,

ilmenite, stilpnomelane, and tourmaline. Primary textures are preserved by pseudomorphs after original minerals and by abrupt differences in secondary grain sizes and mineralogy. Textures are best preserved in primary and reworked pyroclastic rocks, particularly: (1) vesicle and phenocryst shapes and sizes, and, to a lesser degree, fragment shapes and sizes in primary pyroclastic rocks, and (2) fragment, phenocryst, and crystal shapes and sizes in reworked pyroclastic rocks including volcanic conglomerate and sandstone. In porphyritic mafic flows and intrusions, phenocrysts are recognizable from pseudomorphs, but groundmass textures and textures in aphyric units are generally poorly preserved, although felty texture was observed in some flows.

## Chapter III

### STRATIGRAPHIC FRAMEWORK OF THE MANIGOTAGAN RIVER FORMATION

This study is focused on a 1.2-km long segment of the Manigotagan River Formation (Fig. 3) which has a mapped lateral extent of 7.3 km (Weber, 1971). The formation here has been divided into seven lithologically distinct members which include primary and reworked felsic to mafic pyroclastic rocks and minor mafic lava flows (Table 4). The members range in thickness from 5 to 103 m, and, although somewhat variable in thickness, all members are continuous across the study area (Plate 1). The continuity of the members into other parts of the formation is unknown. Two chronologically and compositionally different mafic sills occur in the sequence, one at the base of the formation and the other separating members 3 and 4; discontinuous gabbro intrusions also occur in members 2 and 3 (Plate 1).

Although all lithologies of the Manigotagan River Formation have been studied, only the pyroclastic rocks of Members 1, 2, and 7 will be considered in detail in this thesis. Genetic inferences on intervening units such as reworked pyroclastic rocks, lava flows, and peperite are based on Seneshen (1986) and unpublished data.



Table 4 Summary of members in the Manigotagan River Formation

Member	Thick-ness (m)	Composi-tion	Contacts Upper	Contacts Lower	Rock Types	Components	Structural Features	Genesis
Ignimbrite (7)	15-50**	felsic	unknown	sharp	interlayered lapilli-tuff and tuff	lapilli-tuff and tuff consist of vitric ash, vitric felsic fragments, pumice, dacite fragments, plagioclase, quartz and microcline crystals	thin to very thick bedded; doubly graded	subaerial eruptions generated pyroclastic flows which entered water
Turbidite (6)	11-24	felsic	sharp	sharp	interlayered volcanic sandstone and siltstone	sandstone consists of vesicular to non-vesicular mafic volcanic clasts, felsic volcanic clasts, plagioclase and quartz crystal grains and a siltstone matrix	thin to very thick bedded; normally graded Bouma Ta divisions; possible ripples and load structures	local slumps from the higher parts of the subaqueous fan generated turbidity flows
Lava Flows (5)	6-29	mafic	sharp	sharp	massive and pillowed, locally brecciated flows; minor mafic hyalotuff occurs at base of the sequence; felsic cherty tuff occurs in interpillow areas in the upper part of the sequence	amygdaloidal and plagioclase-phyric with a recrystallized to locally felty groundmass	massive lava flows have brecciated upper and lower zones; lateral trough and from massive to pillowed flows; concentric zoning of vesicles in some pillows; vesicularity increases upwards in the sequence	subaqueous flank fissure eruptions fed by underlying diabase sill (8)
Reperite (4)	5-22	inter-mediate	sharp	sharp	mainly volcanic sandstone; minor volcanic siltstone; intermediate lava pods occur at all levels in the sequence	sandstone consists of felsic volcanic clasts, plagioclase, quartz crystal grains and a mudstone matrix; lava pods are amygdaloidal and plagioclase-phyric with a recrystallized groundmass	thin to very thick bedded; normally graded; local low angle cross-laminations	upper part of progradational subaqueous fan succession was intruded by a shallow diabase sill causing mixing of magma and wet sediment
Mass Flow Deposits; Minor Mafic Lava Flows (3)	32-103	felsic to inter-mediate	sharp	sharp	lower 1/5 is interbedded volcanic sandstone, siltstone and mudstone (outer fan to basin plain); upper 4/5 is channel-fill volcanic conglomerate and sandstone with subordinate interbedded volcanic sandstone and siltstone (Mid-fan); massive and pillowed mafic flows occur mainly in the lower part of the sequence	conglomerate consists of felsic, intermediate, and mafic volcanic clasts, volcanic sandstone clasts, plagioclase and quartz crystal grains and a siltstone matrix; sandstone consists of felsic volcanic lithic grains, plagioclase and quartz crystal grains and a siltstone matrix	thin to very thick bedded; normally graded; scours and load structures are common; local trough and festoon cross bedding; some pillows show concentric zoning of vesicles; vesicularity increases upwards in lava flows	renewed explosive volcanic activity provided felsic to intermediate debris for progradation of the subaqueous fan; mafic lava flows erupted by central or flank eruptions concomitant with fan progradation
Tephra-Fall Deposits; Minor Volcanic Conglomerate And Sandstone (2)	17-91	mafic to inter-mediate	sharp	sharp (fault)	upper 0-20 m: interlayered, mafic to intermediate lapilli-tuff and tuff with minor volcanic sandstone; central 12-64 m: interlayered, mafic lapilli-tuff and tuff; lower 8.3-26 m: interlayered, mafic to intermediate lapilli-tuff and tuff with minor volcanic conglomerate and sandstone	lapilli-tuff and tuff consist of felsic to mafic, vesicular to non-vesicular volcanic clasts, plagioclase and quartz crystals, actinolite porphyroblasts after clinopyroxene crystals and a mafic ash matrix; volcanic conglomerate and sandstone consist of felsic to mafic, vesicular to non-vesicular volcanic clasts, plagioclase and quartz crystal grains and a siltstone matrix	thin to very thick bedded; lapilli-tuff and tuff beds are ungraded and have abrupt contacts; minor volcanic conglomerate and sandstone beds are normally graded; volcanic conglomerate beds have erosive basal contacts	tephra-fall from shallow water or subaerial, flank-fissure, phreatomagmatic eruption (s); volcanic conglomerate and sandstone sequences are either channel-fill deposits within tephra-fall deposits or erosional remnants
Ignimbrite (1)	6-39	felsic	sharp (fault)	sharp, truncated by gabbro	interlayered lapilli-tuff and tuff	lapilli-tuff and tuff consist of vitric ash, dacite fragments, vitric felsic fragments, pumice, and plagioclase and quartz crystals	medium to thick bedded; doubly graded	same origin as upper ignimbrite, but fewer pyroclastic flows reached the site of the examined section

\* will be considered in more detail in subsequent chapters  
 \*\* this is a minimum thickness

Within the Manigotagan River Formation there is an upward transition from felsic and mafic pyroclastic rocks in the lower part, through felsic, reworked pyroclastic rocks and mafic lava flows in the central part to mafic lava flows and felsic pyroclastic rocks in the upper part (Plate 1). Felsic pyroclastic flow deposits at the base and top of the formation (Members 1 and 7; Table 4) were subaqueously deposited but were probably derived from subaerial eruptions. The lower pyroclastic flow deposit is overlain by subaqueous tephra-fall and locally, minor turbiditic sequences (Member 2). The tephra-fall deposits were probably derived from flank fissure-type, phreatomagmatic eruptions. Member 3 represents a marked change in conditions; it is an upward coarsening, progradational, subaqueous fan succession. Thin-bedded turbidites, which are dominant in the lower part of the succession, represent an outer fan to basin plain environment (Shanmugam and Moiola, 1988). These grade upwards to interchannel sandstones and siltstones and upward fining channel-fill conglomerate and sandstone sequences diagnostic of a mid-fan environment (Shanmugam and Moiola, 1988; Walker, 1984). The provenance was probably a subaerial, felsic to intermediate volcano; this is indicated by (1) the composition of clasts in conglomerate, most of which are volcanic, and (2) euhedral to subhedral shapes of plagioclase and embayed quartz grains which resemble pyrogenic crystals in underlying members. Mafic flows intercalated with the lower part of the fan succession

attest to the contemporaneous nature of volcanism and sedimentation. Peperite that comprises Member 4 formed by mixing of magma and wet sediment (Busby-Spera and White, 1987). Mixing occurred where a shallow diabase sill (Unit 8) intruded volcanic sandstone and siltstone of the upper part of the fan succession; irregular pods and dikes extended several meters into the sediment and some broke through the seafloor to feed massive and pillowed lava flows of Member 5. Volcanic sandstone and siltstone (Member 6) that overly the lava flows were probably deposited by turbidity flows generated by local slumps from the higher parts of the subaqueous fan (Members 3, 4).

The Manigotagan River Formation records multiple variations in magma compositions, and in volcanic and sedimentary processes over time. The lower felsic ignimbrite (Member 1) and the mafic to intermediate tephra-fall deposits (Member 2) were apparently erupted in succession and represent the later eruptive phases of the stratovolcano from which dacitic tephra of the underlying Narrows Formation was erupted. The progradational fan succession, which consists largely of resedimented, felsic to mafic pyroclastic debris, probably reflects a renewed, explosive eruptive event. Mafic lava flows in the lower (Member 3) and upper part (Member 5) of the fan succession, were probably erupted through fissures and were fed from the same magma chamber. Following the eruption of the upper mafic lava

flows, there was a hiatus in volcanism, and the turbidites of Member 6 were deposited. Subsequently, another explosive eruption occurred and the felsic ignimbrites of Member 7 were deposited. Subsequent to this final eruptive event, the stratovolcano apparently underwent erosional destruction, subsidence, and burial by the Edmunds Lake flysch sequence. The contact between the Manigotagan River Formation and Edmunds Lake Formation is unexposed, but erosional destruction of the stratovolcano is suggested by the petrographic similarity between sedimentary units of the Edmunds Lake Formation and underlying, felsic pyroclastic units of the Manigotagan River Formation and Narrows Formation (Seneshen and Owens, 1985).

## Chapter IV

### RECOGNITION OF JUVENILE COMPONENTS IN PRECAMBRIAN PYROCLASTIC ROCKS

Primary pyroclastic rocks are composed of variable proportions of vitric, lithic, and crystal particles derived from fragmentation of magma and rocks by magmatic or hydroclastic volcanic eruptions (Fisher and Schmincke, 1984). These particles include juvenile, cognate, and accidental components. According to Fisher and Schmincke (1984), juvenile particles are derived directly from the erupting magma, and they comprise dense or inflated particles of chilled magma together with pyrogenic crystals that were in the magma prior to eruption. Cognate particles are derived by fragmentation of rocks from earlier eruptions of the same volcano, whereas accidental fragments are derived from the subvolcanic basement, and, therefore, can include igneous, sedimentary, or metamorphic rock types.

Recognition of juvenile components in ancient volcanoclastic sequences is hampered by alteration, metamorphism, and deformation; yet the proportion and characteristics of juvenile components are of critical importance because (1) they help to distinguish between pyroclastic and epiclastic rocks, and (2) they facilitate interpretation of the origin and history of the rocks

(Fiske, 1969). In Cenozoic deposits, juvenile components are generally recognized by their shape, internal texture, and internal structure. However, even in Recent deposits, a number of post-eruptive processes can modify or destroy original primary textures of juvenile vitric components. Such processes include: (1) primary compaction and recrystallization (Hildreth et al., 1984; Wright, 1981; Sheridan, 1979), and (2) weathering and transportation (Fisher and Schmincke, 1984; Fiske, 1969). After final deposition, juvenile vitric components can be further modified by diagenesis or low-grade metamorphism. Pyroclastic deposits are highly susceptible to post-depositional alteration because they contain abundant vitric material and have a high initial porosity and permeability (Fisher and Schmincke, 1984). According to Fiske (1969), pumiceous rocks are especially susceptible to alteration because they have large surface areas of unstable glass.

In Precambrian greenstone belts, greenschist facies and higher grade metamorphism has further modified previously altered fragmental rocks. In many belts, including the study area, such rocks now consist of variable proportions of recognizable fragments and crystals enclosed in a fine-grained, granoblastic aggregate produced by the recrystallization of other primary components. The recognition of juvenile components in Precambrian fragmental rocks is thus difficult and requires careful petrographic

analysis. This problem has been considered by a number of workers such as Fiske (1969), who presented diagnostic criteria for the identification of pumice in ancient marine pyroclastic rocks, and Baldwin (1987), who developed a logical process for recognition of both dense and inflated juvenile components in Precambrian pyroclastic deposits. Such criteria have been adopted here for the recognition of juvenile components in pyroclastic rocks of the Manigotagan River Formation. Genetic interpretation of pyroclastic deposits is also facilitated by more readily preserved features such as (1) megascopic primary structures, and (2) field relationships with other rock units.

## Chapter V

### SUBAQUEOUS PYROCLASTIC FLOW DEPOSITS

Interlayered lapilli-tuff and tuff that are interpreted to be ignimbrites comprise 25% of the Manigotagan River Formation. The ignimbrites are felsic in composition and occur at the base (Member 1) and top (Member 7) of the formation (Plate 1). Both the upper and lower ignimbrites are overlain and underlain by rocks of different genesis.

The ignimbrites are composite sheets ranging in thickness from 6 to at least 50 m and can be traced laterally for 1.2 km, the extent of the mapping. Each sheet comprises at least 3, and in places, as many as 12 multiple flow units that range in thickness from 0.7 to 17 m but are generally less than 5 m thick (Table 5). Most flow units consist of a lower, lapilli-tuff division and an upper tuff division; however, some units consist only of a lapilli-tuff division. In most flow units, pumice increases in abundance and to a lesser extent in size upwards and is concentrated in the upper part of lapilli-tuff divisions; it also occurs in ungraded pumice-rich layers in the upper tuff divisions of some flow units. In most lapilli-tuff divisions, vitric felsic fragments and/or dacite fragments are typically normally graded with respect to abundance, and, to a lesser extent size.



**Table 5 Megascopic Features of the Upper and Lower Ignimbrites (Members 7 and 1).**

Member	Thickness (m)	Contacts		Flow Unit Thickness (m)	Internal Features	Comments
		Upper	Lower			
Upper Ignimbrite (Member 7)	*15-50	unexposed	sharp concordant	0.7-17	Composite sheet consisting of 5 to at least 12 flow units; flow units consist of a lower lapilli-tuff division and an upper tuff division or less commonly consist of only a lapilli-tuff division; flow unit contacts are planar and sharp or less commonly are gradational.	Tephra was probably derived from subaerial eruptions and was emplaced subaqueously by pyroclastic flows; the source vent appears to have been in the Gem Lake area, 10 km to the southeast.
Lower Ignimbrite (Member 1)	6-39	sharp concordant (fault)	sharp concordant	5.2-7.5	Composite sheet consisting of at least 3 flow units; flow units consist of a lower lapilli-tuff division and an upper tuff division; flow unit contacts are sharp and planar to locally scoured.	Same origin as upper ignimbrite, but apparently fewer pyroclastic flows reached the site of the examined section.

\* This is a minimum thickness

## 5.1 COMPONENTS OF IGNIMBRITES IN THE MANIGOTAGAN RIVER FORMATION

The ignimbrites are composed of 0 to 40% dacite fragments, 0 to 35% pumice, 0 to 20% vitric felsic fragments, 0 to 2% mafic scoria fragments, 0 to 2% microcline-phyric felsic fragments, 0 to 15% crystal particles, and 55 to 99% fine-grained, largely granoblastic, quartzo-feldspathic aggregate inferred to have replaced vitric ash. In most flow units, the combined abundance of dacite fragments, pumice, and vitric felsic fragments is generally less than 15%, and the abundance of crystal particles is less than 5%.

### 5.1.1 Dacite Fragments

Whitish-grey, 2 to 100 mm long, angular to subrounded, non-vesicular, plagioclase and/or quartz-phyric to aphyric dacite fragments comprise 0 to 40% of the ignimbrites (Tables 6, 7). They occur both in the lower and upper ignimbrites, but are apparently more abundant in the lower (Table 7). Dacite fragments in both the lower and upper ignimbrites have similar phenocryst abundances and plagioclase/quartz ratios, but phenocrysts are somewhat larger in dacite fragments of the lower ignimbrite (Table 6). The dacite fragments are texturally similar to (Fig. 4), or less commonly coarser grained than, the surrounding parts of the rock, which is a fine-grained, largely granoblastic,

**Table 6** Compositional and Textural Features of Fragments in Ignimbrites of Members 1 and 7.  
(see Tables 7 and 8 for data on abundances, sizes, and shapes of fragments)

Member	Fragment Type	Amygdules			Phenocrysts				Groundmass ****		
		Type	%	Size (mm)	Shape	Type	%	Size (mm)		Shape	
Upper Ignim- brite (7)	Dacite Fragments	none recognized			pg	0-12 *** (5)	0.2-2.1 *(0.92)	euhedral to subhedral	0.005-0.1 mm, grano- blastic aggregate composed of pg-qtz- carb-ser-pyrr		
		qtz	0-2	0.2-1.4 *(0.49)	euhedral						
	Pumice	carb and qtz	0-20	0.2-0.6	subcircular	pg	0-15	0.3-2 *(0.80)		subhedral	0.005-0.05 mm, foliated, lace-like aggregate composed of ser-bio-pg-qtz-carb- pyrr-hem
		qtz	0-5	0.1-0.4	subcircular	pg	0-10 *** (9)	0.3-1.4 **		euhedral to subhedral	
	Vitric Felsic Fragments	qtz	0-1	0.1-0.2 **	euhedral	micro	2	0.2-0.5 **		subhedral	0.005-0.01 mm, grano- blastic to foliated aggregate composed of qtz-pg-pyrr-ser-bio
Mafic Scoria	qtz	3-25	0.2-0.5	subcircular	none recognized				0.005-0.01 mm, grano- blastic aggregate composed of hem-pg- carb-bio-pyrr		
Microcline- phyric Felsic Fragments	none recognized			pg	2 *** (2)	0.2-0.7 **	euhedral to subhedral	0.005-0.1 mm, grano- blastic aggregate composed of qtz-pg- micro-chl-pyrr			
	qtz	1	0.2-0.4 **	subhedral							
	micro	2	0.2-0.5 **	subhedral							
Lower Ignim- brite (1)	Dacite Fragments	none recognized			pg	0-15 *** (5)	0.2-5 *(1.18)	euhedral to subhedral	0.005-0.1 mm, grano- blastic aggregate composed of pg-qtz- carb-ser-pyrr		
		qtz	0-3	0.2-1.9 *(0.64)	subhedral						
	Pumice	pg	0-50	0.1-0.4	thin, elongate or subcircular	pg	0-3	0.2-2.8 *(0.87)		subhedral	0.005-0.05 mm, foliated, lace-like aggregate composed of ser-bio-pg-qtz-carb- pyrr-hem
Vitric Felsic Fragments	qtz	0-5	0.1-0.2	subcircular	pg	0-2	0.3-1 **	subhedral	0.005-0.01 mm, grano- blastic aggregate composed of qtz-pg- ser-bio-pyrr		

**Abbreviations**

pg plagioclase  
qtz quartz  
ser sericite  
chl chlorite  
carb carbonate  
hem hematite  
bio biotite  
micro microcline  
pyrr pyrrhotite  
hem hematite

\* Average maximum phenocryst size is the average length of  
5 to 10 of the largest phenocrysts in each fragment  
\*\* Insufficient data to calculate average maximum phenocryst size  
\*\*\* Average plagioclase/quartz ratio  
\*\*\*\* Minerals are listed in decreasing order of abundance



0 1 2 mm

Figure 4: Photomicrographs (plane light, above and x-polars, below) showing an elongate, plagioclase-phyric dacite fragment (beige in plane light, grey in x-polars) composed largely of plagioclase and quartz with minor carbonate, sericite, and pyrrhotite. The texturally similar, fine-grained, quartzo-feldspathic aggregate surrounding the dacite fragment is inferred to be recrystallized vitric ash. The dacite fragment is from the upper ignimbrite (Member 7).

quartzo-feldspathic aggregate inferred to represent recrystallized vitric ash. Because of their uniform texture and generally fine, metamorphic grain size, the dacite fragments were probably originally vitric. In terms of composition, the dacite fragments contain less sericite and biotite, and, thus, contrast with the surrounding quartzo-feldspathic aggregate (Fig. 4).

### 5.1.2 Pumice

Reddish brown to dark green, 5 to 220 mm long, collapsed pumice comprises 0 to 35% of the ignimbrites. It occurs both in the lower (Member 1) and upper (Member 7) ignimbrites, but is generally more abundant in the upper (Tables 7, 8). On outcrop surface, the pumice is thin and elongate with ragged, fish-tail-like terminations (Fig. 5). Such pumice shapes have been documented in ancient marine pyroclastic rocks elsewhere (Fiske, 1969; Howells et al., 1985).

Petrographically, most pumice is plagioclase-phyric to locally aphyric and consists largely of a 0.005 to 0.05 mm, foliated aggregate of sericite and biotite, with minor plagioclase, quartz, carbonate, pyrrhotite, and hematite. In contrast to dacite fragments, the pumice contains fewer plagioclase phenocrysts, more sericite and biotite in its groundmass, and lacks quartz phenocrysts (Table 6). Pumice in both the lower and upper ignimbrites has similar phenocryst sizes, but phenocrysts are more abundant in the

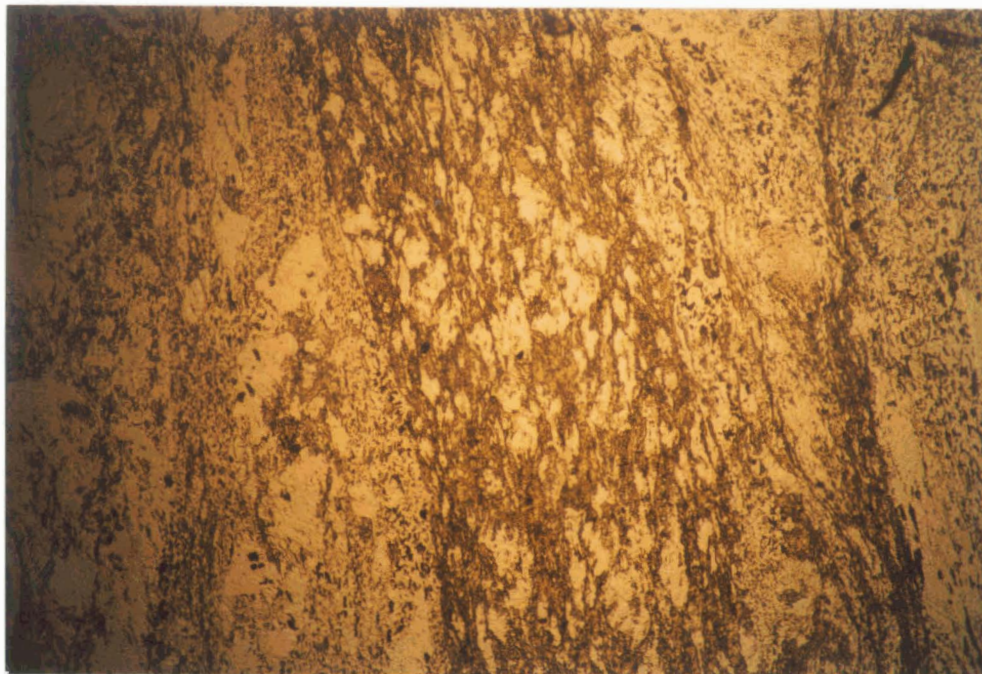


Figure 5: Vertical separation of pumice and vitric felsic fragments in flow unit 3b of upper ignimbrite member. Dark brown, thin, elongate pumice appears to increase in size and abundance upwards. Pinkish grey to dark grey, vitric felsic fragments decrease in size and abundance upwards. Lens cap for scale is 5.5 cm in diameter.

upper ignimbrite (Table 6). In contrast to the surrounding granoblastic, quartzo-feldspathic aggregate, the pumice is foliated and contains more sericite and biotite (Tables 6, 7, 8). Its present composition is consistent with a diagenetically altered glass that was subsequently overprinted by greenschist facies metamorphism. Collapsed pumice composed largely of sericite has also been observed in other Archean, subaqueous ignimbrites (Padgham, 1980).

The original vesicularity of pumice has been largely destroyed by collapse and subsequent recrystallization, but where it is rarely preserved, the pumice contains up to 50% vesicles (Fig. 6). In the lower ignimbrite, pumice vesicles are filled with polycrystalline plagioclase, whereas in the upper ignimbrite they are filled with polycrystalline carbonate and/or polycrystalline quartz (Table 6). In Precambrian pyroclastic deposits elsewhere, there are similar problems, and pumice can only be rarely identified by its original vesicularity (Baldwin, 1987; Tassé *et al.*, 1978).

Another identifying characteristic of pumice is its tendency to separate from lithic fragments and accumulate in the upper parts of graded beds (Fiske, 1969). This feature was observed in the lower lapilli-tuff division of ignimbrite flow units in the Manigotagan River Formation (Fig. 5).



0 1 2 mm

Figure 6: Photomicrograph (plane light) of a 10 mm long, partly collapsed, pumice fragment in which original vesicularity is still preserved. The pumice contains thin, elongate, polycrystalline plagioclase amygdules (white) in a 0.005 to 0.05 mm, foliated aggregate (brown) composed largely of sericite and biotite that has replaced original glass. The white, elongate areas to the left of the pumice are broken plagioclase crystals. Pumice and crystals are enclosed in a fine-grained, quartzo-feldspathic aggregate inferred to be recrystallized vitric ash. The pumice is from the lower ignimbrite (Member 1).

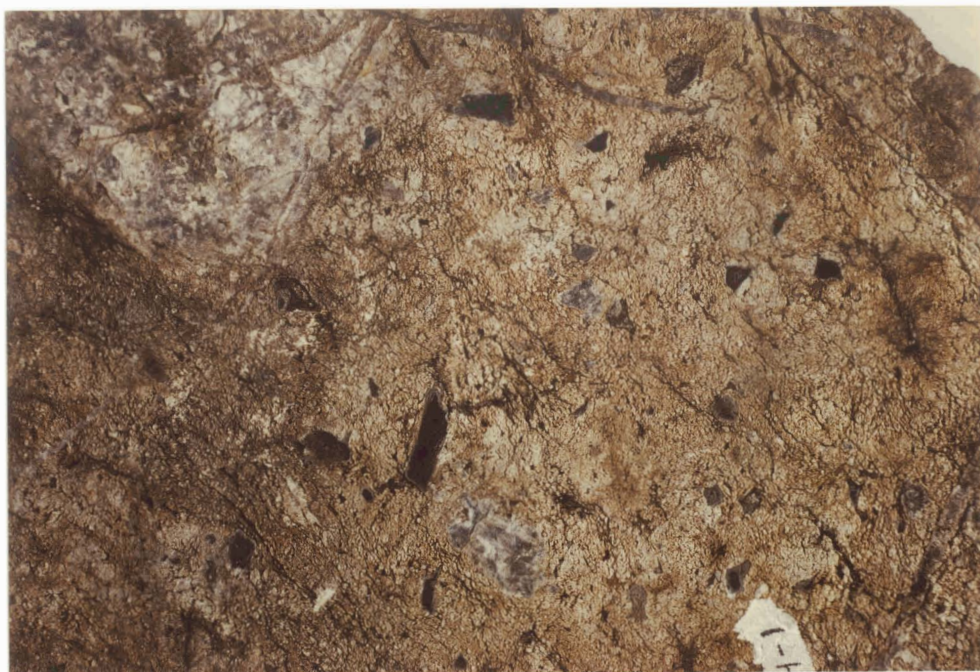


### 5.1.3 Vitric Felsic Fragments

Light grey to black, 0.5 to 180 mm long, vesicular to non-vesicular, plagioclase and/or quartz-phyric to aphyric vitric felsic fragments comprise 0 to 20% of the ignimbrites. They occur in both the lower and upper ignimbrites, but are more abundant in the upper (Table 7). The fragments are angular to rounded and vary from equidimensional to elongate (Fig. 7); they are more elongated in the lower ignimbrite (Fig. 14) than the upper due to a higher degree of deformation.

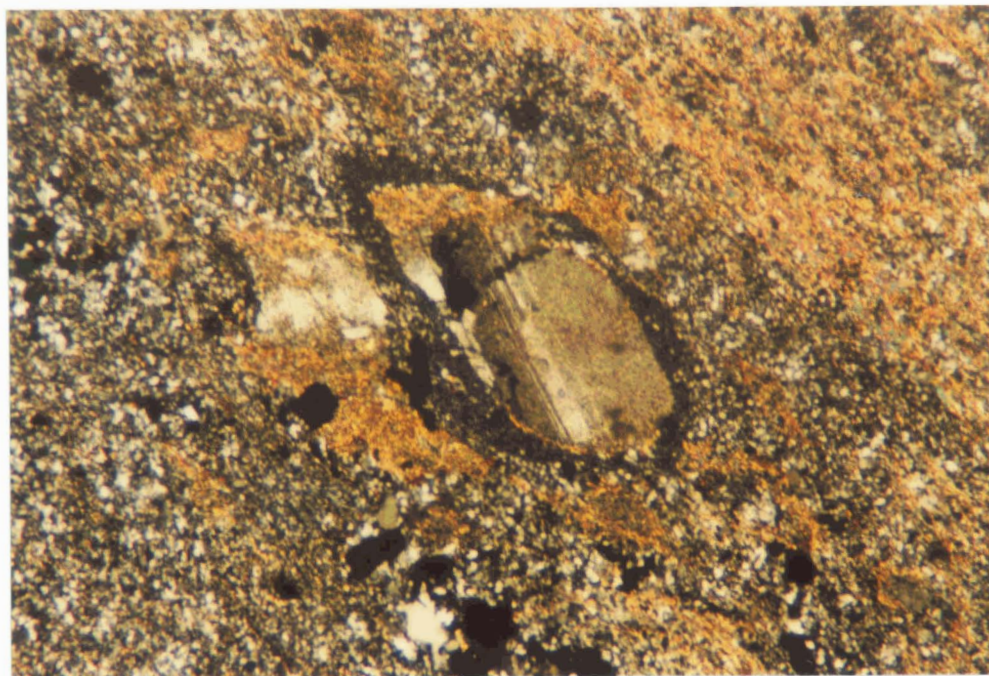
In contrast to the dacite fragments, the vitric felsic fragments are finer grained, are locally amygdaloidal, have higher plagioclase/quartz ratios, and contain smaller plagioclase and quartz phenocrysts and more pyrrhotite in the groundmass (Table 6). Phenocrysts within fragments are subhedral to euhedral, and the original plagioclase is replaced by albite and sericite (Fig. 8). Although these fragments have been metamorphosed, their original glassy nature can be inferred by their: (1) vitreous luster on outcrop surface, (2) local, angular, blocky subconchoidal shapes, and (3) overall very fine, metamorphic grain size (Baldwin, 1987).

The vitric felsic fragments are typically enclosed in the coarser grained, granoblastic, quartzo-feldspathic aggregate inferred to be recrystallized vitric ash (Fig. 8). However,



0 5 cm

Figure 7: Photograph of lapilli-tuff in the upper ignimbrite (Member 7). The lapilli-tuff contains angular, vitric felsic fragments (dark grey to black) and angular, porphyritic dacite fragments (whitish grey). Material surrounding fragments consists of crystal particles and quartzo-feldspathic aggregate inferred to be recrystallized vitric ash.



0 1 2 mm

Figure 8: Photomicrograph (x-polars) of a subrounded, plagioclase-phyric, vitric felsic fragment (black) enclosed in a coarser-grained, quartzo-feldspathic aggregate inferred to be recrystallized vitric ash. Note that the plagioclase phenocryst has been replaced by albite and sericite (orange). The vitric felsic fragment is from the lower ignimbrite (Member 1)

in the upper ignimbrite, vitric felsic xenoliths were observed in some dacite fragments (Fig. 9). Vitric felsic fragments in the quartzo-feldspathic aggregate contain 5 to 10 times more sericite and biotite than vitric felsic xenoliths in dacite fragments. In places, fragments containing up to 70% sericite resemble pumice, but can be distinguished by their typical angular shape, higher pyrrhotite content and smaller plagioclase phenocrysts (Table 6). One fragment, enclosed in the quartzo-feldspathic aggregate, was surrounded by a 0.1 to 0.5 mm thick rim containing up to 70% sericite; sericite content gradually decreased inward to 2% in the fragment core. Originally, this rim could have been largely a potassic clay mineral formed by diagenetic alteration of glass (Fisher and Schmincke, 1984). The less sericitic vitric felsic xenoliths, that are enclosed in presumably impervious dacite fragments, were not altered to the same degree.

#### 5.1.4 Minor Fragment Types

Subangular mafic scoria, and subrounded, microcline-phyric felsic fragments are minor components of the upper ignimbrite, but were not recognized in the lower ignimbrite. They are compositionally and texturally distinct from dacite fragments, vitric felsic fragments, and pumice (Table 6). Mafic scoria shows well preserved vesicularity (Fig. 10),

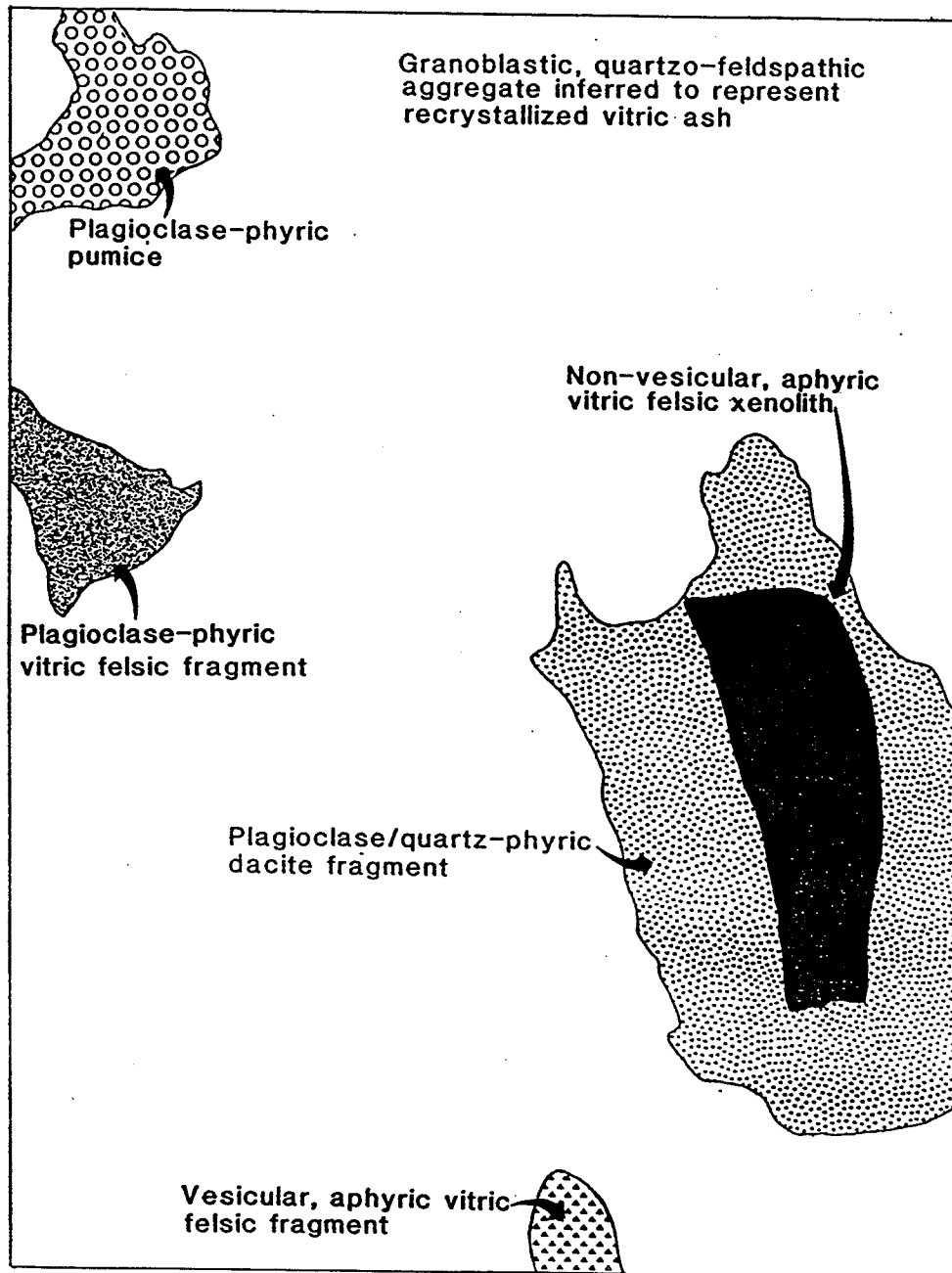


Figure 9: Thin section drawing of lapilli-tuff from the upper ignimbrite (Member 7) showing an aphyric, vitric felsic xenolith enclosed in a dacite fragment. Vesicular to non-vesicular, plagioclase-phyric to aphyric, vitric felsic fragments in the surrounding granoblastic, quartzo-feldspathic aggregate contain 5 to 10 times more sericite than the vitric felsic xenolith.

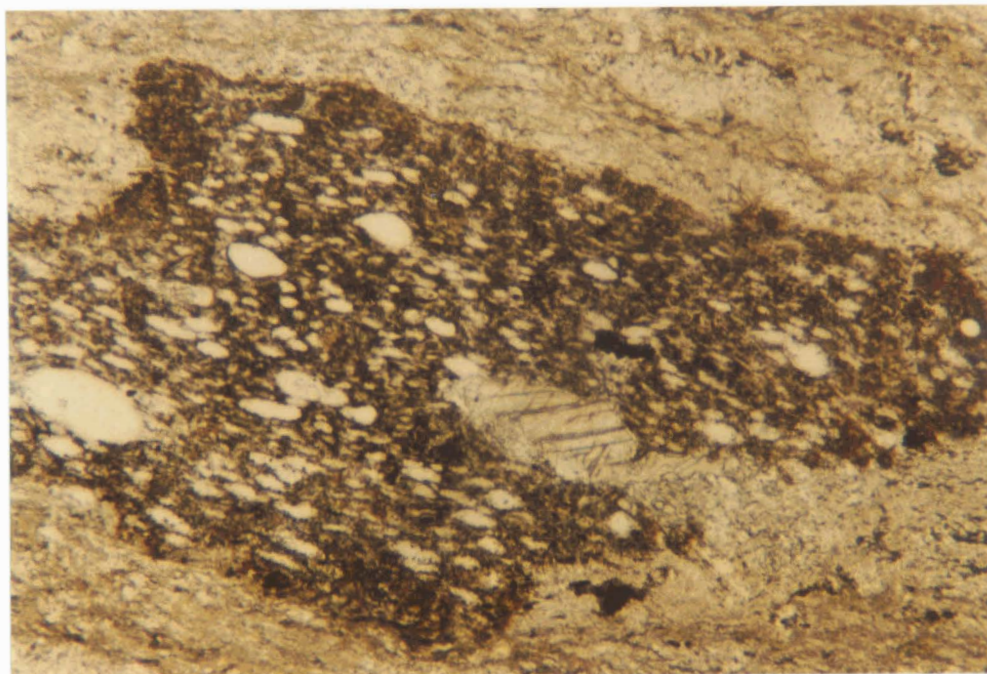


Figure 10: Photomicrograph (plane light) of a sub-angular, mafic scoria fragment in which original vesicularity is still preserved. The scoria contains subcircular, quartz amygdules in a 0.005 to 0.01 mm aggregate composed of hematite, plagioclase, carbonate, biotite, and pyrrhotite. The fine-grained, quartzo-feldspathic aggregate which surrounds the scoria is inferred to be recrystallized vitric ash. The mafic scoria is from the upper ignimbrite (Member 7).

but differs from coexisting pumice in terms of abundance, composition, and texture (Tables 6, 7). Microcline-phyric felsic fragments differ from vitric felsic fragments in distribution, abundance, and composition (Table 6).

#### 5.1.5 Crystal Particles

Crystal particles occur in both the lower and upper ignimbrites, but are larger and more abundant in the lower than in the upper ignimbrite (Tables 7, 8). Crystal types and abundances are 0 to 15% plagioclase, 0 to 5% quartz, and 0 to 5% microcline. The plagioclase/quartz ratio in the crystal population is comparable to that in the phenocryst population of dacite fragments, but it contrasts with other fragments that contain both plagioclase and quartz phenocrysts (cf. Tables 6, 7).

Plagioclase crystals include broken, subhedral to anhedral grains and less common, unbroken, euhedral to locally subhedral crystals. According to Fisher and Schmincke (1984), broken crystals are characteristic of ignimbrites. Crystals have been replaced by single-crystal pseudomorphs of albite, some of which contain sericite and/or carbonate (Fig. 11). Polycrystalline, monomineralic aggregates of albite occur locally and are similar in size and shape to monocrystalline plagioclase crystals. This relationship suggests that the plagioclase aggregates are recrystallized plagioclase crystals.



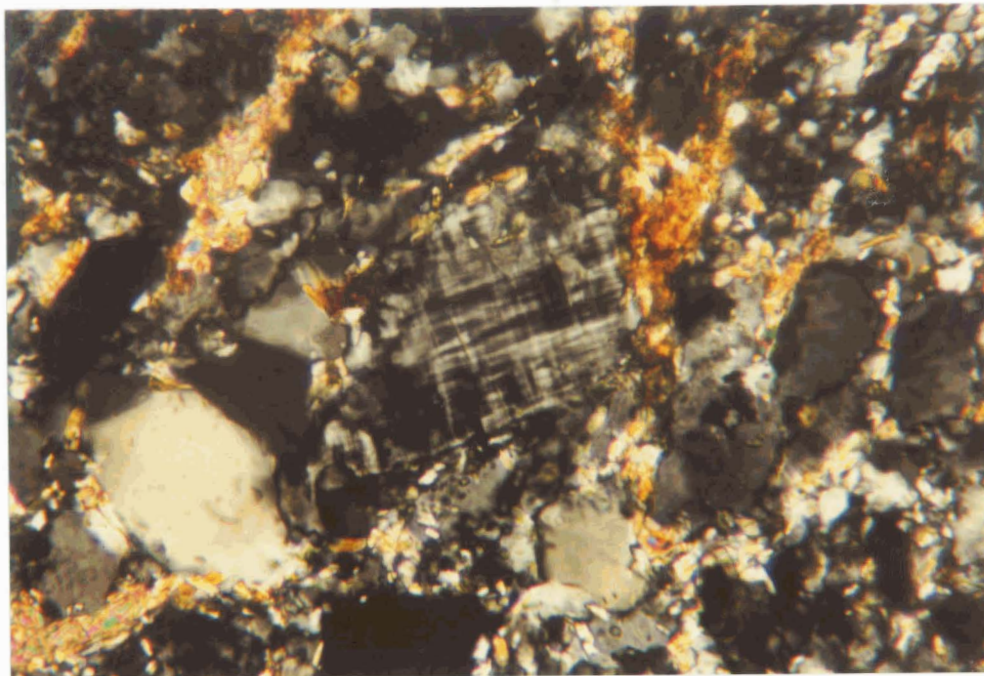
0 1 2 mm

Figure 11: Photomicrograph (x-polars) of a subhedral, apparently, unbroken plagioclase crystal enclosed in a uniform textured, quartzo-feldspathic aggregate inferred to be recrystallized vitric ash. Original plagioclase has been replaced by a single-crystal pseudomorph of albite that here contains some intergrown sericite. The plagioclase crystal is from the upper ignimbrite (Member 7).



Euhedral to subhedral, apparently unbroken plagioclase crystals are similar in shape to phenocrysts in pumice, dacite, and vitric felsic fragments, but they differ in size and abundance. In the upper ignimbrite, the plagioclase crystals are, on average, slightly smaller than phenocrysts in both dacite fragments and pumice (cf. Tables 6, 7, 8). However, in the lower ignimbrite, the crystals are, on average, smaller than phenocrysts in dacite fragments and larger than phenocrysts in pumice (cf. Tables 6, 7, 8). In both the lower and upper ignimbrites, the apparently unbroken crystals are larger than phenocrysts in coexisting vitric felsic fragments. Based on petrographic observation, the plagioclase crystals are generally less abundant than phenocrysts in dacite fragments, but they are more abundant than phenocrysts in pumice and vitric felsic fragments.

Quartz crystals, which include broken, subhedral to anhedral grains (Fig. 12), and less common, unbroken, euhedral to locally subhedral crystals are generally less abundant and smaller, than coexisting plagioclase crystals (Tables 7, 8). Embayments were locally observed in quartz crystals and are typically filled with a fine-grained, quartzo-feldspathic aggregate that is compositionally and texturally similar to the groundmass of dacite fragments, and, thus, probably represents recrystallized glass. Generally quartz crystals are monocrystalline, but locally, there are polycrystalline quartz aggregates that have the



0.0 0.1 0.2 0.3 0.4 0.5 mm

Figure 12: Photomicrograph (x-polars) of an apparently broken, anhedral microcline crystal and coexisting, apparently broken, anhedral to subhedral quartz crystals. Crystals are enclosed in a 0.005 to 0.05 mm, quartzo-feldspathic aggregate inferred to be recrystallized vitric ash. Pink to golden brown mineral is secondary carbonate. The microcline is from the uppermost part of the upper ignimbrite (Member 7).

same size and shape as the crystals and probably represent recrystallized quartz crystals.

Euhedral to subhedral, apparently unbroken quartz crystals are similar in shape to phenocrysts in vitric felsic fragments and dacite fragments, but differ in size and abundance. In both the upper and lower ignimbrites, euhedral to subhedral, apparently unbroken, quartz crystals are, on average, smaller than phenocrysts in dacite fragments; they are larger and more abundant than phenocrysts in vitric felsic fragments (cf. Tables 6, 7, 8). Quartz phenocrysts were not observed in recognizable pumice from the lower or upper ignimbrite members.

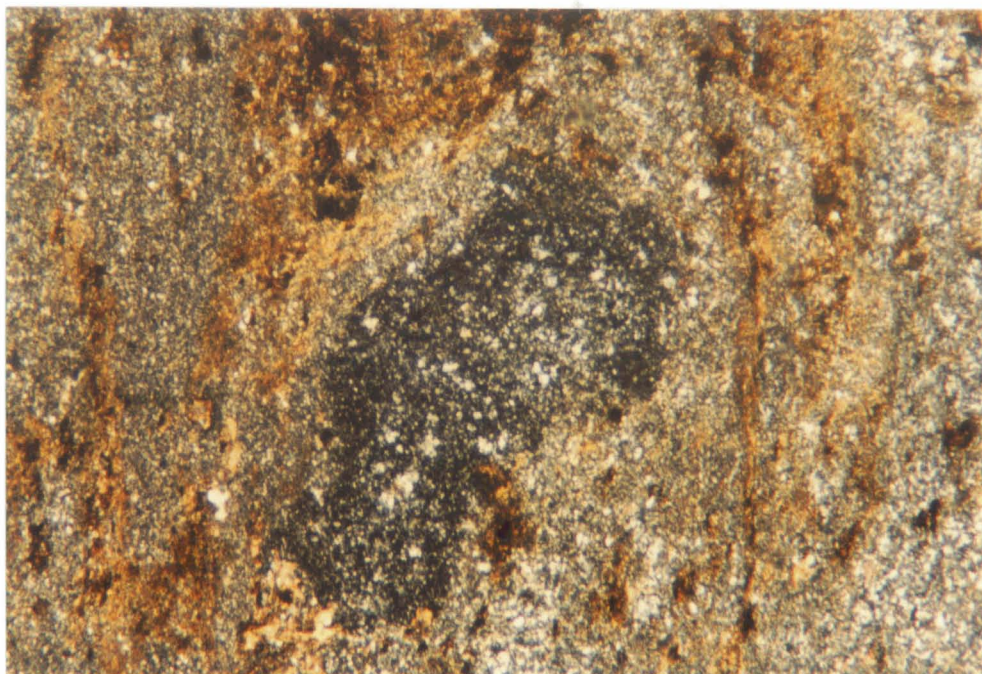
Microcline crystals (Fig. 12), the occurrence of which was confirmed by x-ray diffraction study, were found in low abundance in the uppermost part of the upper ignimbrite member (Tables 7, 8). Microcline crystals, which were probably originally sanidine (Condie *et al.*, 1970), are typically broken and anhedral to subhedral or less commonly are unbroken and subhedral; they are generally somewhat smaller than coexisting plagioclase and quartz crystals (Tables 7, 8). Subhedral, apparently unbroken microcline crystals occur in the same unit as microcline-phyric felsic fragments and are similar in both shape and size to microcline phenocrysts in these fragments; they were probably derived from the same source.

### 5.1.6 Vitric Ash

The dominant component of the ignimbrites is a fine-grained, largely granoblastic aggregate that encloses recognizable fragments and crystal particles. This aggregate ranges in abundance from 56 to 99%, has a grain size of 0.005 to 0.1 mm, and is composed of subequal amounts of plagioclase, quartz, and sericite, with minor carbonate, biotite, hematite, and pyrrhotite and rare microcline and tourmaline (Tables 7, 8).

Typically, the granoblastic aggregate has a uniform, fine-grained texture, probably indicative of an original vitric component. It is texturally similar to the groundmass of recognizable dacite fragments (Fig. 4), but generally, it is coarser grained than the groundmass of vitric felsic fragments (Fig. 8). The granoblastic aggregate contains more sericite than dacite and vitric felsic fragments, but less than pumice. Since vitric, and texturally similar, presumably vitric, dacite fragments are still recognizable (Fig. 4), the aggregate probably consisted of finer vitric particles such as ash-sized glass shards and granules.

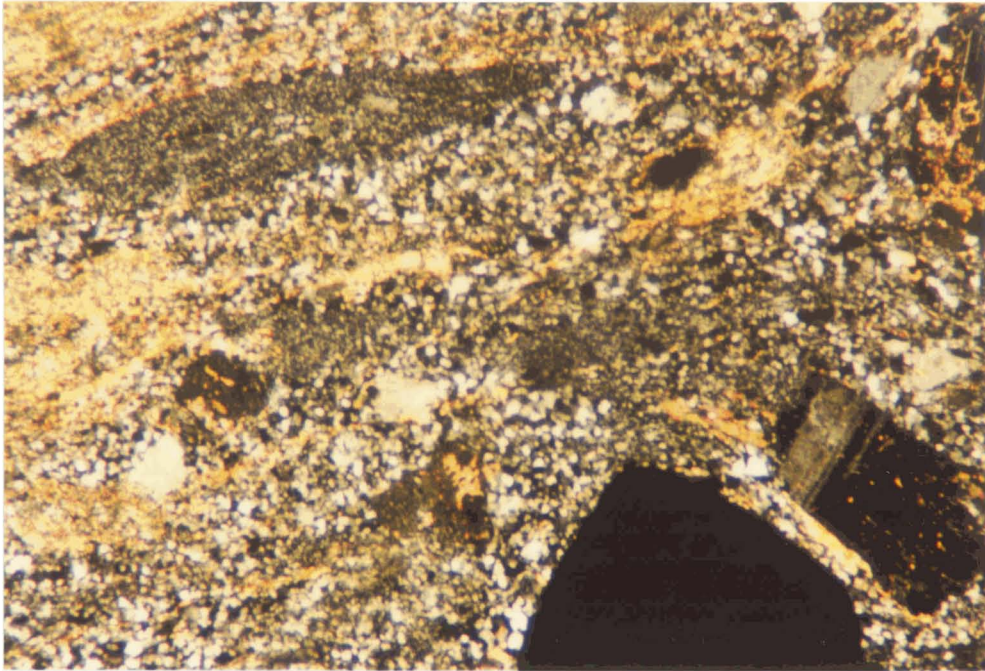
Where pumice is abundant, the granoblastic matrix has a patchy appearance, with irregular patches or lenticles of fine-grained, equigranular, quartzo-feldspathic aggregate partly or entirely surrounded by thin, elongate pumice (Fig. 13). Here, the pumice is clearly distinguishable from the



0 1 2 mm  
Figure 13: Photomicrograph (x-polars) of a subrounded, vitric felsic fragment (dark grey) enclosed in a 0.005 to 0.05 mm, patchy, plagioclase-quartz-sericite aggregate inferred to be recrystallized vitric ash. Grey quartzo-feldspathic patches are partly or entirely outlined by concentrations of sericite and biotite inferred to be recrystallized pumice (brownish-orange). The vitric felsic fragment is from the upper ignimbrite (Member 7).

quartzo-feldspathic aggregate inferred to be recrystallized vitric ash.

Marked textural differences in the granoblastic aggregate are apparent between the lower and upper ignimbrites. The granoblastic aggregate in the lower ignimbrite (Figs. 8, 14) is coarser grained than in the upper ignimbrite (Fig. 11). This marked contrast between the ignimbrites apparently represents differing degrees of recrystallization. The lower ignimbrite is directly underlain by a 20 to 44 m thick gabbro sill (Plate 1) and the greater recrystallization of this unit may be the result of thermal metamorphism by the sill.



0 1 2 mm

Figure 14: Photomicrograph (x-polars) showing lenticular, vitric felsic fragments (grey, finer grained areas), plagioclase crystals (various shades of grey, in places twinned), and quartz crystals (black, lower right) in a 0.005 to 0.1 mm, quartzo-feldspathic aggregate inferred to be recrystallized vitric ash. The fragments and crystals are from the lower ignimbrite (Member 1).

## 5.2 DESCRIPTION OF UPPER IGNIMBRITE (MEMBER 7)

The upper ignimbrite is described first because it is less deformed and better exposed than the lower ignimbrite. It comprises 16% of the Manigotagan River Formation and ranges in thickness from 15 to at least 50 m; it thins to the northwest (Plate 1). The upper boundary with the overlying Edmunds Lake Formation is not exposed; its inferred position is based on the southwestward transition from topographically positive outcrop areas to swampy areas with no outcrop. The lack of outcrop to the southwest could signify the presence of recessive greywacke and mudstone, typical of the Edmunds Lake Formation.

Multiple flow units, which comprise the ignimbrite sheet, have been defined in measured sections and locally in outcrops between sections (Table 5). Twelve flow units were identified in the southeast, where 41 m of the member is exposed, and five in the northwest, where the member is apparently thinner and 26 m is exposed (Fig. 15). Flow units range in thickness from 0.7 to 17 m and can be traced laterally across outcrops 6 to 65 m wide, with little change in thickness. However, over longer distances, changes in unit thicknesses are apparent. For example, the lapilli-tuff division of flow unit 4a (Fig. 15), which was observed in an outcrop 110 m northwest of the measured section, decreased in thickness by 50%, whereas the thickness of the upper tuff division remained relatively constant. Over longer



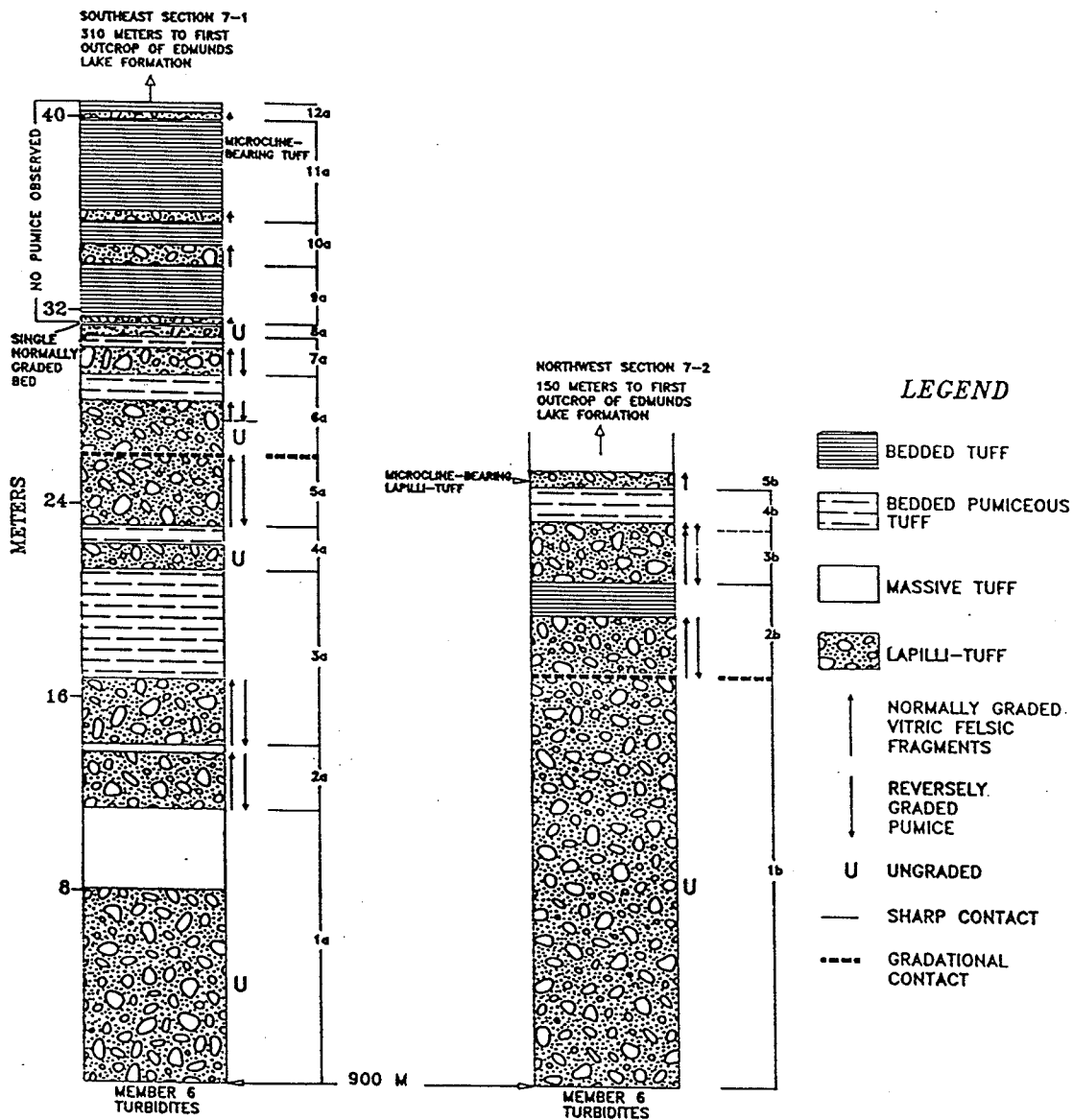


Figure 15: Stratigraphic sections (7-1, 7-2) through the upper ignimbrite (Member 7).

distances, individual flow units cannot be correlated with confidence. Comparison of the two sections through the ignimbrite (Fig. 15) yield the following lateral variations:

1. although average flow unit thicknesses do not change markedly, the number of flow units decreases from 12 in the southeast to 5 in the northwest,
2. in both sections, flow units are compositionally and texturally similar and show similar grading characteristics,
3. there is no apparent change in the proportion or shape of pumice, vitric felsic fragments, and crystal particles, or in the size of crystal particles from southeast to northwest, but the average maximum size of vitric felsic fragments increases from 2.3 cm to 3.5 cm and that of pumice decreases from 5 cm to 4.3 cm,
4. although differing considerably in thickness, the lowermost lapilli-tuff in both sections has a much lower content of vitric felsic fragments than overlying flow units, and
5. microcline crystal particles and microcline-phyric felsic fragments were found in the upper part of the ignimbrite in both sections. The lowermost and uppermost flow units thus appear to be correlative, but many of the intervening flow units do not extend northwestward.

### 5.2.1 Lower Lapilli-tuff Division

Lapilli-tuff divisions comprise the lower 10 to 100% of flow units and range in thickness from 0.25 to 17 m. The lapilli-tuff is thickest in the lowermost flow units of both measured sections (Fig. 15). Upper and lower contacts of each lapilli-tuff division are planar; contacts are sharp where overlain by an upper tuff division, but are gradational where the upper tuff division is absent and the lapilli-tuff is overlain by the next lapilli-tuff division (Fig. 15).

The lapilli-tuff consists of 0 to 3% dacite fragments, 0 to 35% pumice, 2 to 20% vitric felsic fragments, 0 to 2% mafic scoria, 0 to 2% microcline-phyric felsic fragments, 2 to 12% crystal particles, and 55 to 85% fine-grained, quartzo-feldspathic aggregate inferred to have replaced vitric ash (Table 7). The lapilli-tuff divisions lack stratification and are poorly sorted. Characteristically, pumice and vitric felsic fragments are partly separated from each other within flow units (Fig. 5). Vitric felsic fragments are most abundant at the base of units, and show a distinct upward decrease in abundance and a subtle decrease in size within a unit; in some units they are ungraded (Fig. 15). Although pumice was not identified in all units, where observed, its distribution is the reverse of that shown by vitric felsic fragments; it typically increases in abundance and subtly in size upwards or less commonly is ungraded.

Table 7 Internal Characteristics of the Lower Lapilli-Tuff Division

Member and Division Type	Thickness (m)	Internal Features	%	**** Recognizable Fragments			Crystal Particles			**** Granoblastic Matrix	
				Size (mm)	Shape	Type	Type	%	Size (mm)		Shape
Upper Ignimbrite (Member 7) Lapilli-Tuff Division	0.25-17	Upper and lower contacts are planar; contacts are sharp where overlain by an upper tuff division, but are gradational where upper tuff division is absent and the lapilli-tuff is overlain by the next lapilli-tuff division; vitric felsic fragments are normally graded, with respect to abundance and to a lesser extent size, or less commonly are ungraded; pumice was not identified in all flow units, but where identified it is reversely graded with respect to abundance and to a lesser extent size or less commonly is ungraded; internal grading of crystals was not observed.	0-3	3-100	angular to subrounded	dacite fragments	pg	2-12	0.2-1.7 *(0.69)	broken, subhedral to anhedral and less commonly unbroken, euhedral	55-85%, 0.005-0.05 mm, largely granoblastic aggregate composed of pg-qtz-ser-carb-bio-hem-pyrr-micro; qtz, pg, carb, micro, and pyrr are granoblastic; ser, bio, and hem are aligned
			0-35	5-220	thin, elongate, collapsed	pumice	qtz	0-2	0.2-0.7 *(0.36)	broken, subhedral to anhedral and less commonly unbroken, euhedral	
			2-20	5-180	angular to rounded or thin, elongate	vitric felsic fragments	micro	0-5	0.2-0.5 **	broken, anhedral to subhedral and less commonly unbroken, subhedral	
			0-2	1-5	subangular	mafic scoria					
			0-2	3-25	subrounded	microcline-phyric felsic fragments					
Lower Ignimbrite (Member 1) Lapilli-Tuff Division	2.6-7	Upper contacts are planar and sharp; lower contacts are sharp and planar to locally scoured; dacite fragments are normally graded with respect to abundance and to a lesser extent size; pumice was not identified in all flow units, but where identified, it is reversely graded with respect to abundance, but not size; internal grading of crystals was not observed.	2-40	2-40	angular to subrounded	dacite fragments	pg	3-15	0.2-3.1 *(1.07)	broken, subhedral to anhedral and less commonly unbroken, euhedral to subhedral	56-85%, 0.005-0.1 mm largely granoblastic aggregate composed of pg-qtz-ser-carb-bio-hem-pyrr-tour; qtz, pg, carb, and pyrr are granoblastic; ser, bio, and hem are aligned
			0-7	5-66	thin, elongate, collapsed	pumice			*** (4)		
			0-3	2-40	thin, elongate or subangular to rounded	vitric felsic fragments	qtz	1-5	0.2-1.3 *(0.54)	broken, subhedral to anhedral and less commonly unbroken euhedral; local embayments	

Abbreviations

pg	plagioclase	carb	carbonate	* Average maximum crystal size is the average length of 5 to 10 of the largest, apparently unbroken crystals
qtz	quartz	micro	microcline	** Insufficient data to calculate average maximum crystal size
ser	sericite	pyrr	pyrrhotite	*** Average plagioclase/quartz ratio
bio	biotite	tour	tourmaline	**** See Table 6 for descriptions
hem	hematite			***** Minerals are listed in decreasing order of abundance

For example, in flow unit 7a (Fig. 15), vitric felsic fragment abundance decreases from 20% at the base of the lapilli-tuff to 5% at the top over a distance of 1.1 m, whereas average fragment size decreases from 3.8 cm at the base to 1.5 cm at the top. In the same unit, pumice abundance increases from 2% at the base of the lapilli-tuff to 35% at the top and average pumice size increases from 0.8 cm at the base to 1.8 cm at the top. In flow unit 6a, the pumice and vitric felsic fragments are graded only in the upper part (Fig. 15). In flow units 9a, 10a, 11a, 12a, and 5b (Fig. 15), where pumice is apparently absent, vitric felsic fragments are normally graded in abundance, but are poorly size graded. In flow units 1a, 4a, and 1b, pumice and sparse vitric felsic fragments are less than 0.5 cm long and are evenly distributed through the lapilli-tuff division.

Crystal particles are most abundant in flow units 1a and 1b (Fig. 15), where they form about 10% of the division and are evenly distributed. In other lapilli-tuff divisions, the crystal particle content is generally less than 5% and crystals appear to be evenly distributed through divisions. Microcline-phyric felsic fragments and microcline crystals were found only in the lapilli-tuff division of flow unit 5b. However, the presence of microcline in lapilli-tuff divisions of flow units 11a and 12a, which was confirmed by x-ray diffraction analysis, suggests that microcline-phyric

felsic fragments and microcline crystals may also be present here.

### 5.2.2 Upper Tuff Division

The upper tuff division comprises 0 to 90% of flow units and ranges in thickness from 0.02 to 4.5 m. Upper and lower contacts of the tuff division are always sharp and planar. The tuff consists of 0 to 30% pumice, 0 to 1% vitric felsic fragments, 0 to 1% microcline-phyric felsic fragments, 1 to 10% crystal particles and 70 to 99% fine-grained, quartzo-feldspathic aggregate inferred to have replaced vitric ash (Table 8).

Three types of tuff division have been distinguished on the basis of bedding and grading characteristics: (1) bedded tuff (2) bedded pumiceous tuff, and (3) massive tuff (Table 8). Bedded tuff divisions occur in the upper parts of the northwest and southeast sections (Fig. 15). These tuff divisions consist of multiple, or less commonly, single normally graded beds that range in thickness from 0.1 to 24 cm, although most are less than 1 cm thick. Within bed sets, all beds are normally graded, but an overall upward fining or thinning of beds was not observed. The beds have sharp and planar contacts and consist of a lower part composed of 5 to 10%, 0.2 to 1 mm long, crystal particles, rare, 2 to 7 mm long, vitric felsic fragments, and rare, 5 to 20 mm long microcline-phyric felsic fragments in a fine-grained,

Table 8 Internal Characteristics of the Upper Tuff Division

Member and Division Type	Thickness (m)	Internal Features	*** Recognizable Fragments				Crystal Particles			**** Granoblastic Matrix	
			%	Size (mm)	Shape	Type	Type	%	Size (mm)		Shape
Upper Ignimbrite (Member 7)											
1. Bedded Tuff	0.02-2.8	Consists of multiple or less commonly single 1 to 240 mm thick normally graded beds; bed contacts are sharp and planar; in each bed, crystal abundance and size decreases upwards to a locally laminated, fine-grained aggregate composed largely of sericite; division contacts are sharp and planar.	0-1	2-7	lenticular	vitric felsic fragments	pg	1-10	0.2-1 *(0.60)	broken, subhedral to anhedral and less commonly unbroken, subhedral	88-99%, 0.005-0.05 mm largely granoblastic aggregate composed of pg-qtz-ser-carb-bio-hem-pyrr-micro; qtz, pg, micro, and pyrr are granoblastic; ser, bio, and hem are aligned
			0-1	5-20	subrounded	microcline-phyric felsic fragments	qtz	0-1	0.2-0.4 *(0.25)	broken, subhedral to anhedral and less commonly un-	
2. Bedded Pumiceous Tuff	0.44-4.5	Consists of alternating, 0.3 to 10 cm thick, pumice-rich beds and 1 to 29 cm thick, pumice-poor bed sets; bed contacts are planar and sharp; pumice-rich beds are ungraded whereas pumice-poor bed sets consist of multiple, 0.5 to 5 cm thick, graded to locally laminated beds; division contacts are sharp and planar.	0-30	5-65	thin, elongate, collapsed	pumice	pg	1-2	0.1-1.5 *(0.43)	broken, subhedral to anhedral and less commonly unbroken, euhedral to subhedral	70-99%, 0.005-0.05 mm largely granoblastic aggregate composed of pg-qtz-ser-carb-bio-hem-pyrr; qtz, pg, carb, and pyrr are granoblastic; ser, bio, and hem are aligned
			0-1	0.5-60	lenticular	vitric felsic fragments	qtz	0-1	0.2-0.4	broken, subhedral to anhedral and less commonly unbroken, euhedral	
3. Massive Tuff	0.3-3.3	Apparently structureless; faint laminations in the upper part of some divisions; division contacts are sharp and planar.	----- No Data Available -----								
Lower Ignimbrite (Member 1)											
Bedded Tuff	0.5-2.5	Consists of multiple, 1 to 50 mm thick, normally graded beds; bed contacts are sharp and planar; in each bed, crystal abundance and size decreases upwards to a locally laminated, fine-grained, aggregate composed largely of sericite; division contacts are sharp and planar to locally scoured.	0-1	5-8	lenticular	vitric felsic fragments	pg	0-3	0.2-0.7 *(0.42)	broken, subhedral to anhedral and less commonly unbroken, subhedral	94-99%, 0.005-0.1 mm largely granoblastic aggregate composed of pg-qtz-ser-carb-bio-hem-pyrr-tour; qtz, pg, carb, and pyrr are granoblastic; ser, bio, and hem are aligned
						qtz	0-2	0.2-0.5 *(0.34)	broken, subhedral to anhedral and less commonly unbroken, euhedral		

Abbreviations

pg	plagioclase	carb	carbonate	* Average maximum crystal size
qtz	quartz	micro	microcline	** Insufficient data to calculate maximum average crystal size
ser	sericite	pyrr	pyrrhotite	*** See Table 6 for descriptions
bio	biotite	tour	tourmaline	**** Minerals are listed in decreasing order of abundance
hem	hematite			

largely granoblastic aggregate. This grades upwards to a fine-grained, foliated aggregate composed largely of sericite with 0 to 1%, 0.1 to 0.2 mm long, crystal particles; vitric felsic fragments or microcline-phyric felsic fragments were not recognized. Dark grey laminations composed of sericite, biotite, and Fe-oxide occur in the upper parts of many beds. Plagioclase and quartz crystal particles occur in every graded bed, but microcline crystal particles were found only in tuff of flow unit 11a (Fig. 15). In the same flow unit, microcline-phyric felsic volcanic fragments were found locally at the bases of some tuff beds. The presence of microcline in the granoblastic matrix of tuff divisions in flow units 12a and 5b was confirmed by x-ray diffraction analysis.

Bedded pumiceous tuff divisions occur in the central part of the southeast section and upper part of the northwest section (Fig. 15). The tuff divisions consist of alternating pumice-rich beds and pumice-poor bed sets. The pumice-poor bed sets range in thickness from 1 to 29 cm, although most are less than 10 cm thick. Beds in the pumice-poor bed sets have similar bed characteristics as beds in the bedded tuff divisions, although maximum bed thickness is 5 cm and beds are thus thinner (Table 8). The pumice-rich beds occur at random stratigraphic levels within the pumice-poor bed sets and have sharp and planar contacts. The beds range in thickness from 0.3 to 10 cm, although most are less than 5



cm thick. In some beds, the reddish-brown pumice fragments are clearly visible (Fig. 16), whereas in thinner beds the fragments have been amalgamated through recrystallization and are not discernible (Fig. 17). The pumice-rich beds appear to have a higher crystal content than the pumice-poor beds, but this is due to the presence of plagioclase phenocrysts in the pumice (Fig. 16). Grading was not observed in any of the pumice-rich beds.

Massive tuff divisions were observed only in the lower part of the southeast section (Fig. 15). On outcrop surface the tuff divisions are brownish-grey, very fine-grained, and have no visible fragments or crystals. The tuff divisions have sharp and planar contacts and are essentially structureless with the exception of faint laminations that were observed in the upper meter of the tuff division in flow unit 1a.



Figure 16: Photograph of a pumice-rich bed in the bedded pumiceous tuff division of flow unit 4a in the upper ignimbrite. Note the abundance of white plagioclase phenocrysts in pumice fragments. Lens cap for scale is 5.5 cm in diameter.



Figure 17: Photograph showing faint bedding in the bedded pumiceous tuff division of flow unit 3a in the upper ignimbrite (Member 7). Brownish grey pumiceous beds contain more sericite and biotite than light grey beds which are composed largely of quartz and plagioclase. Note the sharp lower contact with the underlying lapilli-tuff division near the bottom of the figure. Lens cap for scale is 5.5 cm in diameter.

### 5.3 DESCRIPTION OF THE LOWER IGNIMBRITE (MEMBER 1)

The lower ignimbrite comprises 9% of the Manigotagan River Formation and ranges in thickness from 6 to 39 m. Where observed, its upper contact with reworked pyroclastic rocks of Member 2 is sharp and concordant. In places, a fractured zone with a breccia-like appearance occurs immediately below the contact (Plate 1). Where best exposed, the fractured zone is at least 2 m wide, and consists of 30 to 40%, variably oriented, quartz-filled fractures in a thin-bedded tuff host. This fracture zone may signify the presence of a fault below the upper contact. The lower contact with a younger gabbro intrusion is concordant and is sharp to locally sheared.

In comparison to the upper ignimbrite, the lower ignimbrite is thinner and consists of thicker, but apparently fewer flow units. (Table 5). Two partial sections, measured in the central and northwestern areas, cover about 55% of the member thickness, and reveal the presence of at least 3 flow units (Fig. 18). Additional flow units are probably hidden under the overburden cover. Flow units can be traced laterally, with little change in thickness, for up to 15 m on outcrop, but the paucity of outcrop precludes the correlation of flow units from outcrop to outcrop, and documentation of any lateral variations.

### 5.3.1 Lower Lapilli-tuff Division

Lapilli-tuff constitutes 52 to 93% of flow units and ranges in thickness from 2.6 to 7 m. The divisions are poorly sorted and lack stratification. Upper and lower bed contacts are typically planar and sharp, but shallow scours were observed locally at the base of some units. The scours penetrate as much as 15 cm into the underlying tuff division and truncate bedding in the tuff. In one scour, at the base of flow unit 2a (Fig. 18), a 20 cm long, subangular, tuff fragment was observed in lapilli-tuff immediately above the base of the scour (Fig. 19); it probably represents a rip-up from the underlying tuff division.

In contrast to the upper ignimbrite, lapilli-tuff divisions in the lower ignimbrite contain more plagioclase and quartz crystals, more dacite fragments, but fewer vitric felsic fragments and pumice; in addition, dacite fragments, vitric felsic fragments, and pumice are smaller, crystals are larger, and mafic scoria, microcline-phyric felsic fragments, and microcline crystals are apparently absent (Table 7). As in the upper ignimbrite, lapilli-tuff shows an internal grading of fragments, but not crystal particles. Dacite fragments are most abundant at the base of lapilli-tuff divisions, and show a distinct upward decrease in abundance and size within divisions. Where pumice was observed, its distribution is the reverse of that shown by dacite fragments, but it is only graded with respect to

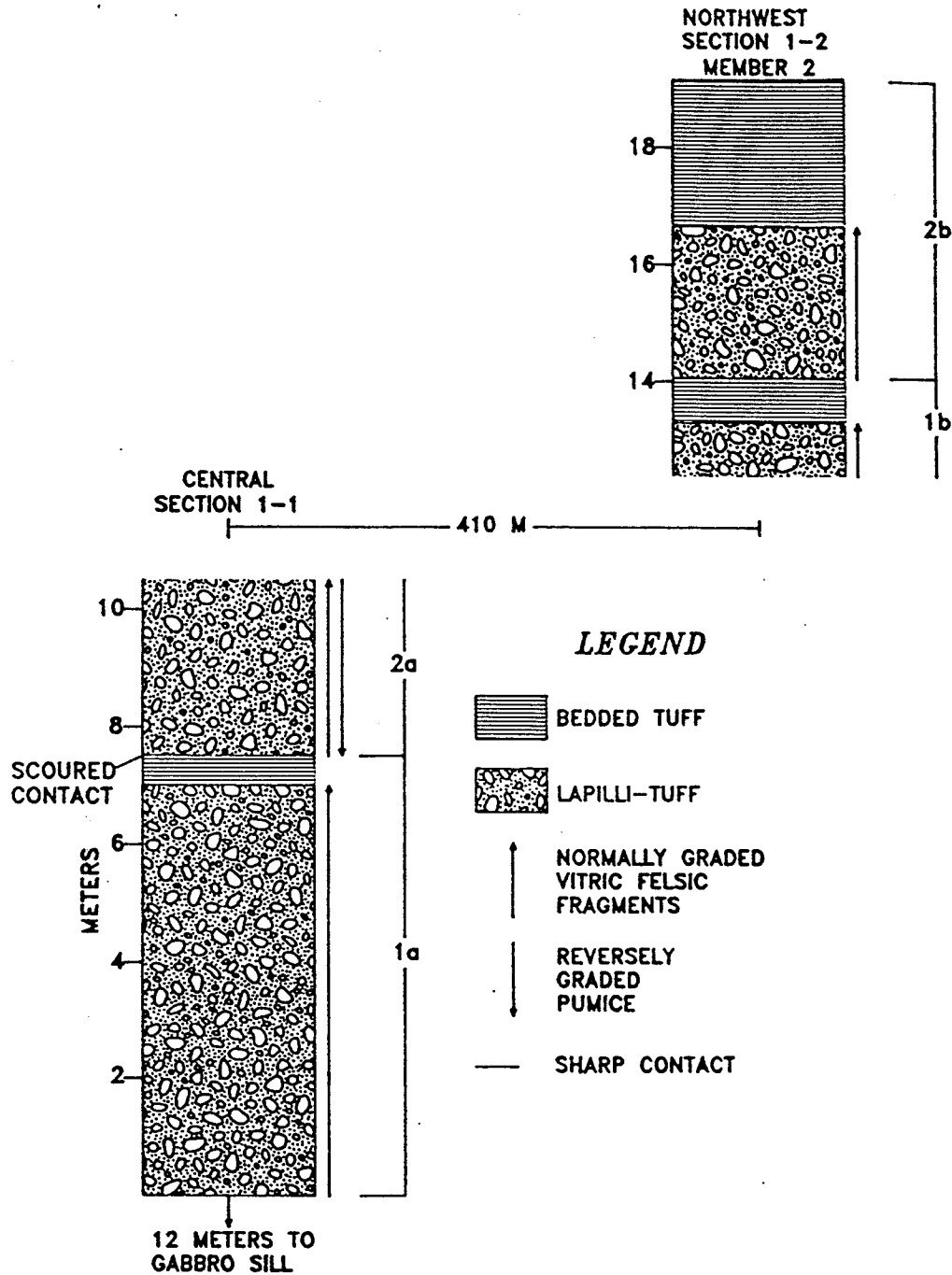


Figure 18: Partial stratigraphic sections (1-1, 1-2) through the lower ignimbrite (Member 1).



Figure 19: Photograph depicting a scour into the tuff division of flow unit 1a at the base of the lapilli-tuff division of flow unit 2a in the lower ignimbrite (Member 1). Note the angular, tuff rip-up (grey-brown area above lens cap) immediately above the scour. Lens cap for scale is 5.5 cm in diameter.

abundance, and not size. For example, in lapilli-tuff of flow unit 2a (Fig. 18), the top of which is not exposed, dacite fragment abundance decreases from 20% at the base of the lapilli-tuff to 5% at the edge of the outcrop over a distance of 2.5 m and average fragment size decreases from 2.8 cm at the base to 1.5 cm at the top. In the same unit, pumice abundance increases from 1% at the base of the lapilli-tuff to 7% at the edge of the outcrop with no significant change in pumice size.

### 5.3.2 Upper Tuff Division

The upper tuff division comprises 7 to 48% of flow units and ranges in thickness from 0.5 to 2.5 m. Its lower contact is always planar and sharp, whereas its upper contact with lapilli-tuff of the overlying flow unit is sharp and planar to locally scoured. The tuff divisions consist of 0 to 1% vitric felsic fragments, 0 to 5% crystal particles and 94 to 99%, fine-grained, quartzo-feldspathic aggregate inferred to have replaced vitric ash (Table 8).

These divisions consist of multiple, 0.1 to 5 cm thick, normally graded beds which typically thin upwards. The beds consist of a lower part composed of 2 to 5%, 0.2 to 0.7 mm long, crystal particles and 0 to 1%, 5 to 8 mm long vitric felsic fragments in a fine-grained, largely granoblastic, quartzo-feldspathic aggregate; this grades upwards to a fine-grained, foliated aggregate composed largely of



sericite with no recognizable crystal particles or vitric felsic fragments. In places, a laminated division was observed in the upper parts of graded beds. In flow unit 1a, interlaminated, but ungraded, light grey and dark grey tuff occurs at the top of a 1.1 cm thick graded bed in the central part of the tuff division (Fig. 20). The grading characteristics of the tuff divisions are similar to bedded tuff divisions in the upper ignimbrite, but beds are thinner and microcline-phyric felsic fragments and microcline crystal particles are absent (Table 8).



Figure 20: Photograph of multiple, light brown to brownish grey, normally graded beds in flow unit 1a in the lower ignimbrite (Member 1). Note the presence of inter-laminated, light grey and dark grey tuff at the top of the graded bed in the central part of the figure. Lens cap for scale is 5.5 cm in diameter.

## Chapter VI

### SUBAQUEOUS TEPHRA-FALL DEPOSITS

Lapilli-tuff and tuff that are interpreted to be tephra-fall deposits are assigned to Member 2 and comprise 20% of the Manigotagan River Formation. The deposit is variable in composition, ranging from mafic to intermediate and it ranges in thickness from 17 to 91 m; it thins to the northwest. Where observed, its lower contact with ignimbrite (Member 1) is sharp and concordant (Plate 1). The deposit is overlain with a sharp and concordant contact by interlayered volcanic sandstone and mafic lava flows (Member 3). In places, the upper surface is hummocky, particularly in the northwest, where there is as much as 10 m relief on the contact (Plate 1).

The member has been divided into three compositionally distinct, laterally continuous, blanket-like units (Plate 1), which, in ascending order, are:

1. mafic to intermediate lapilli-tuff and tuff (2a),
2. mafic lapilli-tuff and tuff (2b), and
3. mafic to intermediate lapilli-tuff and tuff (2c).

All three units are best exposed in the northwestern part of the area, where a continuous section was measured through

each unit (Plate 1). The following unit descriptions are based largely on this section, supplemented by data from other outcrops. More data were collected from unit 2b and, thus, it will be described in more detail than units 2a or 2c.

## 6.1 MAFIC TO INTERMEDIATE LAPILLI-TUFF AND TUFF

Mafic to intermediate lapilli-tuff and tuff comprise the lower part of Member 2 (2a) and range in thickness from 10 to 26 m. Volcanic conglomerate and sandstone are a minor component and occur locally at the base of the unit (Fig. 21). The unit can be traced laterally throughout the map-area and thins to the northwest. Its lower contact with ignimbrite of Member 1 is sharp and planar to locally irregular; it is gradationally overlain by mafic lapilli-tuff and tuff of unit 2b (Fig. 21).

### 6.1.1 Components Comprising the Lapilli-Tuff and Tuff

The lapilli-tuff and tuff consist of variable proportions of recognizable felsic to mafic fragments and quartz crystal particles enclosed in a fine-grained, foliated aggregate composed mainly of subequal amounts of chlorite and quartz. The most abundant recognizable fragments are thin, elongate to equant, poorly to highly amygdaloidal, lapilli to block-sized, felsic volcanic fragments (Tables 9, 10). On outcrop surface, the less deformed fragments contain 10 to 50%

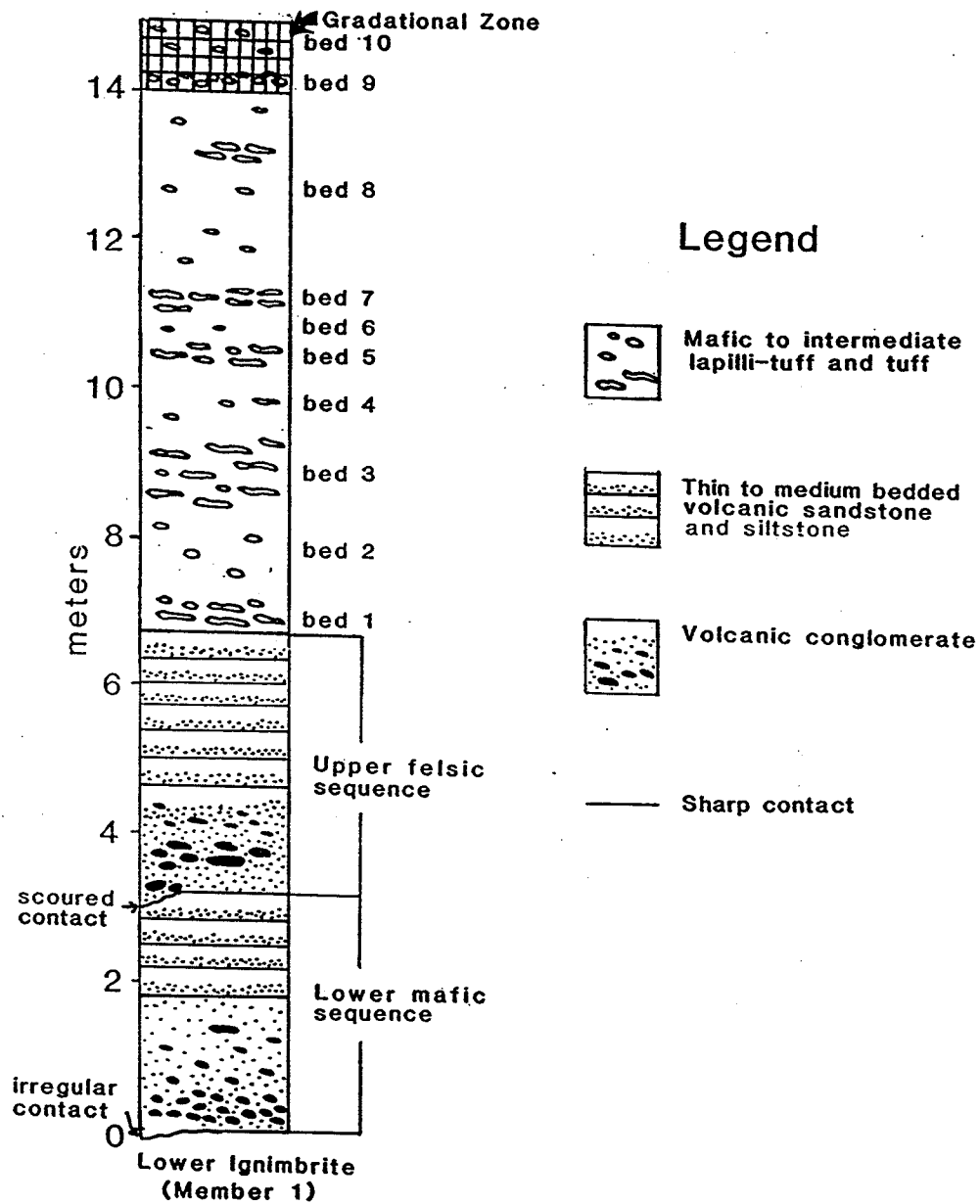


Figure 21: Stratigraphic section 2a-1 through mafic to intermediate lapilli-tuff and tuff and mafic and felsic volcanic conglomerate and sandstone of Unit 2a

**Table 9 Compositional and Textural Features of Fragments from Lapilli-Tuff and Tuff of Member 2**  
(see Table 10 for data on abundances, sizes, and shapes of fragments)

Unit	Fragment Type	Amygdules				Phenocrysts				Groundmass*
		Type	%	Size (mm)	Shape	Type	%	Size (mm)	Shape	
Mafic to Intermediate Lapilli-Tuff and Tuff (2c)	Vesicular Microlitic Mafic Fragments	carb qtz	5-70	0.1-0.5	circular or elliptical	pg	0-2	0.3-0.7	euohedral to subhedral	1-5%, 0.1-0.2 mm pg microlites in a 0.005-0.1 mm granoblastic aggregate composed of hem-chl-pg-qtz-carb-bio-pyrr
	Non-vesicular Microlitic Mafic Fragments		none recognized			pg	0-5	0.2-0.5	euohedral to subhedral	2-15%, 0.05-0.2 mm pg microlites in a 0.005-0.05 mm foliated aggregate composed of chl-hem-pg-epd-bio-carb-pyrr
	Porphyritic Felsic Fragments		none recognized			pg	0-10	0.2-2	euohedral to subhedral	0.005-0.05 mm granoblastic aggregate composed of pg-qtz-carb-chl-pyrr
Mafic Lapilli-Tuff and Tuff (2b)	Rimmed, Vesicular, Microlitic Mafic Fragments (Type 1)	qtz,pg	15-70	0.1-7 (core)	circular, elliptical, or less commonly amoeboid	pg	0-3	0.3-1	euohedral to subhedral	Core: 5-30%, 0.1-0.3 mm pg microlites in a 0.005-0.01 mm granoblastic aggregate composed of hem-pg-chl-bio-epd Rim: 0.005-0.05 mm foliated aggregate composed of chl-hem-act-epd
		pg,qtz	2-10	0.1-1 (rim)		act (after cpx)	0-2	0.3-5.5		
	Partly Rimmed, Vesicular, Microlitic Mafic Fragments (Type 2)	pg,qtz	2-20	0.1-1.5 (core)	elliptical, circular, or less commonly amoeboid	pg	0-2	0.3-1	euohedral to subhedral	Core: 0-5%, 0.1-0.2 mm pg microlites in a 0.005-0.05 mm foliated aggregate composed of chl-hem-pg-act-epd Partial Rim: 0.005-0.2 mm largely granoblastic aggregate composed of pg-hem-chl-act-bio-epd-carb-qtz-pyrr; pg, qtz, carb, epd, and pyrr are granoblastic; hem, chl, act, and bio, are aligned
		pg	2-10	0.1-1.7 (partial rim)	elliptical, or less commonly circular or amoeboid					
	Non-vesicular Microlitic Mafic Fragments (Type 3)		none recognized			pg	0-2	0.3-0.7	subhedral	0-5%, 0.1-0.2 mm pg microlites in a 0.005-0.05 mm foliated aggregate composed of chl-hem-pg-act-epd

Table 9 Continued

Unit	Fragment Type	Amygdules			Phenocrysts				Groundmass *	
		Type	%	Size (mm)	Shape	Type	%	Size (mm)		Shape
Mafic to Intermediate Lapilli-Tuff and Tuff (2a)	Vesicular Felsic Fragments	carb	10-50	0.2-3.5	circular or elliptical			none recognized	0.005-0.05 mm granoblastic aggregate composed of qtz-pg-carb-hem-bio-chl	
	Non-vesicular Microlitic Mafic Fragments			none recognized		pg	0-3	0.4-1.1	euhedral	5-10%, 0.05-0.2 mm pg microlites in a 0.005-0.05 mm granoblastic aggregate composed of hem-chl-carb-qtz-pg-pyrr
	Non-vesicular Felsic Fragments			none recognized		pg	0-2	0.1-0.5	euhedral	0.005-0.05 mm granoblastic aggregate composed of qtz-pg-chl-bio-carb
	Vesicular Microlitic Intermediate Fragments	carb	10-40	0.3-2.5	circular or elliptical	pg	0-2	0.5-1	euhedral to subhedral	15%, 0.05-0.03 mm pg microlites in a 0.005-0.01 mm granoblastic aggregate composed of pg-chl-hem-bio-pyrr

## Abbreviations

\* Minerals are listed in decreasing order of abundance

pg	plagioclase	act	actinolite
qtz	quartz	cpx	clinopyroxene
chl	chlorite	carb	carbonate
hem	hematite	bio	biotite
epd	epidote	pyrr	pyrrhotite

**Table 10 Internal Characteristics of Tephra-Fall and Channel-Fill Deposits of Member 2**

Unit	Thick-ness (m)	Contacts		Internal Features	* Recognizable Fragments			Crystal Particles			** Matrix		
		Upper	Lower		X	Size (mm)	Shape	Type	X	Size (mm)		Shape	
Mafic to Intermediate Lapilli-Tuff and Tuff (2c)	0-20	sharp	sharp	consists of multiple, 20-400 cm thick beds which show bed to bed variations in fragment abundance and fragment size; beds are ungraded and contacts are gradational rather than sharp, but the transition from one bed to the next normally occurs within a vertical distance of less than 5 cm; locally, in the upper 1 to 2 m of the unit, there are 30 to 50 cm thick felsic tuff interbeds.	0-15	10-50	thin, elongate, or subangular	vesicular mafic fragments	pg	2-7	0.1-1	broken, sub-hedral to anhedral or less commonly unbroken, eu-hedral	75-95%, 0.005-0.05 mm foliated aggregate composed of chl-qtz-pg-hem-bio-epd-act-pyrr
					1-15	5-20	thin, elongate, or angular	non-vesicular mafic fragments	qtz	0-3	0.1-0.7	broken, sub-hedral to anhedral; local embayments	
					0-15	2-20	angular to subrounded	porphyritic felsic fragments					
Mafic Lapilli-Tuff and Tuff (2b)	12-64	sharp	gradational	consists of multiple, 5-250 cm thick beds which show bed to bed variations in fragment abundance and fragment size; bed are ungraded and contacts are gradational rather than sharp, but the transition from one bed to the next normally occurs within a vertical distance of 1 to 5 cm.	1-35	10-340	subangular to rounded or thin, elongate	vesicular mafic fragments (type 1)	pg	0-3	0.1-1	broken, sub-hedral to anhedral or less commonly unbroken, eu-hedral	35-92%, 0.005-0.2 mm largely granoblastic aggregate composed of pg-hem-chl-act-bio-epd-carb-qtz-pyrr; pg, qtz, carb, epd, and pyrr are granoblastic; hem, chl, act, and bio are aligned
					1-20	3-80	thin, elongate or subangular	vesicular mafic fragments (type 2)	act (after cpx)	0-2	0.2-1	unbroken, eu-hedral to sub-hedral	
					1-7	1-20	elongate to oval	non-vesicular mafic fragments (type 3)					
Mafic to Intermediate Lapilli-Tuff and Tuff (2a)	8.3-26	gradational	sharp	consists of multiple, 20-270 cm thick beds which show bed to bed variations in fragment abundance and fragment size; beds are ungraded and contacts are gradational rather than sharp, but the transition from one bed to the next normally occurs within a vertical distance of 2 to 5 cm.	5-30	10-460	thin, elongate, or angular to subrounded	vesicular felsic fragments	qtz	0-2	0.2-0.5	broken, sub-hedral to anhedral	65-94%, 0.005-0.05 mm foliated aggregate composed of chl-qtz-pg-carb-hem-bio-ser-pyrr
					1-10	5-30	thin, elongate, or subangular	non-vesicular mafic fragments					
					0-2	10-100	thin, elongate	non-vesicular felsic fragments					
Felsic Turbiditic Sequence	0-3.5	sharp	scoured	consists of a single, 140 cm thick, normally graded volcanic conglomerate bed which is overlain by a succession of 15 to 63 cm thick, normally graded volcanic sandstone beds; bed contacts are sharp and planar to locally scoured.	2-30	5-1270	thin, elongate, or subangular to rounded	non-vesicular felsic fragments	pg	1-8	0.1-0.7	broken, sub-hedral to anhedral or less commonly unbroken, eu-hedral	66-94%, 0.005-0.05 mm largely foliated aggregate composed of ser-qtz-pg-carb-bio-pyrr
					0-10	30-220	subrounded to well rounded	vesicular intermediate fragments	qtz	3-5	0.2-0.8	broken, sub-hedral to anhedral; local embayments	
Mafic Turbiditic Sequence	0-3.25	sharp	irregular scoured?	consists of a single, 180 cm thick, normally graded volcanic conglomerate bed which is overlain by a succession of 1 to 12 cm thick, normally graded volcanic sandstone beds; bed contacts are sharp and planar to locally irregular.	2-15	5-60	thin, elongate, or subrounded	non-vesicular mafic fragments	pg	1-3	0.2-0.5	broken, sub-hedral to anhedral	80-96%, 0.005-0.1 mm foliated aggregate composed of chl-qtz-pg-carb-bio-pyrr
					1-3	1-60	thin, elongate, or subrounded	non-vesicular felsic fragments	qtz	0-3	0.2-0.3	broken, sub-hedral to anhedral	

\*\* Minerals are listed in decreasing order of abundance

Abbreviations		* See Table 9 for descriptions	
pg	plagioclase	act	actinolite
qtz	quartz	cpx	clinopyroxene
chl	chlorite	hem	hematite
ser	sericite	carb	carbonate
		bio	biotite
		epd	epidote
		pyrr	pyrrhotite



vesicles that are filled with carbonate (Fig. 22). Amygdules are enclosed in a uniform, fine-grained, quartzo-feldspathic aggregate that may have originally been vitric.

Less abundant fragment types identified in the unit include non-vesicular, microlitic, mafic lapilli and sparse, non-vesicular, felsic lapilli and blocks; both fragment types are plagioclase-phyric. Free quartz crystals were locally observed in the unit, but free plagioclase crystals were not observed. Recognizable fragments and crystal particles are enclosed in a texturally and mineralogically uniform, fine-grained, foliated aggregate, which is the dominant component of the lapilli-tuff and tuff (Table 10). It is composed largely of chlorite and quartz with lesser plagioclase and carbonate (Table 10). Although totally recrystallized, the aggregate probably represents the original matrix, and, because of its present composition and uniform texture, it may have originally been mafic and vitric.

Felsic and many mafic fragments can be distinguished from the surrounding foliated aggregate by sharp boundaries and textural and mineralogical differences. Felsic fragments are granoblastic and contain more quartz than the surrounding aggregate (cf. Tables 9, 10). Mafic fragments contain plagioclase microlites and more hematite than the surrounding aggregate (cf. Tables 9, 10). In places, however, mafic fragments are more obscure and are



Figure 22: Photograph of a subangular, felsic volcanic fragment (pale grey) in lower unit (2a) of Member 2, showing preservation of original vesicularity. The dark green aggregate surrounding fragments is largely recrystallized but probably mimics the original matrix, which may have originally been vitric. Lens cap for scale is 5.5 cm in diameter.

represented by 2 to 10 mm long, lenticular patches that comprise 0 to 5% of the lapilli-tuff and tuff. These patches are mineralogically similar to the enclosing foliated matrix, but differ by the presence of 5 to 10%, 0.1 to 0.2 mm long, euhedral, randomly oriented, plagioclase microlites and 0 to 3%, 0.3 to 0.7 mm long, euhedral, plagioclase crystals. Because of the mineralogical similarity of these fragments and the matrix, particle boundaries are diffuse. They probably represent aphyric to plagioclase-phyric mafic fragments whose boundaries have been obscured by recrystallization. The matrix abundance given in Table 10 is a maximum value because these poorly defined, microlitic fragments have been included in the total matrix abundance.

#### 6.1.2 Bedding Characteristics

On outcrops, the mafic to intermediate lapilli-tuff and tuff is stratified, consisting of multiple, poorly sorted, 20 to 270 cm thick beds defined by variations in fragment abundance and fragment size; fragment-rich beds normally alternate with fragment-poor beds (Fig. 21). Bed contacts are gradational rather than sharp, but the transition from one bed to the next normally occurs within a vertical distance of 2 to 5 cm. Individual beds maintain a constant thickness across outcrops for up to 10 m, but they cannot be correlated between outcrops with confidence, and, thus, their lateral continuity is unknown.

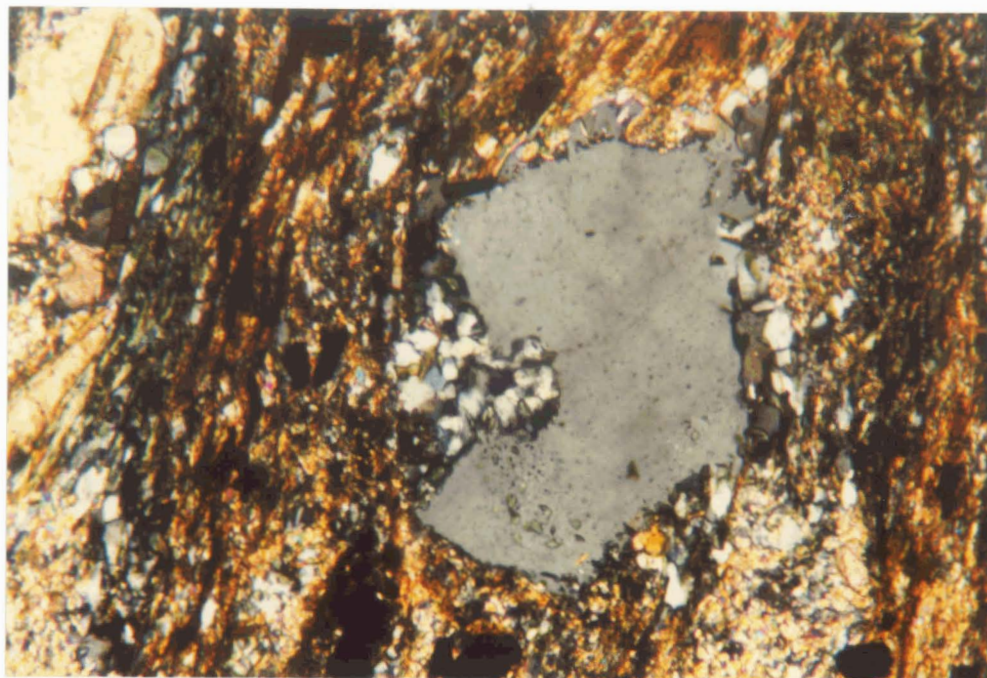
The fragment-rich beds contain 20 to 30%, 0.5 to 46 cm long fragments, whereas fragment-poor beds contain 5 to 10%, 0.5 to 10 cm long fragments. In some fragment-poor beds, there are isolated, 10 to 30 cm thick, lenticular, fragment-rich zones (Fig. 21). Vertically in the succession, there is no apparent change in the matrix composition or in the size and abundance of crystals. However, the abundance of vesicular felsic fragments decreases upwards and that of both recognizable and poorly defined mafic fragments increases. In the measured section, lapilli-tuff and tuff is underlain by a laterally restricted volcanic conglomerate and sandstone sequence about 7 m thick (Fig. 21). The lapilli-tuff and tuff component here is thus much thinner than elsewhere in the unit where volcanic conglomerate and sandstone are absent, but otherwise it is identical.

## 6.2 MINOR VOLCANIC CONGLOMERATE AND SANDSTONE

Volcanic conglomerate and sandstone sequences were observed only on one outcrop in the northwestern part of the lapilli-tuff unit. At this locality, a lower mafic sequence and an upper felsic sequence comprise about 40% of stratigraphic section 2a-1 (Fig. 21). The sequences are laterally continuous across outcrops for up to 5 m, but cannot be traced to adjacent outcrops. Based on the distances to adjacent outcrops, the sequences have a maximum possible lateral extent of 150 m.

In contrast to the mafic to intermediate lapilli-tuff and tuff, the volcanic conglomerate and sandstone contain vesicular intermediate fragments, lack vesicular felsic fragments, and have a higher abundance of non-vesicular felsic fragments and crystal particles including both quartz and plagioclase (Table 10). In contrast to vesicular felsic fragments in the lapilli-tuff, the intermediate fragments are better rounded, plagioclase-phyric, and slightly less vesicular. In addition, the groundmass of the fragments lacks quartz but contains plagioclase microlites and more chlorite. Non-vesicular felsic fragments occur in both the lower and upper sequences, but are more abundant in the upper (Table 10). Vesicular, intermediate volcanic fragments were observed only in the basal part of the upper sequence. Recognizable, non-vesicular, mafic fragments were observed only in the lower sequence.

Crystal particles are larger and more abundant in the upper sequence than the lower (Table 10). Plagioclase crystals are typically broken or less commonly unbroken, and show evidence of significant abrasion. All quartz crystal particles observed in the lower and upper sequences are broken, but they are not as extensively abraded as coexisting plagioclase crystals. Well preserved embayments were observed in some of the quartz crystals (Fig. 23) implying an original volcanic origin.



0 0.1 0.2 0.3 0.4 0.5 mm

Figure 23: Photomicrograph of a partly hexagonal, embayed quartz crystal (x-polars) from volcanic sandstone of the upper felsic sequence in the lower part of unit 2a. The embayment is filled with quartzo-feldspathic aggregate that probably represents recrystallized juvenile magma from which the crystal was liberated. The foliated aggregate surrounding the crystal is composed largely of sericite, quartz, and plagioclase and, although totally recrystallized, may have originally been felsic vitric ash.

In each sequence, the dominant component is a fine-grained recrystallized aggregate that surrounds recognizable fragments and crystals and probably represents the original matrix (Table 10). In the lower mafic sequence, the aggregate is foliated and is composed of chlorite, quartz and plagioclase in subequal proportions and minor carbonate, biotite, and pyrrhotite. It is texturally similar to the foliated matrix aggregate in the mafic to intermediate lapilli-tuff, and, thus, it may have originally been vitric. In the upper felsic sequence, the aggregate is largely foliated and contains more sericite and quartz than matrix in the lower mafic sequence (Table 10); it may have originally been felsic vitric ash.

In both the mafic and felsic sequences a single, normally graded conglomerate bed is overlain by a thickening upward succession of normally graded sandstone beds (Fig. 21). In the upper felsic sequence, the base of the conglomerate bed appears to be a scour because sandstone beds in the underlying mafic sequence are apparently truncated (Fig. 24). Here, fragments are largest and most abundant immediately above the scour and decrease in size and abundance upwards. To the northwest of the scour, however, the conglomerate appears to show reverse to normal grading (Fig. 21). In the lower mafic sequence, the contact between normally graded conglomerate and underlying ignimbrite is irregular (Fig. 25) and could represent a pre- or



Figure 24: Photograph showing a scour at the base of the conglomerate bed in the upper felsic sequence. Note the truncation of the sandstone bed in the underlying mafic sequence. Lens cap for scale is 5.5 cm in diameter.





Figure 25: Photograph showing the irregular contact between ignimbrite of Member 1 (white) and overlying pebbly sandstone (dark green) of the lower mafic sequence. This could represent a pre- or syndepositional scour or alternatively, a drag fold. Lens cap for scale is 5.5 cm in diameter.

syndepositional scour. Sandstone beds, which overlie the conglomerate in both sequences, have sharp, planar to locally scoured contacts and generally maintain a constant thickness across an outcrop, but some beds pinch out along strike. In the lower mafic sequence, 1 to 2 mm thick, light and dark grey laminae occur in the upper 1 to 2 cm of some of the thicker sandstone beds. The dark grey laminae are composed largely of chlorite whereas the light grey laminae are composed mainly of quartz and plagioclase. An internal grading was not observed in such laminae.

### 6.3 MAFIC LAPILLI-TUFF AND TUFF

Mafic lapilli-tuff and tuff comprise the central part of Member 2 (2b) and range in thickness from 12 to 64 m. The unit is thickest in the central part of the mapped area and thins to the southeast and northwest (Plate 1). The lower contact with mafic to intermediate lapilli-tuff and tuff (2a) is gradational over a distance of about 2 m (Figs. 21, 33). This gradational zone consists of alternating fragment-rich and fragment-poor beds. Within this zone, vesicular felsic fragments decrease in abundance upwards and eventually disappear, whereas the abundance of vesicular mafic fragments increases. In a similar manner, the abundance of chlorite in the matrix decreases upwards, but that of plagioclase and actinolite increases.

In contrast to the underlying mafic to intermediate lapilli-tuff, the mafic lapilli-tuff and tuff is thicker and more mafic; fragments are generally smaller and are all mafic; plagioclase crystal particles are present but quartz crystal particles are apparently absent; plagioclase dominates over chlorite in the matrix; actinolite is present in the matrix (Table 10); and actinolite pseudomorphs after clinopyroxene were identified in both fragments (Table 9) and in the granoblastic aggregate surrounding fragments (Table 10).

### **6.3.1 Components Comprising the Lapilli-Tuff and Tuff**

The lapilli-tuff and tuff are composed of variable proportions of fragments and crystal particles in a fine-grained, largely granoblastic aggregate that presumably represents recrystallized matrix. Mafic fragments comprise 3 to 62% of the unit and range in length from 1 to 340 mm, although most are less than 60 mm long. Fragments were originally angular to rounded, but are now moderately to highly elongate due to tectonic flattening. The larger fragments were more competent and are subequant; most of the smaller fragments are chlorite-rich and more ductile, and they now occur as thin lenticles. Three types of mafic fragments have been recognized based on differences in vesicularity and internal texture (Table 9).

### 6.3.1.1 Rimmed, Vesicular, Microlitic Mafic Fragments (Type 1)

Type 1 mafic fragments are the largest, most abundant, and generally most vesicular fragments in the unit (Tables 9, 10). They consist of an inner, commonly fractured, vesicular, microlitic core, completely or partly surrounded by a less vesicular chloritic rim.

Fragment cores are nearly opaque in plane light and consist of rare plagioclase phenocrysts and poikiloblastic actinolite pseudomorphs after clinopyroxene phenocrysts (Fig. 26) in a groundmass composed largely of randomly oriented, plagioclase microlites and hematite (Table 9, Fig. 27). Fragment core vesicularity ranges from 15 to 70%. Vesicles are circular, elliptical, or less commonly amoeboid and range from 0.1 to 7 mm in diameter or length, although most are 0.1 to 0.5 mm. Vesicles are typically filled with polycrystalline quartz (Fig. 27) or, less commonly, monocrystalline quartz, but locally they are filled by polycrystalline albite (Fig. 28) or polycrystalline quartz plus albite (Fig. 29) aggregates. The plagioclase amygdules consist of multiple, radiating plagioclase laths. In the quartz-plagioclase amygdules, plagioclase laths are intergrown with polycrystalline quartz. In both types of amygdules, plagioclase has been partly replaced by epidote and/or carbonate. Within fragments, there is no change in amygdule abundance, size or shape from the outer to the inner part of the core.

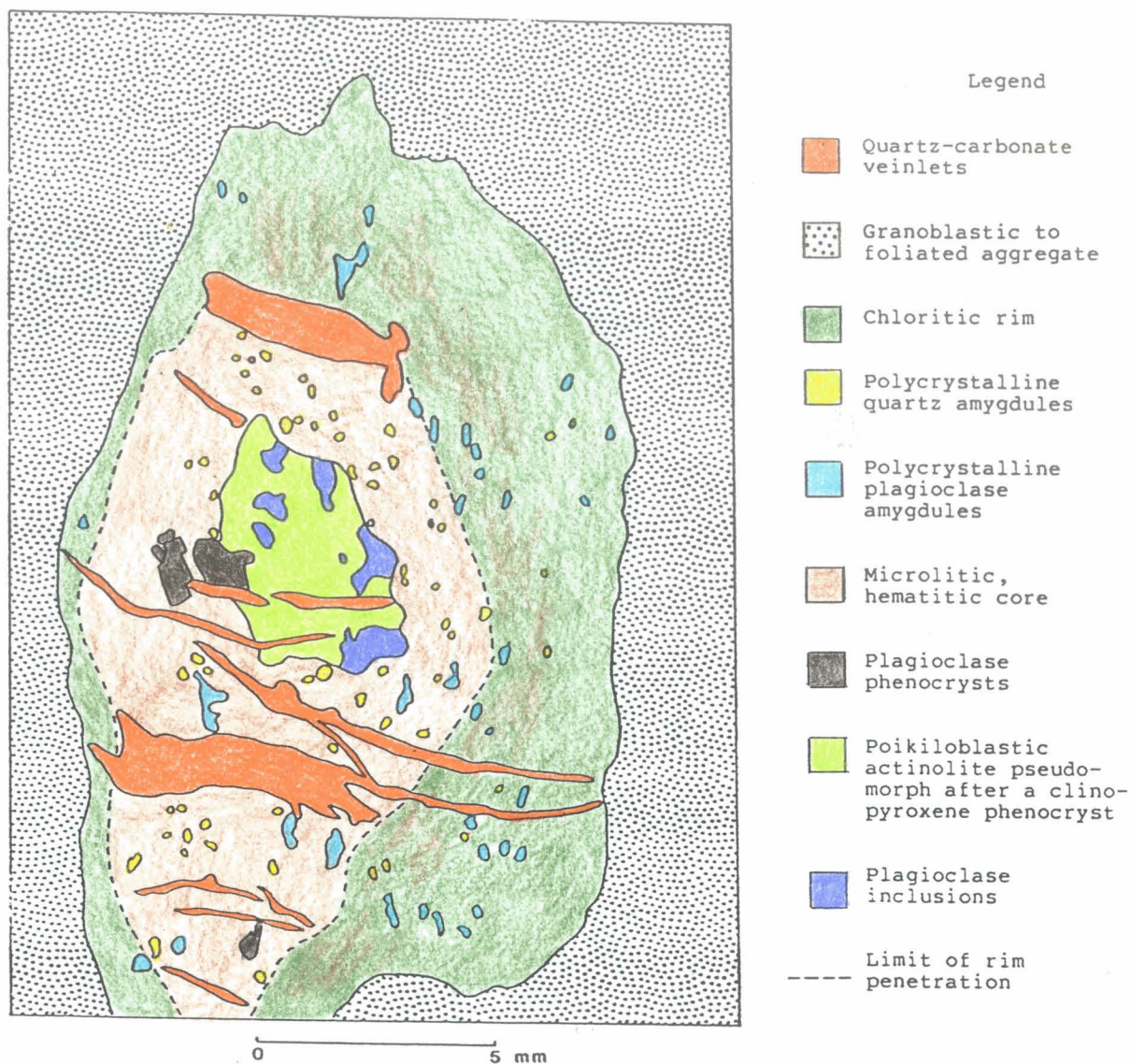


Figure 26: Thin section drawing of a type 1 mafic fragment from mafic lapilli-tuff of unit 2b. The fragment core contains quartz and plagioclase amygdules and consists of plagioclase phenocrysts and rare poikiloblastic actinolite pseudomorphs after clinopyroxene phenocrysts in a microlitic groundmass composed largely of hematite. The core is asymmetrically surrounded by an amygdaloidal rim composed largely of chlorite with lesser hematite, epidote and actinolite. Secondary quartz-carbonate veinlets cross-cut the core and rim, but do not penetrate the surrounding granoblastic aggregate.

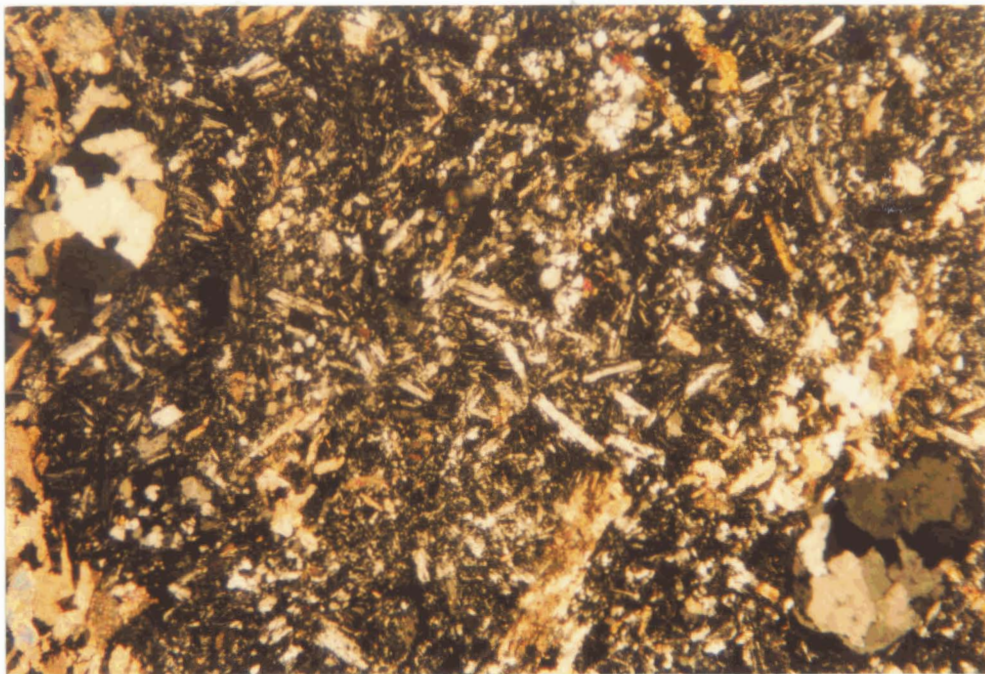
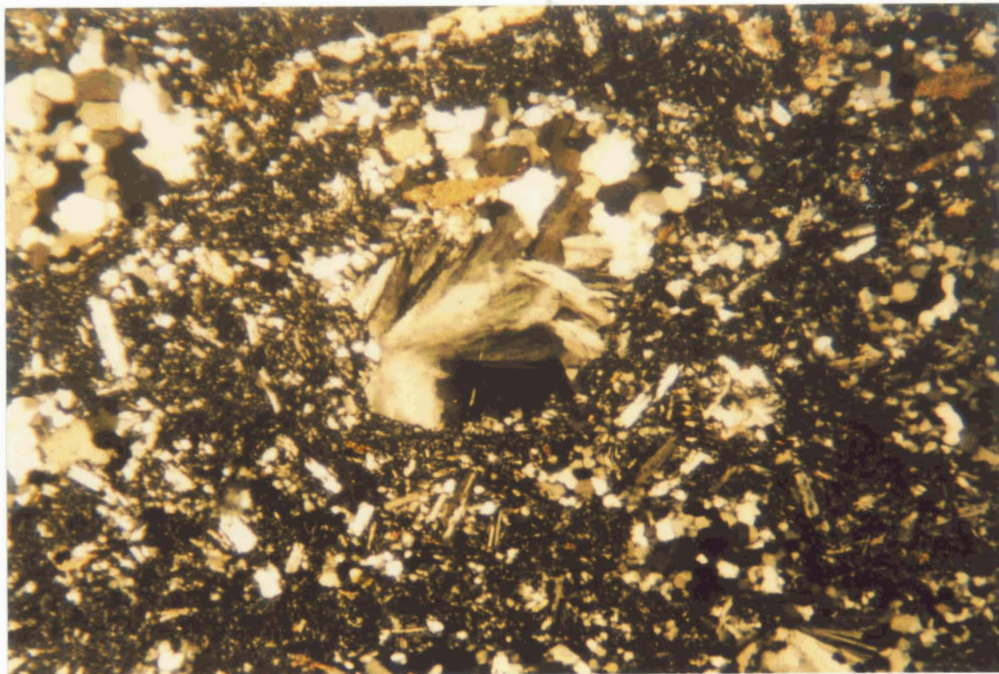


Figure 27: Photomicrograph (x-polars) of the core of a type 1 mafic fragment from mafic lapilli-tuff of unit 2b. The core consists of polycrystalline quartz amygdules (top left and bottom right) in a groundmass composed of randomly oriented, plagioclase microlites (white) and hematite (black) with lesser chlorite, carbonate, and epidote. The left margin of the photograph is a cross-cutting carbonate veinlet (golden brown). The rectangular grain in the lower center of the photograph is a plagioclase phenocryst that has been largely replaced by carbonate.



0.0 0.1 0.2 0.3 0.4 0.5 mm

Figure 28: Photomicrograph (x-polars) of a polycrystalline albite amygdale in a type 1 fragment from mafic lapilli-tuff of unit 2b.

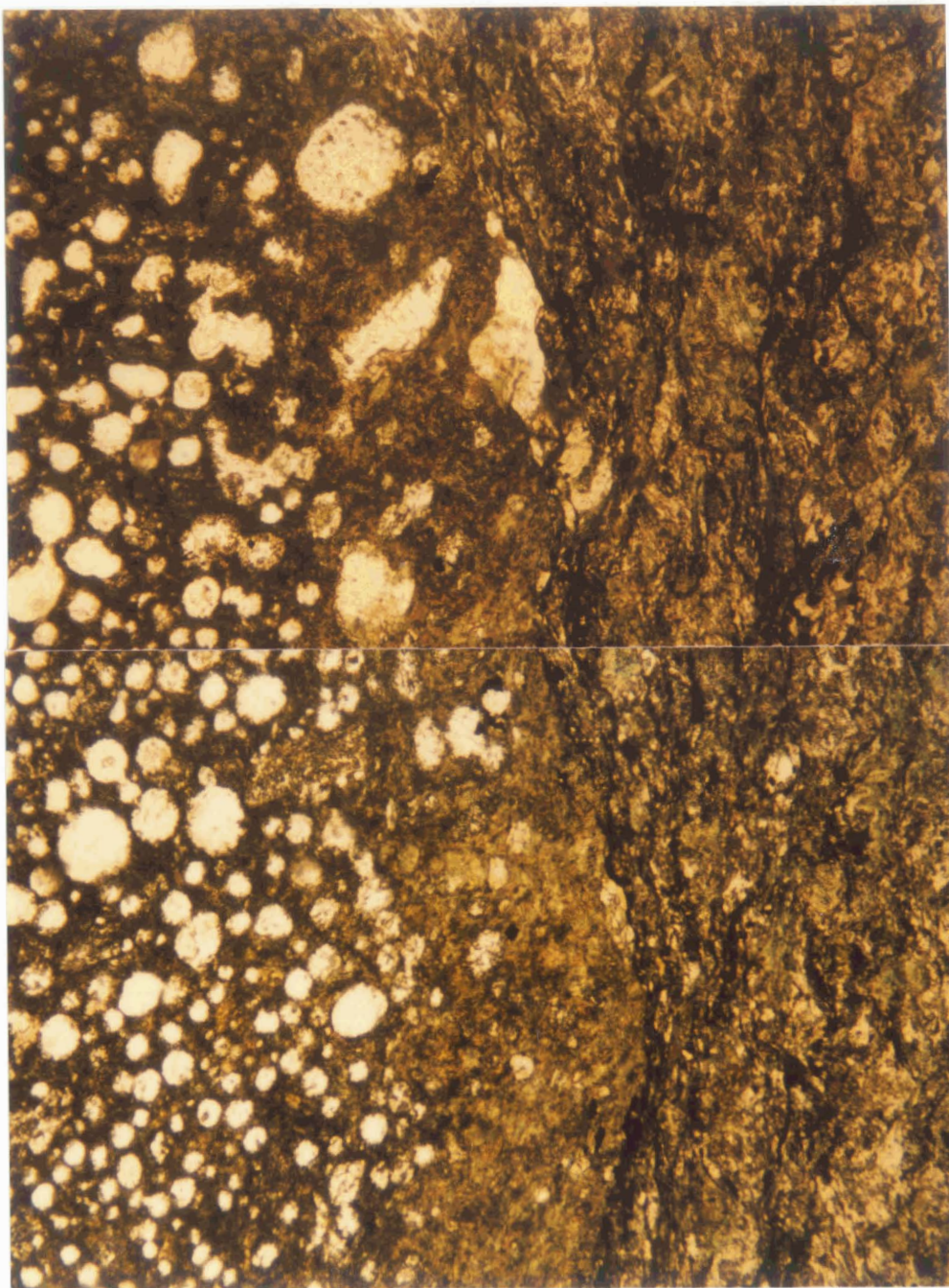


0 1 2 mm

Figure 29: Photomicrograph (x-polars) of a polycrystalline quartz plus albite amygdale in a type 1 fragment from mafic lapilli-tuff of unit 2b.



The rims observed on type 1 mafic fragments are 0.5 to 10 mm thick, completely or partly surround fragments, and contain 2 to 10% amygdules in a foliated aggregate composed largely of chlorite with lesser hematite, actinolite and epidote. Generally, the rim thickness in individual fragments is not constant, and it also varies in thickness among fragments in the same bed. A small proportion of fragments, which are only partly surrounded by a rim, appear broken and the core is in sharp contact with the surrounding largely granoblastic matrix aggregate. In most fragments, the boundary between the rim and core is gradational, but in some fragments it is sharp. Where the boundary is gradational, the chlorite content increases, and the contents of hematite and plagioclase decrease gradually outwards across the entire width of the rim. Where the boundary is sharp, there is an abrupt increase in chlorite and a decrease in hematite and plagioclase across the core-rim interface. Amygdules in the rims are typically composed of polycrystalline plagioclase or less commonly, polycrystalline quartz. Unlike the plagioclase amygdules in the core, which consist of radiating plagioclase laths, those in the rim are an aggregate of subequant, anhedral, 0.1 to 0.5 mm, sutured plagioclase grains with 1 to 5%, 0.1 to 0.2 mm long, actinolite or biotite needles. In addition, the amygdules in the rim are typically sporadically distributed and less abundant than those in the core (Fig. 30). However, in one fragment there was no variation in amygdule distribution or abundance between the rim and core.



0 1 2 mm

Figure 30: Photomicrograph (plane light) of a type 1 mafic fragment from mafic lapilli-tuff of unit 2b. The fragment consists of a highly vesicular, hematitic core (greenish black) and a poorly vesicular, chloritic rim (light green). All vesicles are filled with polycrystalline quartz (white). The granoblastic to foliated aggregate that encloses the fragment consists of plagioclase, chlorite and hematite in subequal proportions and lesser actinolite, epidote, carbonate and quartz. Although totally recrystallized, the aggregate probably consisted originally of ash-sized vitric mafic particles or granules.

Quartz-carbonate veinlets comprise 0 to 20% of fragments. They are oriented almost perpendicular to the long axis of fragments and bed contacts; they cross-cut fragment cores and less commonly rims, but do not extend into the surrounding granoblastic to foliated aggregate that forms the matrix (Fig. 26). The fractures are tectonic because they show a consistent orientation throughout the unit; they may represent tension fractures that developed in competent fragments, but not in the surrounding ductile matrix.

#### **6.3.1.2 Partly-Rimmed, Vesicular, Microlitic Mafic Fragments (Type 2)**

In comparison to type 1 mafic fragments, type 2 mafic fragments are smaller, less abundant, more elongate, and less vesicular; they also contain more chlorite, a higher proportion of plagioclase amygdules, and fewer microlites, and they lack quartz-carbonate veinlets, actinolite pseudomorphs after clinopyroxene phenocrysts, and well developed chloritic rims although poorly defined, partial rims are present on some fragments (Tables 9, 10). The fragments consist of rare plagioclase phenocrysts in a microlitic, foliated aggregate composed largely of chlorite and hematite (Table 9). In terms of mineralogy, some type 2 fragments closely resemble the rims of type 1 fragments, but, in terms of mineralogical and textural characteristics, most are intermediate between the cores and rims of type 1 fragments.

Fragment vesicularity ranges from 2 to 20%, but is generally less than 10%. Vesicles are typically filled with polycrystalline albite, but locally are filled with polycrystalline quartz. The plagioclase amygdules are elliptical, circular, or less commonly amoeboid, and, like amygdules in the rims of type 1 fragments, they are aggregates of sutured plagioclase grains with minor actinolite or biotite needles. In the type 2 mafic fragments, amygdules occur throughout the entire fragment, but they have a non-random distribution. Within fragments, they are either clustered in irregular, 1 to 7 mm long patches or are isolated from one another. Plagioclase phenocrysts, which locally coexist with the amygdules, can be clearly distinguished by their subhedral to euhedral shapes, monocrystallinity, and albite-Carlsbad twins.

The groundmass of type 2 mafic fragments consists of 0 to 5%, randomly oriented, plagioclase microlites in a fine-grained, foliated aggregate composed largely of chlorite and hematite in subequal proportions. Typically, the groundmass is mineralogically homogeneous, but in some fragments a non-uniform distribution of chlorite and hematite produces a patchy appearance. In these fragments, irregular, 1 to 5 mm long, hematite-rich areas are entirely enclosed by, or intergrown with, chlorite-rich areas. The boundary between the hematite-rich and chlorite-rich areas is always gradational. In one fragment, a 5-mm long, oval patch

composed of subequal amounts of plagioclase and hematite, subordinate chlorite and actinolite, and minor biotite, epidote, carbonate and quartz was enclosed in the chloritic groundmass. The oval patch, differs compositionally from the hematite-rich areas, and, additionally, its boundaries with the enclosing chloritic groundmass are sharp rather than gradational.

Some of these fragments appear to have a partial vitric rim that can be distinguished from the recrystallized granoblastic matrix only by the presence of plagioclase amygdules that are similar in size, shape, composition, and abundance to those in the readily recognizable parts of the fragments (Fig. 31). These rims appear to be 1 to 3 mm thick and occur on about 10% of the fragments as defined in planar thin sections. They are a fine-grained aggregate composed of plagioclase and hematite in subequal proportions, subordinate chlorite and actinolite and minor biotite, epidote, carbonate, quartz and pyrrhotite. The plagioclase, quartz, carbonate, epidote, and pyrrhotite are granoblastic, whereas chlorite, actinolite, and biotite are aligned; hematite typically occurs as anastomosing stringers. The aggregate is texturally and mineralogically indistinguishable from adjacent, non-amygdaloidal areas that are believed to represent recrystallized matrix. The original nature of the rims cannot be defined precisely, but they were probably texturally and/or compositionally

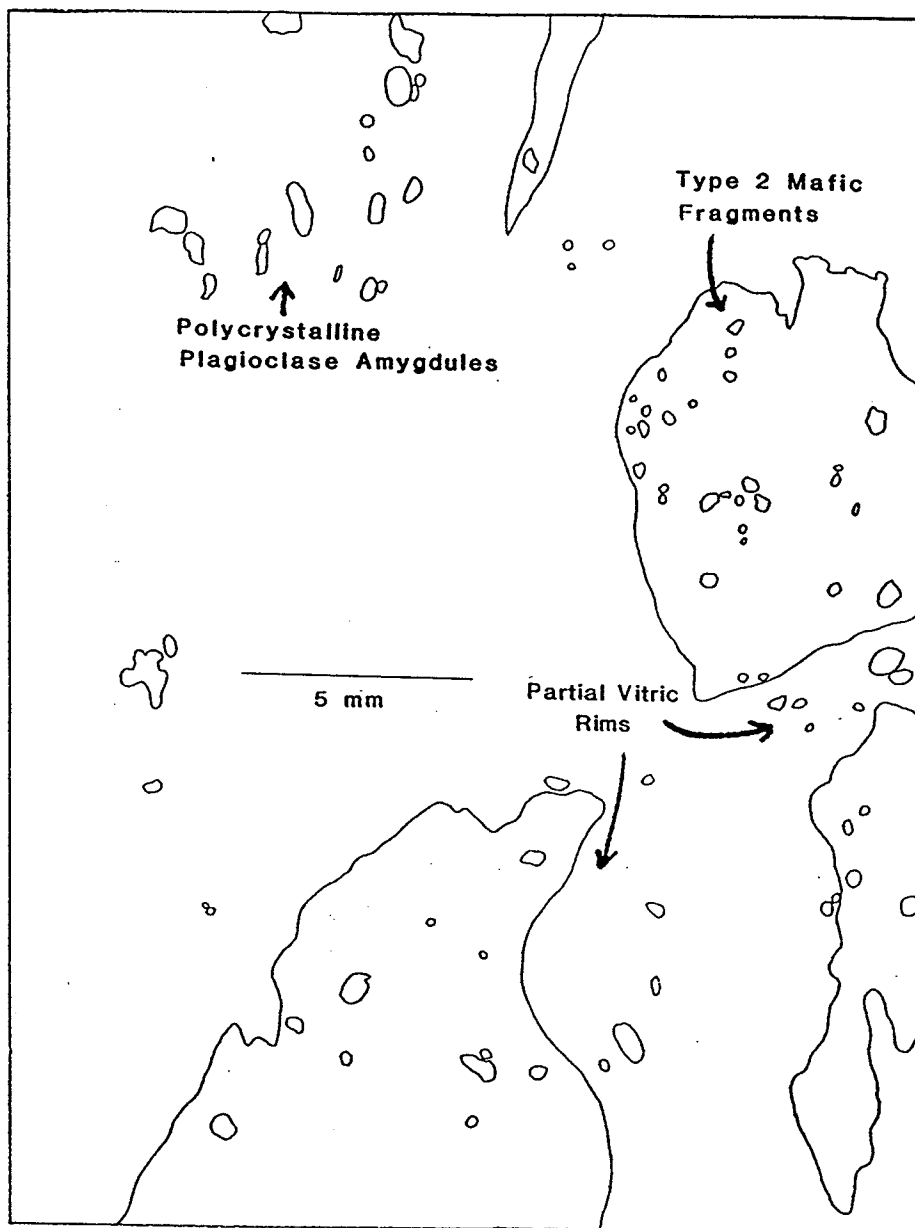


Figure 31: Thin section drawing showing the distribution of polycrystalline plagioclase amygdules in the granoblastic aggregate of mafic lapilli-tuff in unit 2b. Amygdule clusters adjacent to type 2 mafic fragments presumably represent partial vitric rims on type 2 mafic fragments. Apparently isolated amygdules may represent the vitric edges of type 2 mafic fragments, small vitric mafic fragments, tuff vesicles, or a combination of the three.

different than type 1 and 2 mafic fragments in which plagioclase microlites can be identified. The uniform texture of the rims implies that they may have originally been vitric.

Locally, amygdule clusters and less common single amygdules are isolated in the granoblastic aggregate (Fig. 31). The isolated amygdules may represent (1) the vitric edge of a type 2 mafic fragment, the more crystallized part of which was not intersected by the thin section, (2) separate, vitric mafic fragments, or (3) tuff vesicles.

#### **6.3.1.3 Non-Vesicular, Microlitic Mafic Fragments (Type 3)**

Type 3 mafic fragments are smaller and less abundant than type 1 and 2 mafic fragments (Tables 9, 10). The fragments occur as thin lenticles and consist of rare plagioclase phenocrysts in a uniform textured, microlitic, foliated aggregate composed largely of chlorite. The fragments lack amygdules, but otherwise they are compositionally and texturally similar to type 2 fragments (Table 9).

#### **6.3.1.4 Crystal Particles**

Crystal particles are a minor component of the mafic lapilli-tuff and tuff (Table 10). They include single crystal albite pseudomorphs after plagioclase and actinolite pseudomorphs after clinopyroxene. Plagioclase crystals are

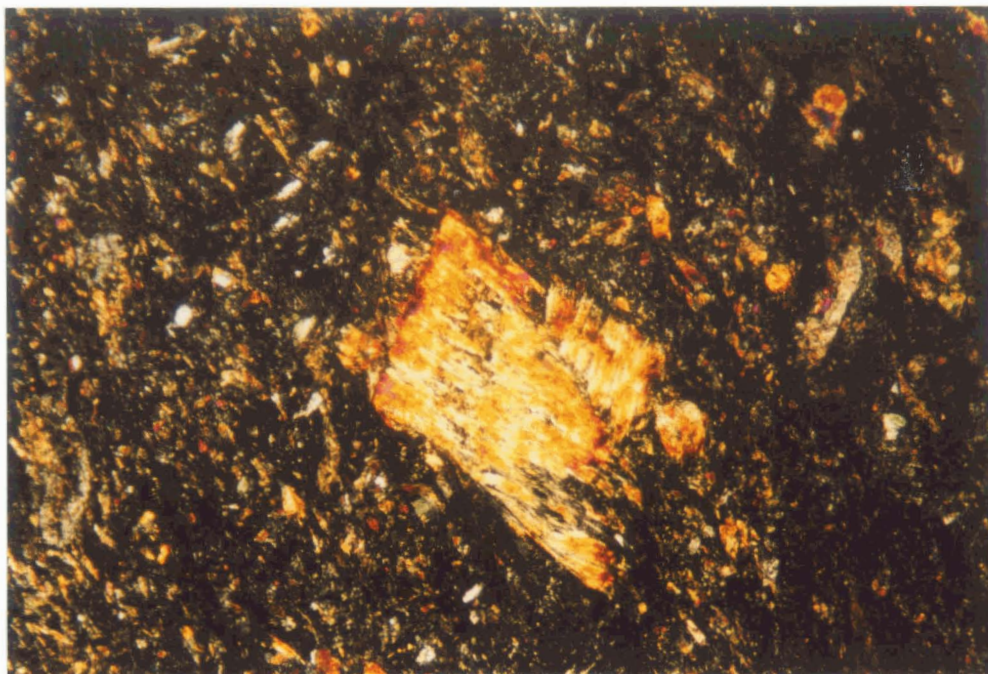
typically isolated in the recrystallized matrix, and can be clearly distinguished from isolated plagioclase amygdules by their generally angular shape, monocrystallinity, and albite-Carlsbad twins. The crystals are typically broken, but do not show evidence of extensive abrasion; lesser unbroken crystals are euhedral.

Isolated single-crystal actinolite pseudomorphs after clinopyroxene were locally observed in the recrystallized matrix of the mafic lapilli-tuff and tuff. The pseudomorphs are tabular, or less commonly rhombic (Fig. 32), and unbroken.

#### **6.3.1.5 Granoblastic Matrix**

The granoblastic aggregate that surrounds mafic fragments and crystal particles is, in most places, the dominant component of the mafic lapilli-tuff and tuff. It is mineralogically and texturally identical to the partial vitric rims on type 2 mafic fragments (cf. Tables 9, 10) and therefore, may have also originally been vitric. The aggregate typically has a uniform, largely granoblastic texture, but, locally, it has a granular-like appearance with 0.2 to 0.5 mm long knots of actinolite, chlorite, and plagioclase enveloped partly or completely in hematite stringers (Fig. 30). Because of its fine metamorphic grain size the aggregate probably originally consisted of ash-sized, vitric mafic particles or granules.





0 1 2 mm

Figure 32: Photomicrograph (x-polars) of an actinolite pseudomorph after an original clinopyroxene crystal. The pseudomorph is enclosed in a fine-grained granoblastic aggregate composed of subequal amounts of plagioclase and hematite, subordinate chlorite, and actinolite, and minor biotite, epidote, carbonate, quartz and pyrrhotite. Although totally recrystallized, the aggregate probably originally consisted of ash-sized, vitric mafic particles or granules.

### 6.3.2 Bedding Characteristics

In the mafic lapilli-tuff and tuff, multiple, ungraded beds were defined by variations in fragment abundances and fragment size. The beds have abrupt contacts and are 5 to 250 cm thick with an average thickness of 70 cm. They are poorly sorted and generally maintain a constant thickness for up to 20 m across outcrops, but beds cannot be correlated between outcrops with confidence, and, thus, their longer range continuity is unknown.

A stratigraphic section measured in the northwestern part of the unit revealed the presence of at least 45 beds (Fig. 33); about 10% of the section is covered, and the total number of beds may be greater. The bed to bed variation in fragment abundance is commonly greater than 20% fragments, but is locally less than 10% fragments. The variation in average maximum fragment size from bed to bed is generally less than 50 mm but can be as much as 115 mm. Bed contacts are gradational rather than sharp, but the transition from one bed to the next normally occurs within a vertical distance of 1 to 5 cm (Fig. 34).

Size or abundance grading were not observed in any of the beds, but generally there is a higher abundance of larger fragments in the upper 1/3 of the succession as opposed to the lower 2/3 of the succession (Fig. 33). Generally, fragments are evenly distributed within the beds, but, in

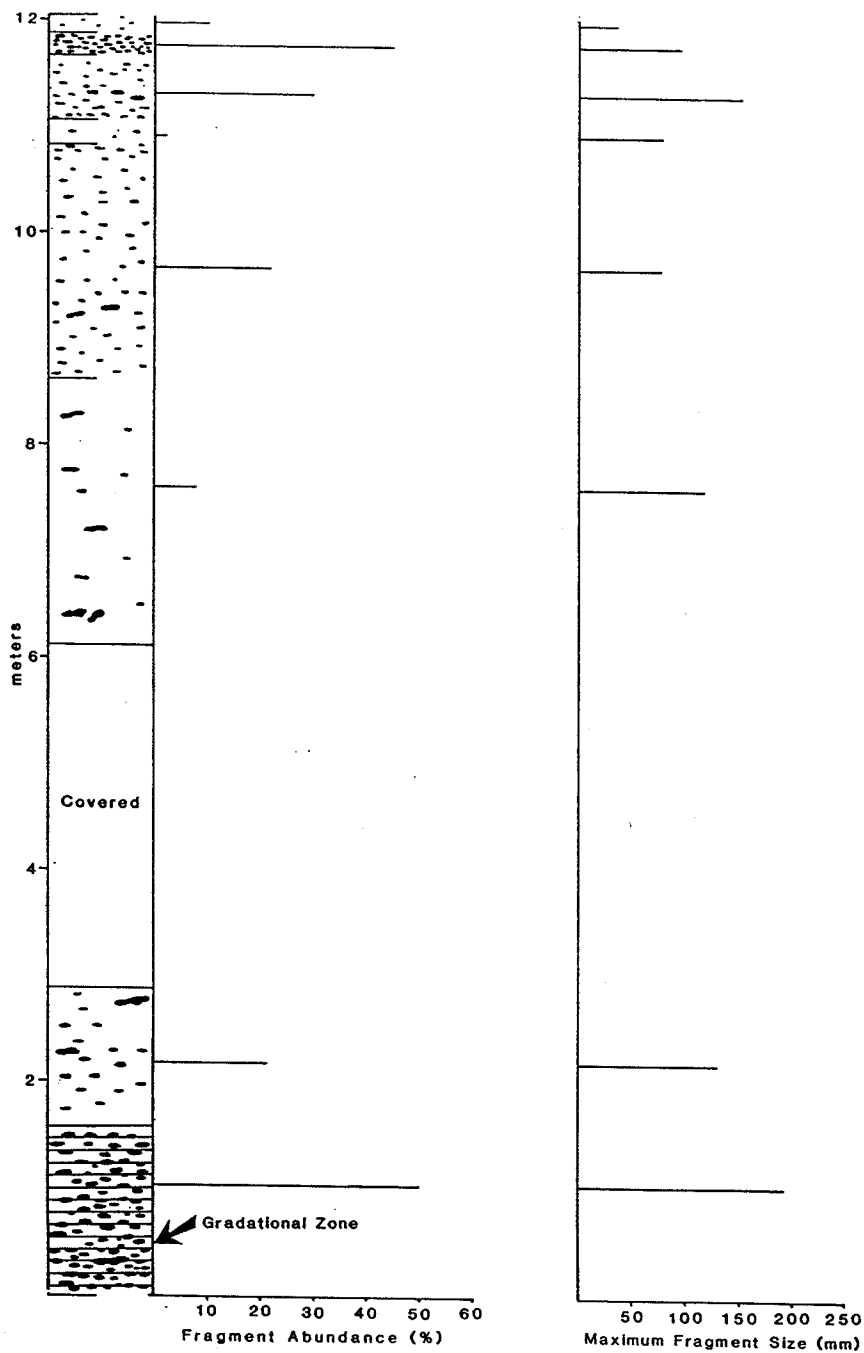


Figure 33: Stratigraphic section 2b-1 through mafic lapilli-tuff and tuff of unit 2b. The succession consists of at least 45 beds which show bed to bed variations in fragment abundance and average maximum fragment size. Fragment abundance was determined by counting about 600 points for each bed using a 1 cm by 1 cm grid. Maximum fragment size in each bed is the average length of the ten largest fragments.

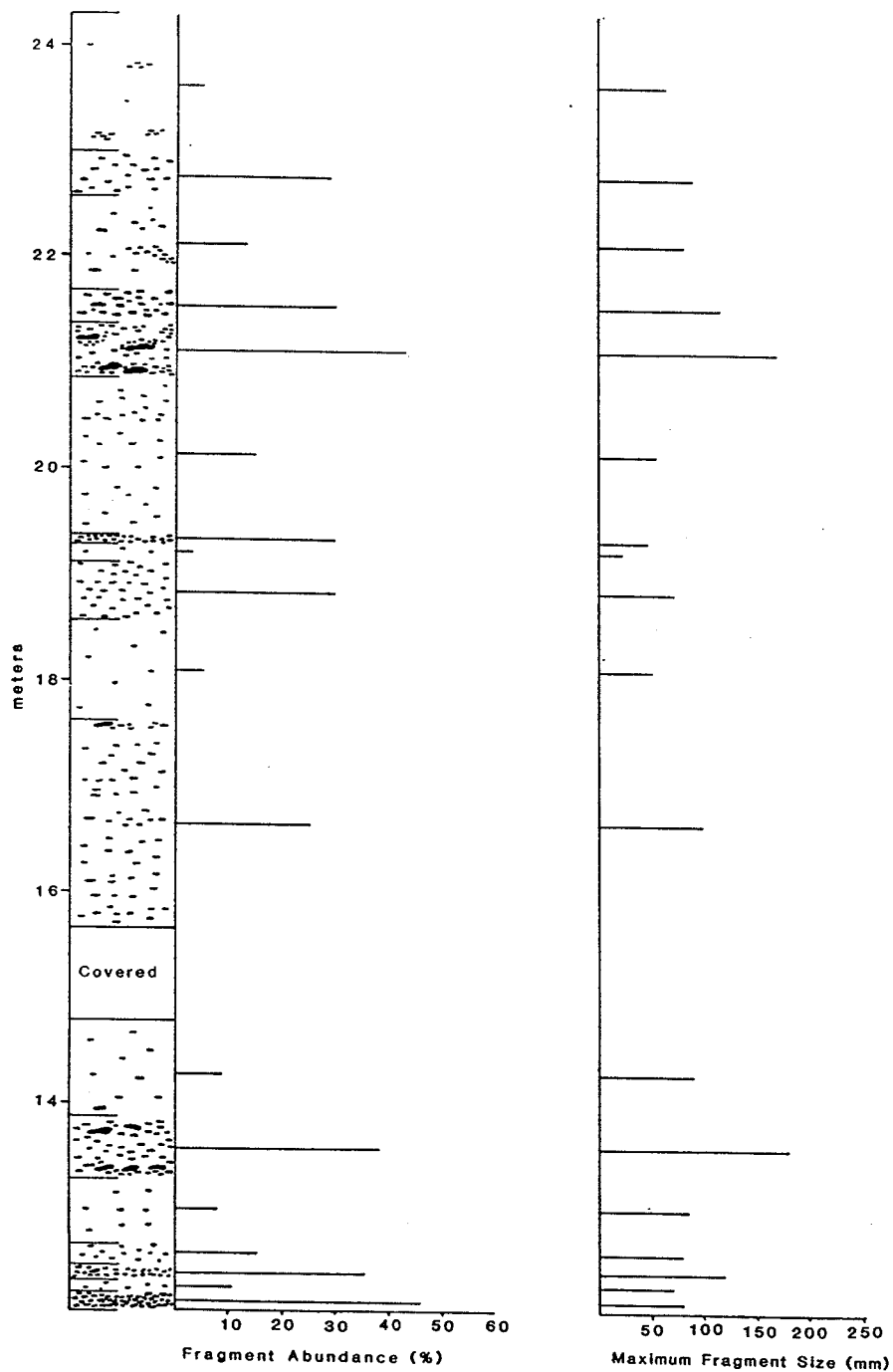


Figure 33 (continued)

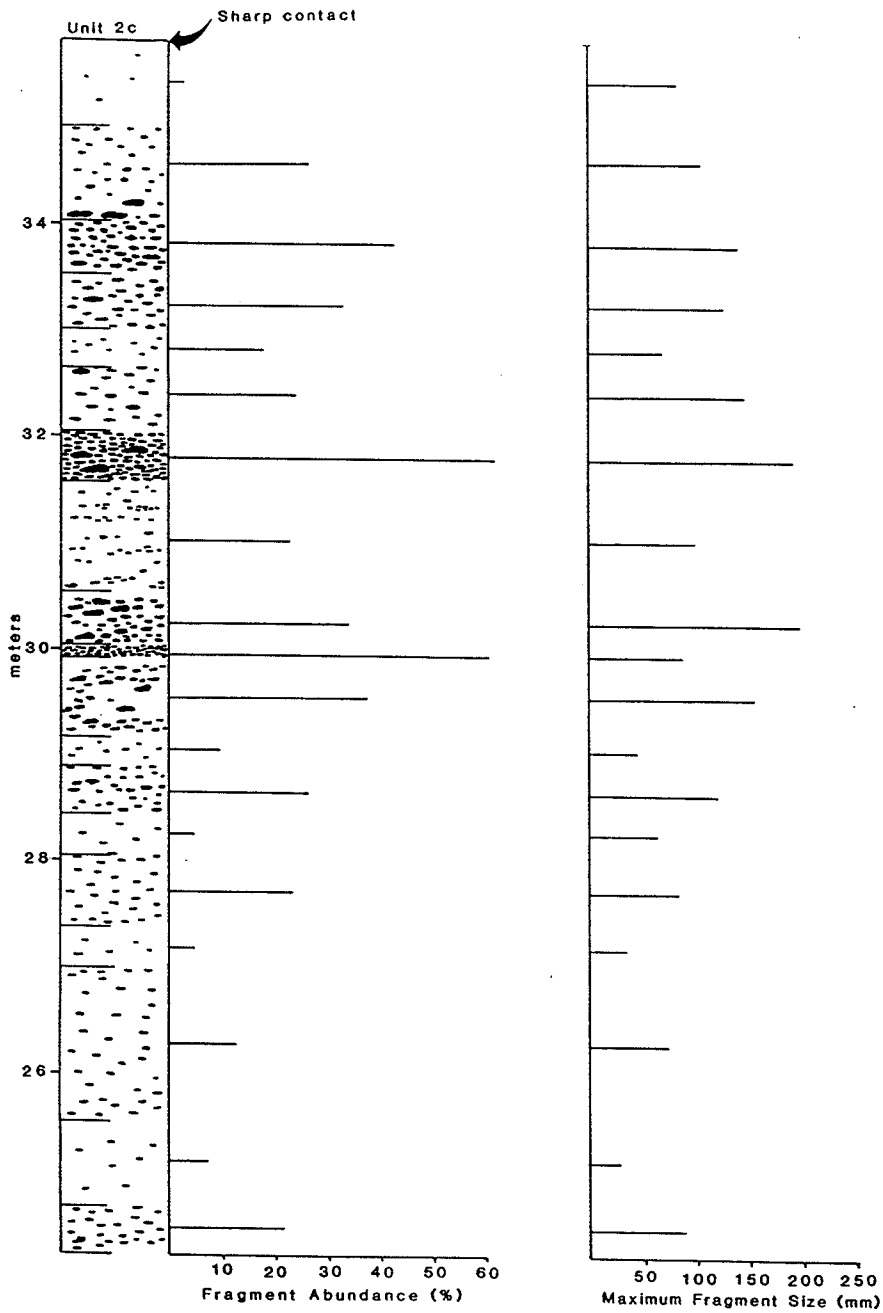


Figure 33 (continued)

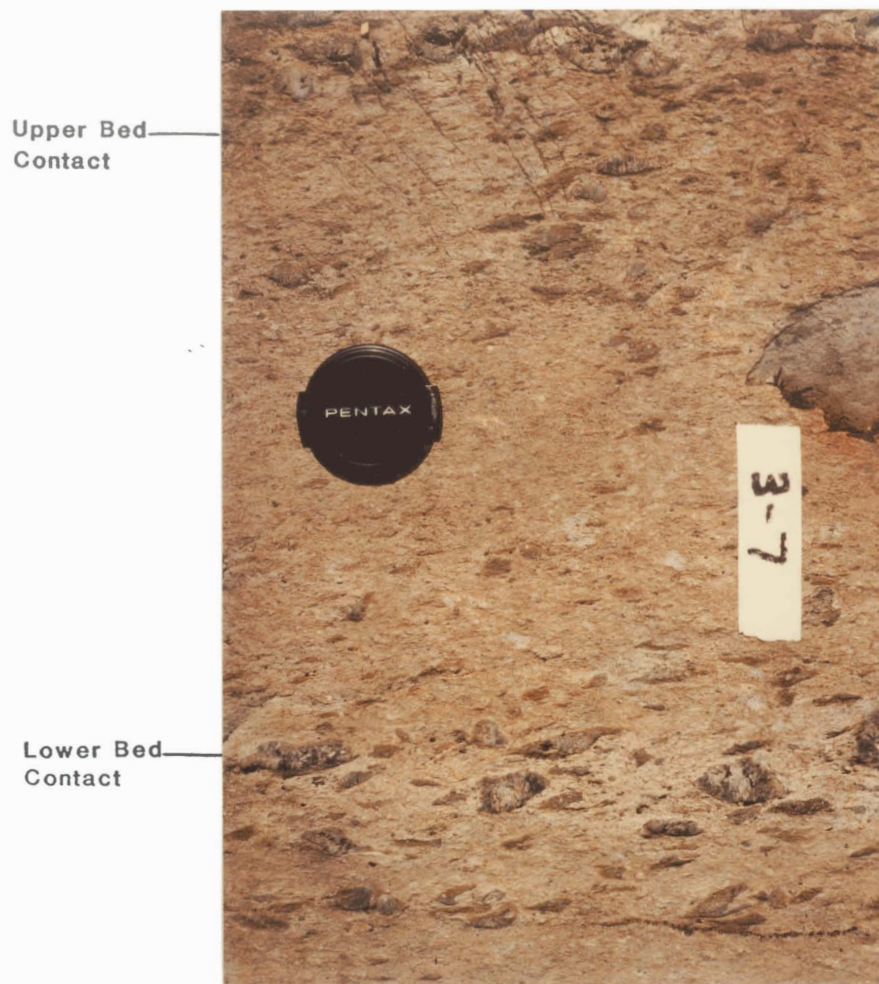


Figure 34: Photograph of mafic lapilli-tuff and tuff from unit 2b. Note the gradational contact between the lapilli-tuff bed (lower) and the overlying tuff bed (center). Also note the irregular fragment-rich area in the upper part of the tuff bed which may represent a load cast. Lens cap for scale is 5.5 cm in diameter.

some beds, isolated, 10 to 20 cm long, oval to irregular, fragment-rich areas were observed in fragment-poor beds (Figs. 33, 34); they may represent differentially compacted beds or a soft sediment deformation feature. Because the fragment-rich areas are nearly equidimensional, they are probably not differentially compacted beds. Instead, the fragment-rich areas could be load casts formed by the sinking of the overlying coarser grained beds into underlying finer grained beds. Alternatively, the fragment-rich areas could have been produced by elutriation of ash-sized particles. In some beds, isolated, block-sized, rounded, type 1 mafic fragments were observed (Fig. 35). The fragments could be volcanic bombs that were rounded aerodynamically.

Crystal particles are a minor component of the mafic lapilli-tuff and tuff (Table 10). No vertical variations in size or abundance of crystal particles, or composition or texture of the granoblastic matrix were observed within beds or through the sequence.

#### **6.4 MAFIC TO INTERMEDIATE LAPILLI-TUFF AND TUFF**

Mafic to intermediate lapilli-tuff and tuff comprise the upper part of Member 2 (2c); it is thinner and more felsic than the underlying mafic lapilli-tuff and tuff (2b). The unit thins and thickens along strike, ranging in thickness from 5 to 20 m, and in the northwestern part of the mapped



Figure 35: Photograph of mafic lapilli-tuff from unit 2b. Note the isolated, rounded, type 1 mafic fragment in a thin, lapilli-rich bed (center). The fragment could be a volcanic bomb that was rounded aerodynamically. Lens cap for scale is 5.5 cm in diameter.



area, it is abruptly truncated by Member 3 (Plate 1). The lower contact with underlying mafic lapilli-tuff and tuff is sharp and is marked by a change in fragment type and matrix composition. The upper contact with overlying interlayered volcanic sandstone and lava flows of Member 3 is sharp and hummocky in places. Locally, felsic tuff is interbedded with lapilli-tuff in the upper 1 to 2 m of the unit.

#### **6.4.1 Components Comprising the Lapilli-Tuff and Tuff**

The lapilli-tuff and tuff are composed of variable proportions of mafic and felsic fragments and crystal particles in a fine-grained, foliated mafic aggregate that probably represents recrystallized matrix (Tables 9, 10). Most fragments are mafic and these are commonly elongate due to tectonic flattening, but some fragments are subequant and angular to subangular; the less abundant, more competent felsic fragments are subequant and angular to subrounded. Vesicular mafic fragments are texturally similar to the cores of type 1 mafic fragments in the underlying unit, but they contain fewer plagioclase microlites and lack actinolite pseudomorphs after clinopyroxene phenocrysts; in addition, the granoblastic groundmass contains carbonate and quartz, has less plagioclase, and lacks epidote (Table 9). The fragments also lack chloritic rims and are generally smaller than type 1 mafic fragments (Table 10). Non-vesicular mafic fragments are comparable in size and texture

to type 3 mafic fragments in the underlying unit, but they contain more plagioclase phenocrysts and microlites, and the groundmass contains carbonate and biotite but lacks actinolite (Table 9). Porphyritic felsic fragments in the mafic to intermediate lapilli-tuff and tuff (2c) are not comparable to any fragments in the underlying unit.

Unlike the underlying unit, the mafic to intermediate lapilli-tuff and tuff contain quartz crystals and a higher abundance of plagioclase crystals (Table 10). Plagioclase crystals are typically broken, but do not show evidence of extensive abrasion. All quartz crystals are broken, but again, they do not show evidence of extensive abrasion; embayments were locally observed in the quartz crystals.

Fragments and crystal particles are surrounded by a uniform, fine-grained, foliated aggregate that contains more chlorite and quartz and less plagioclase, hematite, and actinolite than the granoblastic aggregate in the underlying unit (Table 10). Although totally recrystallized, the aggregate probably represents matrix, and, because of its uniform texture and fine metamorphic grain size, it may have originally been vitric. It probably consisted of ash-sized, vitric mafic particles or granules.

#### 6.4.2 Bedding Characteristics

Like the underlying unit, the mafic to intermediate lapilli-tuff consists of multiple, poorly sorted beds that are defined by variations in fragment abundance and size. The beds are 20 to 400 cm thick; bed contacts are gradational rather than sharp, but the transition from one bed to the next normally occurs within a vertical distance of less than 5 cm. The beds can be traced across outcrops for up to 6 m, but cannot be correlated between outcrops with confidence. Locally, 30 to 50 cm thick felsic tuff beds occur in the upper 1 to 2 m of the unit.

A stratigraphic section measured in the northwestern part of the unit revealed the presence of 8 lapilli-tuff and tuff beds and 1 felsic tuff bed (Fig. 36). The lapilli-tuff and tuff beds are ungraded and show bed to bed variations in fragment abundance and fragment size. Fragment-rich beds contain 15 to 20%, 0.5 to 5 cm long fragments whereas fragment-poor beds contain 2 to 5%, 0.5 to 3 cm long fragments. Unlike the underlying unit, however, the relative proportions of fragments and crystals changes vertically. In bed 1 (Fig. 36), vesicular and non-vesicular mafic fragments are present in subequal proportions with minor crystal particles; porphyritic felsic fragments are absent. In bed 2, porphyritic felsic fragments and crystal particles are abundant, but vesicular and non-vesicular mafic fragments are a minor component. In beds 3 to 9,

Member 3  
Interlayered tuffaceous  
sandstone and mafic flows

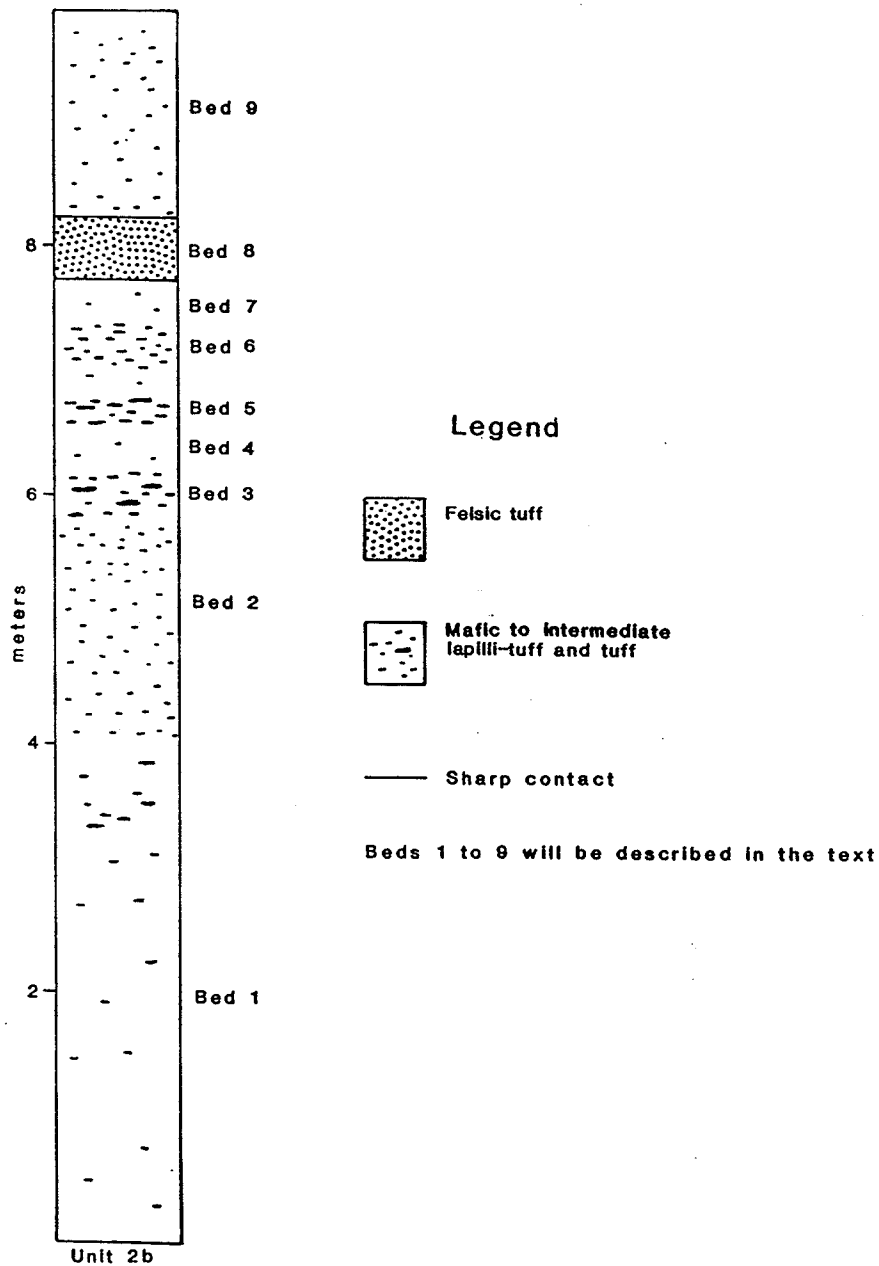


Figure 36: Stratigraphic section 2c-1 through mafic to intermediate lapilli-tuff of Unit 2c.

vesicular and non-vesicular mafic fragments are present in subequal proportions with minor porphyritic felsic fragments and crystal particles. The matrix composition and texture does not change upwards in the unit.

A sample of the felsic tuff bed was unobtainable, but, in contrast to the lapilli-tuff and tuff, it is more felsic and lacks recognizable fragments. Its upper and lower contacts are sharp, but no scours were observed. The tuff is sheared and iron stained, and, thus, grading characteristics could not be determined.

## Chapter VII

### DISCUSSION

#### 7.1 INTRODUCTION

Felsic to mafic pyroclastic rocks comprise an integral part of Precambrian greenstone belts, but the origin of such rocks is commonly nebulous because many of the primary textures and structures necessary for genetic interpretation have been destroyed by metamorphic recrystallization and deformation. However, in some greenstone belts primary pyroclastic rocks have been identified. These include pyroclastic flow deposits (Baldwin, 1987; Dimroth and Demarke, 1978; Dimroth and Rocheleau, 1979; Padgham, 1980; Thurston, 1980; Tassé et al., 1978), air-fall deposits (Buck, 1978; Padgham, 1980), and phreatic breccia (Dimroth and Rocheleau, 1979). In the Manigotagan River Formation, many of the primary structures and textures necessary for genetic interpretation have been preserved. These textures and structures can then be compared with other pyroclastic deposits for the purpose of establishing genetic models. Genetic aspects that will be examined in this particular study include (1) environment of eruption and deposition, (2) emplacement mechanisms, and (3) eruptive sources.

## 7.2 SUBAQUEOUS PYROCLASTIC FLOW DEPOSITS

The ignimbrites of the Manigotagan River Formation consist of variable proportions of dacite fragments, vitric felsic fragments, pumice, rare mafic scoria and microcline-phyric felsic fragments, and plagioclase and lesser quartz crystals enclosed in a largely granoblastic, quartzo-feldspathic aggregate inferred to be recrystallized vitric ash. They are composite sheets consisting of multiple flow units, most of which consist of a lower, massive lapilli-tuff division and an upper, unbedded to planar bedded tuff division. In the upper ignimbrite, however, some flow units lack the upper tuff division and consist only of a lapilli-tuff division.

### 7.2.1 Comparison With Ignimbrites In The Literature

Members 1 and 7 of the Manigotagan River Formation are considered to be ignimbrites on the basis of similarities in thickness and structural characteristics to those of other ignimbrites. The members range in thickness from 6 to at least 50 m, and ignimbrites of similar thickness have been documented elsewhere (Niem, 1977; Bond, 1973; Lowman and Bloxam, 1981). According to Sheridan (1979), many ignimbrites are composite sheets composed of flow units that range in thickness from 0.5 to 40 m. The thicknesses of flow units comprising the Manigotagan River Formation ignimbrites are within this thickness range (Table 4). In

addition, lapilli-tuff and tuff divisions that comprise individual flow units (Tables 7, 8) are similar in thickness to those documented in subaqueous pyroclastic flow deposits (Niem, 1977; Bond, 1973; Lowman and Bloxam, 1981).

Structures observed in the ignimbrites of the Manigotagan River Formation include:

1. reverse grading of pumice,
2. normal grading of dacite and/or vitric felsic fragments, and
3. pumice-rich and pumice-poor bed sequences.

Reverse grading of pumice and normal grading of dense vitric fragments has also been documented in younger pyroclastic flow deposits (Fiske, 1963; Yamazaki et al., 1973; Self and Rampino, 1981; Kano et al., 1988). Pumice-rich and pumice-poor beds of similar thickness to those in the Manigotagan River Formation have been documented in Mississippian subaqueous pyroclastic flow deposits (Niem, 1977).

### **7.2.2 Environment of Eruption and Deposition**

In ancient volcanic and sedimentary successions, such as the Manigotagan River Formation, eruptive environments are difficult, if not impossible, to deduce because metamorphic recrystallization has destroyed many of the primary characteristics of components that are diagnostic of eruptive environments (Wright and Mutti, 1981). In addition,



a direct comparison with other subaqueously and subaerially erupted pyroclastic flow deposits will not be applicable because the structural characteristics of the deposits do not necessarily reflect eruptive environment. Although the ignimbrites of the Manigotagan River Formation lack features indicative of eruptive environment, there are other indirect lines of evidence which suggest that they were erupted in a subaerial environment, such as:

1. the relatively high volume of volcanic conglomerate in the subaqueous fan succession (Member 3) which suggests that a large landmass had once existed, and
2. the presence of tephra-fall deposits (Member 2).

Ignimbrites can be deposited in subaerial or subaqueous environments and the distinction between such environments is normally based on indirect lines of evidence such as the presence of fossils (Fiske and Matsuda, 1964; Carey and Sigurdsson, 1980; Wright and Mutti, 1981), pillows in nearby parts of the sequence (Tassé et al., 1978; Howells et al., 1985), and/or structures within the deposits. The ignimbrites of the Manigotagan River Formation occur in a volcanic and sedimentary sequence that shows evidence of subaqueous deposition. Moderately to highly vesicular, pillowed lava flows occur throughout the sequence (Plate 1), and the intervening sedimentary rocks show evidence of subaqueous deposition such as shallow scours, low angle cross-bedding, argillite rip-ups, and load and slump

structures (Seneshen, 1986 and unpublished data). In addition, the Manigotagan River Formation is underlain by subaqueous pyroclastic debris flows of the Narrows Formation (Weber, 1971) and is overlain by subaqueous flysch-type sediments of the Edmunds Lake Formation (Campbell, 1971).

At present there is controversy about the usefulness of structures for deducing the depositional environment of ignimbrites. Some workers have argued that primary structures and structure sequences are not valid criteria for distinguishing between subaerial and subaqueous environments (Lajoie, 1984; Howells et al., 1985), whereas other workers believe that structures of subaqueous pyroclastic flow deposits are different from those of subaerial deposits (Fisher and Schmincke, 1984; Fisher, 1984). In terms of primary structures, the lapilli-tuff divisions of the Manigotagan River Formation ignimbrites are analogous to subaerial ignimbrites (Sparks, 1976; Fisher, 1979), but the regular repetition of lapilli-tuff and tuff has not been documented in subaerial ignimbrites. Fine-grained surge deposits can be intercalated with subaerial ignimbrites (Sparks, 1976), but these are commonly cross-stratified. In addition, preceding pumice-fall deposits, which commonly underlie subaerial ignimbrites, (Koch and McLean, 1975; Leat, 1985; Druitt and Sparks, 1982; Sparks, 1975; Wright, 1981) were not observed beneath the Manigotagan River Formation ignimbrites.

In summary, the ignimbrites of the Manigotagan River Formation occur in an apparently subaqueous volcanic and sedimentary sequence and differ substantially from subaerial ignimbrites in terms of structural characteristics. Although the ignimbrites were apparently deposited in a subaqueous environment, other indirect lines of evidence suggest that they were erupted subaerially.

### 7.2.3 Emplacement of the Ignimbrites

Although some subaqueous pyroclastic flows are welded (Francis and Howells, 1973; Lowman and Bloxam, 1981; Reedman et al., 1987), most subaqueous deposits lack welding and were apparently emplaced by sediment gravity flows (Fiske and Matsuda, 1964; Carey and Sigurdsson, 1980; Wright and Mutti, 1981; Fisher, 1977; Tassé et al., 1978), or a combination of sediment gravity flows and tephra-fall (Niem, 1977; Bond, 1973; Fiske, 1963). Identification of welding in ancient ignimbrites is hampered by metamorphic recrystallization, but the structural features of the Manigotagan River Formation ignimbrites suggest that they were emplaced as cold sediment gravity flows rather than hot pyroclastic flows. Such features include:

1. a repetitive sequence of lapilli-tuff and tuff divisions (Fiske, 1963; Yamada, 1973; Fisher, 1977; Tassé et al., 1978),

2. lapilli-tuff divisions showing reverse grading of pumice and normal grading of dense, vitric felsic fragments (Fiske, 1963),
3. tuff divisions that consist of bedded tuff, bedded pumiceous tuff, or massive tuff (Niem, 1977; Bond, 1973; Fiske and Matsuda, 1964),
4. sharp and planar to locally scoured basal contacts (Fiske and Matsuda, 1964),
5. a lack of quartz nodules which represent the fillings of original gas cavities (Howells et al., 1985; Wright and Coward, 1977),
6. a lack of funnel-shaped structures interpreted to be rootless vents (Wright and Coward, 1977), and
7. a lack of columnar joints.

In many deposits elsewhere, the boundary between the lower lapilli-tuff division and upper tuff division is gradational (Fisher, 1977; Niem, 1977; Bond, 1973; Wright and Mutti, 1981) reflecting one depositional event. In the ignimbrites of the Manigotagan River Formation, however, the lower lapilli-tuff divisions and upper tuff divisions are separated by sharp boundaries reflecting separate depositional events, and, possibly, different depositional processes.

### 7.2.3.1 Emplacement of the Lapilli-Tuff Division

The lapilli-tuff divisions of the Manigotagan River Formation ignimbrites have a number of distinct characteristics.

1. They consist of angular to subrounded vitric felsic fragments and/or dacite fragments, pumice, broken and lesser unbroken crystals, and 55 to 85% recrystallized vitric ash.
2. They show a wide range in thickness.
3. They occur in all flow units and generally comprise more than 50% of flow units.
4. They are poorly sorted and apparently lack stratification.
5. Vitric felsic fragments and/or dacite fragments show normal (density and poorly developed size) grading or less commonly are ungraded; pumice shows reverse (density or density and poorly developed size) grading or less commonly are ungraded; crystals are apparently ungraded.
6. Contacts are planar and sharp to locally scoured or they are gradational where two lapilli-tuff divisions are in contact.
7. Although the lowermost and uppermost flow units in the upper ignimbrite appear to correlate, the central units are apparently laterally discontinuous.

These characteristics could be indicative of deposition from either (1) debris flows, or (2) high density turbidity flows.

### **Debris Flows**

Debris flows are viscous, high strength, sediment gravity flows in which large grains are supported by the cohesiveness of a sediment-water matrix or dispersive pressure (Lowe, 1982; Blatt et al., 1980). The flows typically move in a laminar fashion, but can become turbulent by incorporating water (Lowe, 1982; Nemec and Steel, 1984). Lowe (1982) has speculated that cohesive debris flows can evolve through grain flows and high density turbidites into low density turbidites. The diagnostic features of subaerial and subaqueous debris flows have been reviewed by Nemec and Steel (1984).

Some of the characteristics of the lapilli-tuff divisions of the Manigotagan River Formation ignimbrites resemble the general characteristics of subaqueous debris flows. Such characteristics include:

1. bed thicknesses that are within the proposed thickness range for subaqueous debris flow deposits (Cas and Wright, 1987),
2. a poorly sorted, matrix supported framework, and an apparent lack of stratification (Nemec and Steel, 1984; Walker, 1984; Blatt et al., 1980),

3. divisions that are graded or less commonly ungraded (Nemec and Steel, 1984),
4. sharp basal contacts with limited erosion (Fisher, 1982; Nemec and Steel, 1984), and
5. poorly developed size grading of coarser components, but no apparent grading of finer components (Nemec and Steel, 1984).

Despite these similarities, the lapilli-tuff divisions apparently lack reversely graded basal zones which are characteristic of subaqueous debris flows.

Reversely graded basal zones have been reported in other lapilli-tuff divisions interpreted as debris flow deposits (Tassé et al., 1978; Yamazaki et al., 1973). The reverse grading indicates that shearing at the base of the debris flow produced dispersive pressure which acted to buoy larger fragments up into the flow (Walker, 1975). The apparent paucity of reversely graded zones at the bases of lapilli-tuff divisions in this study could imply that the flows were somewhat turbulent (Nemec and Steel, 1984; Cas, 1979) and/or they travelled over relatively low slopes (Walker, 1975).

Although the lapilli-tuff divisions have many of the characteristics of debris flow deposits, the lack of reversely graded basal zones suggests deposition from somewhat turbulent, and possibly more distal, sediment gravity flows. An emplacement mechanism that could better

account for the characteristics of the lapilli-tuff divisions in this study would be high density turbidity flows, which possibly evolved from debris flows (Nemec and Steel, 1984; Lowe, 1982).

### **High Density Turbidity Flows**

High density turbidity flows are sediment gravity flows in which clasts are supported by a combination of intergranular dispersive pressure and turbulence (Lowe, 1982). The support mechanism is governed by the relative abundance of gravel and sand in the flow.

The lapilli-tuff divisions of the Manigotagan River Formation ignimbrites have many of the characteristics of high density turbidites including:

1. a similar thickness range (Fiske, 1963; Niem, 1977; Wright and Mutti, 1981),
2. normally graded or ungraded to normally graded lapilli-tuff divisions (Cas, 1979),
3. grading that is confined to the coarser components (Cas and Wright, 1987; Lowe, 1982), and
4. a matrix-supported framework, poor sorting, and an apparent lack of internal stratification (Fiske, 1963; Niem, 1977; Wright and Mutti, 1981).

Despite these similarities, the lapilli-tuff divisions in this study lack other features of high density turbidites,



especially (1) the entire sequence of graded divisions (Cas, 1979; Lowe, 1982) and (2) reversely graded basal zones (Lowe, 1982). The lack of these features may indicate relatively distal deposits (Lowe, 1982; Walker, 1975).

### **Comparison of the Two Models**

It is difficult to choose between debris flow and high density turbidite models because the lapilli-tuff divisions in this study have characteristics of both. However, reversely graded basal zones are common in debris flow deposits and proximal high density turbidites; the lack of these zones in the lapilli-tuff divisions would, however, agree with more distal, gravelly high density turbidity flows (Lowe, 1982). As noted elsewhere, the high density turbidites may have evolved from debris flows by the incorporation of water (Nemec and Steel, 1984; Lowe, 1982).

#### **7.2.3.2 Emplacement of the Upper Tuff Division**

The upper tuff divisions have been divided into three types on the basis of bedding characteristics. In decreasing order of abundance, these are: (1) bedded tuff, (2) bedded pumiceous tuff, and (3) massive tuff. All three tuff division types occupy the same stratigraphic position relative to the lower lapilli-tuff divisions, and, thus, were probably emplaced by the same mechanism. The tuff divisions have a number of typifying characteristics.

1. They consist of multiple, or less commonly single, 1 to 240 mm thick, normally graded beds with or without pumice-rich beds; less commonly the divisions are apparently massive.
2. In normally graded beds, crystals decrease in size and abundance upwards to a locally laminated, crystal-free zone.
3. Bed contacts are sharp and planar.
4. Pumice-rich beds are typically confined to tuff divisions overlying pumiceous lapilli-tuff.
5. The divisions show lateral changes in aggregate thickness.

The characteristics of the tuff divisions suggest that they could be either (1) subaqueous tephra-fall deposits, or (2) low density turbidites.

#### **Subaqueous Tephra-Fall Deposits**

The tuff divisions have some of the features of subaqueous tephra-fall deposits which include:

1. normal grading from crystal-rich bases to sericitic (shard-rich?) crystal-free tops (Fisher and Schmincke, 1984),
2. sharp and planar bed contacts (Fiske, 1963),
3. beds that are less than 50 cm thick (Fisher and Schmincke, 1984), and

#### 4. pumice-rich beds (Niem, 1977).

Despite these similarities, there are a number of other features that are not typical of subaqueous tephra-fall deposits. These features are: (1) lateral changes in aggregate thickness, and (2) a close spatial relationship with lapilli-tuff divisions.

The fine-grained, equigranular, recrystallized vitric ash which comprises the upper tuff divisions in this study, would have probably had a uniform fall velocity, and therefore, would have produced a deposit of more uniform thickness (Fisher and Schmincke, 1984). The tuff divisions in this study show lateral changes in aggregate thickness over relatively short distances. In addition, in the southeast part of the upper ignimbrite, pumice is typically confined to bedded tuff and bedded pumiceous tuff divisions that overlie pumiceous lapilli-tuff divisions implying that there is a spatial relationship between the lapilli-tuff and tuff divisions.

The lateral changes in aggregate thickness in conjunction with the spatial relationship to the underlying lapilli-tuff suggest that the deposition of the tuff was genetically related to deposition of the lapilli-tuff and was not an independent process such as tephra-fall. An emplacement mechanism that could better account for the features of the tuff divisions in this study would be low density turbidity flows.

### Low Density Turbidites

Low density turbidity flows are sediment gravity flows in which grains (clay to medium-grained sand) are supported entirely by turbulence (Lowe, 1982; Walker, 1984). The diagnostic features of low density turbidites have been well reviewed (Walker, 1984). Features of the tuff divisions in this study that resemble the general features of turbidites are:

1. bed thicknesses,
2. normal grading,
3. parallel laminations in the upper parts of some beds,  
and
4. sharp and planar contacts.

The tuff divisions range in thickness from 0.02 to 4.5 m and internal bed thicknesses range in thickness from 0.1 to 24 cm. These thickness ranges are similar to those of other bedded tuff divisions interpreted to be low density turbidites (Wright and Mutti, 1981; Fiske and Matsuda, 1964; Tassé et al., 1978).

The normally graded beds and normally graded beds with laminations resemble the lower parts of Bouma sequences (Bouma, 1962). The normally graded part (Ta) is formed by very rapid settling of grains from suspension and laminations (Tb) are formed by traction of grains in a high flow regime (Walker, 1984). The paucity of other Bouma

divisions (Tcde) could indicate deposition in a relatively proximal environment where such divisions are commonly absent (Cas and Wright, 1987; Walker, 1984). Alternatively, the beds could be storm generated shelf turbidites (Cas and Wright, 1987). These commonly lack upper Bouma divisions due to low degrees of expansion, low slopes, and low potential energy.

Although sharp and planar contacts are characteristic of turbidites, the beds apparently lack shallow basal scours which are also common in turbidites (Walker, 1984). The apparent paucity of basal scours could signify that (1) the turbidite flows were not erosive as a result of travelling over low slopes, or (2) shallow scours have been obliterated by deformation.

The origin of the pumice-rich beds that occur in some bedded tuff divisions in the upper ignimbrite is problematic. The pumice-rich beds generally occur within a sequence of normally graded beds suggesting that the pumice could have been deposited by pelagic settling between periods of turbidite deposition (Niem, 1977). Alternatively, the pumice may have been separated by density sorting in a turbidity flow (Carey and Sigurdsson, 1980) implying that the turbidity flows had variable pumice contents.

Although most tuff divisions consist of normally graded beds, which appear to have been emplaced by low density

turbidity flows, the massive tuff divisions have less diagnostic features indicative of their origin. However, because the massive tuff divisions have sharp and planar contacts with lapilli-tuff divisions and occur at the same relative stratigraphic position as other tuff divisions interpreted to be low density turbidites, they were probably also emplaced by low density turbidity flows. The apparent lack of grading in these divisions could be due to extremely good sorting of tephra by reworking or aeolian fractionation prior to resedimentation by a turbidity flow. Alternatively, grading may have been destroyed by metamorphic recrystallization or may be too subtle to be observed on outcrop surfaces.

#### **7.2.4 Significance of Lateral Variations**

In the upper ignimbrite, where lateral variations could be documented, it is apparent that lapilli-tuff and tuff divisions are discontinuous along strike. This discontinuity suggests that the divisions have an overall lenticular morphology and this lenticularity probably reflects the attitude of the exposed section.

According to Car (1980), most sections through Precambrian volcanoes are at a high angle to flow vectors. In the Manigotagan River Formation, the morphology of channels in the subaqueous fan succession (Member 3) suggests that flow was at a high angle to present plane of

exposure (Seneshen, 1986 and unpublished data). Therefore, the lapilli-tuff and tuff divisions could be a stacked sequence of laterally discontinuous lobes. The negligible change in the size and abundance of components between measured sections further supports flow vectors at a high angle to the plane of exposure. The higher number of flow units in the south section could reflect a longer sustained channel-way for the passage of high and low density turbidity flows.

#### **7.2.5 Source of Components Comprising the Ignimbrites**

The components comprising the Manigotagan River Formation ignimbrites have the following general characteristics:

1. dacite fragments occur in both the lower and upper ignimbrites, but they are apparently more abundant in the lower (Table 7); their uniform texture and fine metamorphic grain size suggests that they were originally vitric;
2. pumice occurs in both the lower and upper ignimbrites, but it is generally more abundant in the upper (Tables 7, 8); its present composition is consistent with a diagenetically altered glass that was subsequently metamorphosed to greenschist facies;
3. vitric felsic fragments occur in both the lower and upper ignimbrites, but they are more abundant in the upper; the fragments differ markedly from the

- surrounding quartzo-feldspathic aggregate in composition and texture (cf. Tables 6, 7); locally they occur as xenoliths in dacite fragments;
4. rare mafic scoria and microcline-phyric felsic fragments occur only in the upper ignimbrite; microcline-phyric felsic fragments occur only in the uppermost flow units;
  5. unbroken crystals are similar in shape to phenocrysts in pumice, dacite, and vitric felsic fragments, but they differ in terms of size and abundance;
  6. unbroken plagioclase and quartz crystals are, on average, slightly smaller than plagioclase and quartz phenocrysts in dacite fragments; the plagioclase/quartz ratio of the crystal population is similar to that of the phenocryst population in dacite fragments (cf. Tables 6, 7);
  7. based on observation, most unbroken plagioclase crystals and all quartz crystals are larger than plagioclase and quartz phenocrysts in vitric felsic fragments; where quartz phenocrysts were observed in vitric felsic fragments, the plagioclase/quartz ratio of the phenocryst population exceeds that of the crystal population (cf. Tables 6, 7);
  8. unbroken plagioclase crystals are, on average, smaller than phenocrysts in pumice from the upper ignimbrite, but are larger than phenocrysts in pumice from the lower ignimbrite; quartz phenocrysts were



not observed in pumice from the lower or upper ignimbrites;

9. in microcline-bearing units, unbroken plagioclase, quartz, and microcline crystals are similar in shape and size to plagioclase, quartz, and microcline phenocrysts in coexisting microcline-phyric felsic fragments; and
10. fragments and crystals are enclosed in a fine-grained, largely granoblastic, quartzo-feldspathic aggregate inferred to be recrystallized vitric ash; it is texturally similar to the groundmass of most dacite fragments.

The fine-grained, quartzo-feldspathic aggregate that surrounds fragments and crystals is the dominant component comprising the ignimbrites. Because of its fine metamorphic grain size and generally uniform texture, it is inferred to be recrystallized vitric ash. The aggregate typically consists of subequal amounts of plagioclase, quartz, sericite, and biotite and is thus intermediate in composition between pumice and dacite; in places, it is texturally similar to the groundmass of dacite fragments. The aggregate was probably originally a mixture of ash-sized, pumice and dacite particles.

In terms of size and relative abundance, unbroken plagioclase and quartz crystals are similar to phenocrysts in dacite fragments, but differ from phenocrysts in vitric

felsic fragments and pumice. On this basis, the crystals were probably liberated during explosive fragmentation of dacitic magma, and, thus, the dacite fragments represent a juvenile component.

The apparent absence of quartz phenocrysts in pumice implies that the pumice was not produced from the same magma as the dacite fragments, and is thus a cognate component. However, the structural characteristics and thicknesses of units comprising members 1 and 7 are indicative of ignimbrites, and in such units, pumice would normally be a juvenile component. Assuming that the units comprising members 1 and 7 are indeed ignimbrites, then the pumice must have been incorporated from some other source. There are three possible mixing mechanisms for the incorporation of pumice:

1. dome explosions and mixing in the eruption column prior to column collapse and the generation of pyroclastic flows,
2. eruption (s) of a zoned magma chamber with subsequent mixing in the eruption column prior to collapse and generation of pyroclastic flows, and
3. erosion of pumice from an earlier plinian air-fall blanket by pyroclastic flows.

Domes can contain a significant abundance of pumiceous and non-pumiceous components (Fink, 1983). The pumice in

the Manigotagan River Formation ignimbrites could have been liberated from domes during explosive eruptions, then mixed in the eruption column, and later carried away in pyroclastic flows. Although this process seems viable, some features of the ignimbrites preclude domes as a source of pumice, such as:

1. the lack of compositionally different sedimentary units between lapilli-tuff divisions which suggests that there was insufficient time between eruptions for the redevelopment of domes, and
2. the lack of compositionally similar non-pumiceous components.

Since pumice in most ignimbrites is a juvenile component (Fisher and Schmincke, 1984), the pumice in the Manigotagan River Formation ignimbrites is probably also a primary component. The pumice may have been erupted from a zoned magma chamber in which volatiles accumulated in the upper part. The upper part of the chamber contained plagioclase phenocrysts whereas the deeper part was richer in plagioclase and quartz phenocrysts (Smith, 1979). The initial phase of the eruption produced plagioclase-phyric pumice; as the eruption continued, quartz-plagioclase phyric particles were produced from deeper in the chamber. The components were mixed in the eruption column prior to collapse and onset of pyroclastic flows. To produce the stacked sequence of flow units in the Manigotagan River

Formation ignimbrites, rezoning of the magma chamber would have to occur after each eruption to provide pumice and quartz crystals for subsequent mixing and transport in pyroclastic flows. However, the lack of compositionally different sedimentary units between lapilli-tuff divisions implies that the eruptions occurred in rapid succession so that there was insufficient time for rezoning of the chamber prior to the onset of each pyroclastic flow. Therefore, this mixing model does not account for the stacked sequence of mixed flow units comprising the Manigotagan River Formation ignimbrites.

Another possible source of the pumice could be an earlier plinian air-fall blanket. In this model, plagioclase-phyric pumice, produced during initial plinian eruptive phases from a zoned magma chamber, would have covered the gullied flanks of a stratovolcano. Subsequent collapse of the eruption column, perhaps reflecting decreased eruptive energy, would have produced successive quartz-bearing pyroclastic flows that travelled along different channel-ways on the gullied flank of the stratovolcano and eroded pumice in their path. During eruptive hiatuses, slumping of the channel slopes would have provided new pumice for erosion by pyroclastic flows from subsequent eruptions. Features of the ignimbrites that fit this model are:

1. the coexistence of plagioclase-phyric pumice and quartz crystals in flow units,

2. the variable abundance of pumice in flow units, which probably reflects the amount of pumice available for erosion, and
3. lenticular flow units that probably represent a series of lobes.

The following features of the vitric felsic fragments suggest that they are a cognate component:

1. they differ markedly from the dacite fragments in composition, phenocryst size, and relative phenocryst abundance,
2. although the fragments could have been a source for some of the plagioclase crystals, they could not have provided the larger quartz crystals observed in the granoblastic matrix, and
3. the presence of vitric felsic xenoliths in some dacite fragments indicates that they solidified prior to the eruption of dacitic magma.

The presence of vitric felsic xenoliths in some dacite fragments suggests that solidified vitric felsic fragments were incorporated into dacitic magma at the vent, rather than having been eroded by pyroclastic flows. It is improbable that the fragments were produced by dome explosions, because, in the upper ignimbrite, they occur in every flow unit, and there would be insufficient time for the redevelopment of a dome during presumably short eruption

hiatuses. An alternative source could be erosion of vitric felsic fragments from the vent walls. The fragments could have been mixed in the eruption column and/or in subsequent pyroclastic flows.

Microcline-phyric felsic fragments and microcline crystals occur only in the uppermost flow units of the upper ignimbrite. Unbroken microcline crystals are similar in shape and size to phenocrysts in the microcline-phyric felsic fragments implying that both are juvenile components and were probably derived from the same source. The restriction of microcline to the uppermost flow units could signify that the source magma became more alkaline with depth, or, alternatively, the microcline-bearing units may have been derived from a different magma chamber.

The mafic scoria fragments are a minor component of the upper ignimbrite and are compositionally and texturally different from other components. They are probably cognate and could have been torn from the vent walls or were eroded by pyroclastic flows.

#### 7.2.6 Composite Model for the Emplacement of the Ignimbrites

Analysis of the ignimbrites of the Manigotagan River Formation has yielded the following information:

1. the ignimbrites were apparently erupted in a subaerial environment, but were deposited subaqueously,
2. lapilli-tuff divisions were apparently emplaced by high density turbidity flows,
3. upper tuff divisions were apparently emplaced by low density turbidity flows,
4. flow vectors appear to be at a high angle to the present plane of exposure, and
5. the ignimbrites are composed of a mixture of juvenile and cognate components.

This data best fits the following composite model of emplacement (Fig. 37):

1. an early plinian eruptive phase produced a blanket air-fall deposit composed mainly of plagioclase-phyric pumice,
2. subsequent column collapse produced quartz-bearing pyroclastic flows that travelled along different channels and eroded plagioclase-phyric pumice from the underlying air-fall deposit; the pyroclastic flows entered the sea, transformed into high density turbidity flows and deposited lapilli-tuff divisions farther out in the basin,
3. the relatively high volume of fine ash comprising the upper tuff divisions was probably produced by a combination of processes including (a) separation of

EARLY PLINIAN ERUPTIVE  
PHASE PRODUCES A BLANKET  
AIR-FALL DEPOSIT

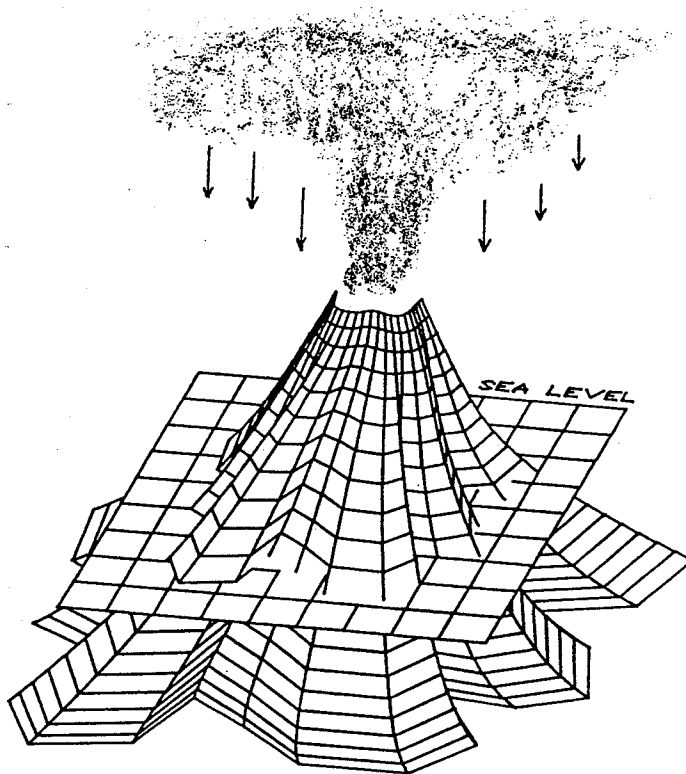


Figure 37: Composite model for the generation and emplacement of the ignimbrites of the Manigotagan River Formation



SUBSEQUENT COLUMN COLLAPSE  
PRODUCES QUARTZ-BEARING  
PYROCLASTIC FLOWS WHICH  
ERODE PLAGIOCLASE-PHYRIC  
PUMICE FROM THE PRECEDING  
AIR-FALL DEPOSIT; THE  
PYROCLASTIC FLOWS ENTER  
THE SEA, TRANSFORM INTO  
HIGH DENSITY TURBIDITY  
FLOWS, AND DEPOSIT LAPILLI-  
TUFF DIVISIONS FARTHER OUT  
IN THE BASIN

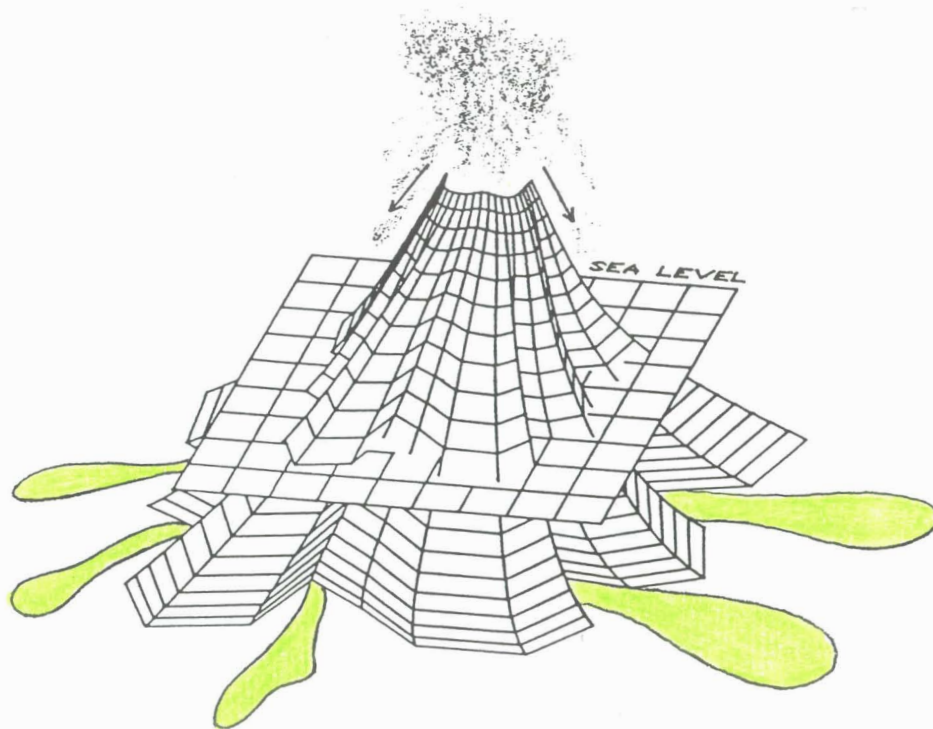


Figure 37: (continued)

FINE ASH WAS PROBABLY  
PRODUCED BY MULTIPLE  
MECHANISMS INCLUDING  
(A) SEPARATION OF FINES  
FROM A COLLAPSING  
ERUPTION COLUMN, (B)  
ELUTRIATION OF FINES  
FROM A FLUIDIZED  
PYROCLASTIC FLOW, (C)  
LITTORAL EXPLOSIONS,  
AND, (D) WAVE WINNOWING  
OF THE PROXIMAL PART  
OF THE LAPILLI-TUFF  
DIVISION; LOW DENSITY  
TURBIDITY FLOWS,  
TRIGGERED BY EARTHQUAKES  
AND/OR WAVE ACTIVITY  
TRANSPORTED AND DEPOSITED  
THE FINE ASH OVER THE  
PRECEDING LAPILLI-TUFF  
DIVISIONS TO FORM THE  
UPPER TUFF DIVISIONS

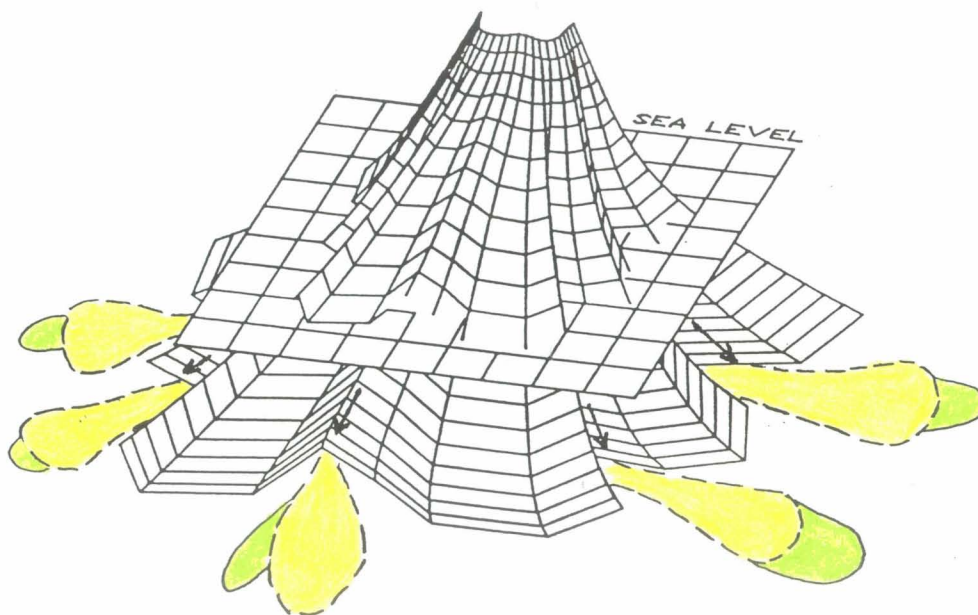


Figure 37: (continued)

finer above a collapsing eruption column (Sparks and Walker, 1977), (b) elutriation of fines from fluidized pyroclastic flows (Walker, 1981; Walker et al., 1980), (c) littoral explosions (Walker, 1979), and (d) wave winnowing of the proximal parts of the lapilli-tuff division; successive, low density turbidity flows triggered by earthquakes and/or wave activity transported and deposited the fine ash over the preceding lapilli-tuff divisions to form the upper tuff divisions, and

4. the cycle was repeated with subsequent eruptions.

This model accounts for the following features of the Manigotagan River Formation ignimbrites:

1. the repetitive sequence of compositionally similar lapilli-tuff and tuff divisions,
2. the mixture of quartz crystals and plagioclase-phyric pumice in flow units,
3. the variable content of pumice in flow units reflecting the amount of available pumice in various channels, and
4. the lenticular morphology of flow units which probably mimics a stacked sequence of lobes.

Wright and Mutti (1981) have proposed a similar model for the genesis of the Dali Ash. In their model, a subaerially erupted pumiceous pyroclastic flow entered the sea,

transformed into a high density turbidity flow, and deposited a lower normally graded division. Subsequently, a series of ash turbidites, representing slumps from the submarine slopes of the lower subaqueous pyroclastic flow deposit, or later, lower concentration pumice flows, deposited a thin-bedded, upper tuff division over the preceding pyroclastic flow deposit. Features of the Manigotagan River Formation ignimbrites that resemble the general features of the Dali Ash are:

1. the presence of lower normally graded divisions interpreted to be high density turbidites, and
2. the presence of thin-bedded upper divisions interpreted to be low density turbidites.

In contrast to the ignimbrites of the Manigotagan River Formation, the Dali Ash consists of only one flow unit enclosed in marine mudstone and its lower massive division is composed of tuff rather than lapilli-tuff. These differences only reflect the eruptive source rather than the emplacement mechanism. The Manigotagan River Formation ignimbrites, which, in contrast to the Dali Ash, are a stacked sequence of coarser flow units, were emplaced by pyroclastic flows fed by a succession of presumably short-lived eruptions, and the tephra that comprises the lower lapilli-tuff divisions was coarser than the Dali Ash. Although the ignimbrites of the Manigotagan River Formation apparently had a different eruptive source than the Dali Ash, they were probably emplaced by a similar mechanism.

### 7.3 SUBAQUEOUS TEPHRA-FALL DEPOSITS

Lapilli-tuff and tuff of Member 2, which ranges in thickness from 17 to 91 m and thins to the northwest, are interpreted to be subaqueous tephra-fall deposits. The deposit has been divided into three compositionally distinct, laterally continuous, blanket-like units. The lower (2a) and upper (2c) units are variable in composition and consist of both mafic and felsic fragments and sparse crystal particles in a dominantly mafic matrix. In contrast, the middle unit (2b) is compositionally uniform and is composed of mafic fragments and sparse crystal particles enclosed in a mafic matrix. Each unit consists of alternating, ungraded, fragment-rich and fragment-poor beds.

#### 7.3.1 Environment of Eruption and Deposition

Eruptive environments for the lapilli-tuff and tuff of Member 2 are difficult to deduce with absolute certainty, but the following data suggests that the eruptions occurred in relatively shallow water (<500 m), or, possibly even in a subaerial environment:

1. the presence of highly vesicular fragments indicating a low ambient confining pressure (Cas and Wright, 1987), and
2. an abundance of conglomerate in the overlying subaqueous fan succession indicative of a large, nearby landmass.

Lapilli-tuff and tuff of Member 2 were apparently deposited in a subaqueous environment for the following reasons:

1. pillowed lava flows and turbidites of Member 3 occur immediately above Member 2,
2. inferred subaqueous pyroclastic flow deposits (Member 1) occur immediately below Member 2, and
3. tuff vesicles, accretionary lapilli, and impact sags, which are indicative of subaerial deposition (Moore, 1985), were not observed.

It is difficult to deduce the water depth in which the preserved succession accumulated, but the apparent lack of abundant tractional structures in the deposit could imply that most of the tephra was deposited below storm wave base (Cas et al., 1989).

### 7.3.2 Evidence of Hot Particles

A unique feature of the mafic lapilli-tuff and tuff unit (2b) is the presence of well defined rims on type 1 mafic fragments. These rims have the following characteristics:

1. they are composed largely of chlorite with lesser hematite, actinolite, and epidote,
2. they have a variable thickness from 0.5 to 10 mm,
3. rim/core boundaries are gradational or less commonly they are sharp,

4. rims typically contain fewer amygdules and plagioclase microlites than fragment cores, and
5. amygdules in the rim are dominantly polycrystalline plagioclase as opposed to polycrystalline quartz amygdules that are dominant in fragment cores.

Baldwin (1987) proposed a post-depositional alteration model to explain the development of rims on hot fragments that were incorporated into a debris flow. In his model, a heat-induced reaction occurred between hot fragment cores and the surrounding, relatively cold, water saturated matrix. The reaction continued until the temperature of the fragments became equal to that of the water-saturated matrix. The rims on the type 1 fragments were probably also produced by heat-induced alteration on partly or completely chilled fragments.

The lower abundance of amygdules and microlites in the rims on type 1 fragments suggests that alteration could have been focused on, and limited by previously chilled, and, thus, more reactive rims. However, the very fine-grain size and low crystallinity of the fragments suggests that they were completely chilled, either in air or water, prior to alteration. Post-depositional, heat-induced, alteration of completely chilled fragments accounts for:

1. fewer microlites in the rim,
2. the variable thickness of the rims,

3. the chlorite-rich nature of the rim,
4. the difference in amygdule composition between rim and core, and
5. the development of both gradational and sharp boundaries between rim and core.

Although post-depositional, heat-induced alteration could account for the lower abundance of plagioclase microlites in the rims, the lower abundance of amygdules is more difficult to explain. The heat-induced alteration could have initially produced a ductile rim, which, in turn, promoted the collapse of vesicles.

The type 2 and 3 mafic fragments typically contain more chlorite than type 1 fragments indicating that they were more pervasively altered. The more thorough alteration of these fragments could be due to their smaller size and/or lower crystallinity (more reactive). The presence of mafic fragments showing variable degrees of post-depositional, heat-induced alteration indicates that most of the fragments in the mafic lapilli-tuff and tuff were still hot when they were incorporated in the deposit.

### **7.3.3 Emplacement of Lapilli-Tuff and Tuff of Member 2**

Lapilli-tuff and tuff that comprise Member 2 have the following general characteristics:



1. beds defined by bed to bed variations in fragment abundance and fragment size; fragment-rich lenses occur in some beds,
2. beds are poorly sorted, matrix supported, ungraded, and range in thickness from 5 to 400 cm,
3. some beds contain outsized volcanic bombs, and
4. bed contacts are gradational rather than sharp, but the transition from one bed to the next normally occurs within a vertical distance of 1 to 5 cm.

These characteristics could be indicative of (1) subaqueous redeposition by mass flow processes, or (2) subaqueous tephra-fall deposits.

#### **7.3.3.1 Subaqueous Mass Flow Deposits**

The lapilli-tuff and tuff units have some features that resemble subaqueous mass flow deposits. These are:

1. poor sorting and a matrix-supported framework with local outsized fragments (Fisher, 1982; Nemec and Steel, 1984),
2. massive to diffusely layered, amalgamated, tabular beds (Cas et al., 1989),
3. fragment concentrations in discrete pockets or lenses (Cas et al., 1989), and
4. ungraded beds (Norin, 1958).

Despite these similarities, the lapilli-tuff and tuff units lack many of the other characteristics of subaqueous mass flow deposits which include:

1. reverse grading (Nemec and Steel, 1984),
2. sharp, but not obviously erosive contacts (Fisher, 1982),
3. tractional structures (Cas et al., 1989), and
4. sandy cappings (Nemec and Steel, 1984).

An alternative emplacement mechanism that could account for the characteristics of the lapilli-tuff and tuff units is tephra-fallout from subaerial eruptions.

#### **7.3.3.2 Subaqueous Tephra-Fall Deposits**

The lapilli-tuff and tuff units of Member 2 have many features that resemble the general features of other relatively coarse-grained, mafic tephra-fall deposits. Such features include:

1. regular internal bedding with a narrow bed thickness range (Kokelaar, 1986; Houghton and Hackett, 1984; Cas et al., 1989),
2. gradational (diffuse) bed contacts (Cas et al., 1989; Ross, 1986; Houghton and Hackett, 1984), and
3. isolated, outsized volcanic bombs (Cas et al., 1989; Moore, 1985).

The great thickness of lapilli-tuff and tuff (up to 91 m) comprising Member 2, the regular internal bedding with gradational bed contacts, and the presence of isolated, outsized volcanic bombs are all consistent with the succession being emplaced by tephra-fall in proximity to a vent (Fisher and Schmincke, 1984; Cas et al., 1989). However, if the tephra was emplaced in a proximal setting, then cone-like, radially dipping bedding attitudes should be apparent (Cas et al., 1989). In contrast, the three units comprising Member 2 are laterally continuous, blanket-like deposits. This blanket-like morphology could indicate that the tephra was more widely dispersed from central vent-type eruptions (Sparks et al., 1983; Barberi et al., 1989; Rowley, 1978; Fiske and Sigurdsson, 1982), or that it was erupted from flank fissures (Walker et al., 1984).

Flank fissure eruptions are favoured because central vent-type eruptions, that widely disperse tephra (phreatoplinian), typically produce thin, fine-grained deposits (Fisher and Schmincke, 1984). In addition, flank fissure eruptions could account for the presence of mafic lava flows in the lower part of Member 3 (Plate 1).

#### **7.3.4 Emplacement of Volcanic Conglomerate and Sandstone**

At one outcrop in the northwestern part of the map area (Fig. 21), volcanic conglomerate and sandstone sequences were observed at the base of the mafic to intermediate

lapilli-tuff and tuff unit (2a). The volcanic conglomerate and sandstone sequences have a maximum possible lateral extent of 150 m and cannot be traced laterally to adjacent outcrops.

The volcanic conglomerate and sandstone sequences share many of the structural characteristics of the repetitive lapilli-tuff and tuff divisions of the upper and lower ignimbrites. Therefore, the volcanic conglomerate and sandstone may also represent the products of subaqueous pyroclastic flows that were fed directly from subaerial eruptions. However, although there is a similarity in structural characteristics between the conglomerate and sandstone sequences and ignimbrites, there are other significant differences. The two sequences differ markedly from each other, and from the underlying ignimbrite, in terms of composition and they lack pumice (cf. Tables 7, 8, 10). The conglomerate and sandstone sequences are thus compositionally different from the ignimbrites and were probably not fed directly from subaerial eruptions.

Similar structural characteristics imply that the conglomerate and sandstone units were emplaced by the same mechanisms as the ignimbrites, namely high and low density turbidity flows. The conglomerate beds, like the lapilli-tuff divisions, have many of the characteristics of high density turbidites, including (1) erosive basal contacts (Lowe, 1982), (2) similar bed thicknesses (Cas, 1979), (3)

normal, or reverse to normal grading (Cas, 1979; Lowe, 1982), and (4) poor sorting and a matrix-supported framework (Lowe, 1982; Wright and Mutti, 1981). Thus, they were apparently emplaced by high density turbidity flows. The sandstone beds, like the upper tuff divisions, have the characteristics of low density turbidites (Walker, 1984; Bouma, 1962) including (1) similar bed thicknesses, (2) sharp, planar, and locally scoured contacts, and (3) normally graded to locally laminated beds. Thus, they were apparently emplaced by low density turbidity flows that possibly evolved from high density turbidity flows (Lowe, 1982). The apparently isolated occurrence of conglomerate and sandstone sequences at the base of unit 2a suggests that the sequences could be either channels within tephra-fall deposits or erosional remnants that were subsequently draped by mafic to intermediate, lapilli-tuff and tuff, fall deposits.

#### 7.3.5 Eruption Type

The morphological characteristics of volcanic particles have been used to characterize eruption types (Sheridan and Wohletz, 1983; Heiken, 1974). In the lapilli-tuff and tuff of Member 2, the original characteristics of ash-sized particles have been destroyed by metamorphic recrystallization, and only the larger, lapilli- to block-sized particles retain some diagnostic characteristics of

their fragmentation history. The general characteristics of the components comprising lapilli-tuff and tuff of Member 2 suggest that the tephra was produced by phreatomagmatic eruptions. Features of the deposit that are consistent with phreatomagmatic deposits are:

1. a high abundance (35 to 97%) of fine-grained, mafic particles inferred to be recrystallized mafic vitric ash (Cas and Wright, 1987; Fisher and Schmincke, 1984),
2. a high abundance of angular to subangular particles (Moore, 1985; Sheridan and Wohletz, 1983),
3. a high abundance of accessory particles, especially in the lower (2a) and upper (2c), mafic to intermediate lapilli-tuff and tuff units (Rowley, 1978),
4. mafic fragments that show a wide range in vesicularity (0 to 70%) and have a low crystallinity (Houghton and Wilson, 1989), and
5. the local occurrence of outsized, volcanic bombs (Cas et al., 1989).

Non-vesicular to highly vesicular mafic fragments were probably produced by phreatomagmatic explosions of vesiculating magma where fragmentation occurred by both magmatic explosions and contact surface steam explosions. Lava flows were not an important source of tephra as indicated by the low crystallinity of the mafic fragments.

Accessory felsic fragments, were probably derived from the underlying felsic volcanic substrate (Member 1 ignimbrite and the Narrows Formation) during the initial phreatomagmatic eruptive phases. Accessory fragments, that were derived from underlying units, have also been observed elsewhere (Walker et al., 1984).

## Chapter VIII

### CONCLUSIONS

A number of conclusions can be drawn from this study of three pyroclastic members of the Manigotagan River Formation.

1. The abundance of conglomerate in the subaqueous fan succession (Member 3), indicative of a large, nearby landmass, and the presence of tephra-fall deposits (Member 2) suggest that the ignimbrites were erupted subaerially.
2. The ignimbrites of this study differ from subaerial ignimbrites in terms of structural characteristics and occur in a volcanic and sedimentary sequence that shows evidence of subaqueous deposition. Therefore, the ignimbrites were apparently emplaced in a subaqueous environment.
3. The structural characteristics of the lower lapilli-tuff divisions suggest that they were deposited by gravelly, high density turbidity flows.
4. The structural characteristics of the upper tuff divisions and their spatial association with lapilli-tuff divisions suggests that they were emplaced by a series of low density turbidity flows.



5. The repetitive sequence of compositionally similar, lapilli-tuff and tuff divisions without intercalated, compositionally different, sedimentary units implies that flow units were emplaced in rapid succession and were probably fed directly from multiple, shortspaced eruptions.
6. The morphology of channels in the subaqueous fan succession (Member 3) indicates that flow vectors are at a high angle to the present plane of exposure. Therefore, the lenticular flow units probably represent a series of lobes.
7. A comparison of phenocryst sizes, free crystal sizes, and plagioclase/quartz ratios has revealed that dacite fragments in the ignimbrites are juvenile, but pumice and vitric felsic fragments are cognate. The pumice was probably eroded from an earlier, plinian air-fall deposit by pyroclastic flows. Vitric felsic fragments were apparently eroded from the vent walls, mixed in the eruption column, and subsequently incorporated into pyroclastic flows.
8. The best composite model to account for the characteristics of the ignimbrites involves a number of stages: (a) an early plinian eruptive phase produced a blanket air-fall deposit composed largely of plagioclase-phyric pumice, (b) subsequent column collapse produced quartz-bearing pyroclastic flows that travelled along different channels and eroded

plagioclase-phyric pumice from the underlying air-fall deposit; the pyroclastic flows entered the sea, transformed into high density turbidity flows, and deposited lapilli-tuff divisions farther out in the basin, (c) fine ash was probably produced by a multiple mechanisms including (i) separation of fines from a collapsing eruption column, (ii) elutriation of fines from fluidized pyroclastic flows, (iii) littoral explosions, and (iv) wave winnowing of the proximal part of the lapilli-tuff division; successive low density turbidity flows, triggered by earthquakes and/or wave activity, transported and deposited fine ash over the preceding lapilli-tuff divisions to form the upper tuff divisions, and (d) the cycle was repeated with subsequent eruptions.

9. The presence of highly vesicular fragments and abundant channel-fill conglomerate in the overlying subaqueous fan succession (Member 3) suggest that tephra comprising lapilli-tuff and tuff of Member 2 were derived from shallow water or subaerial eruptions.
10. Lapilli-tuff and tuff of Member 2 are underlain and overlain by subaqueously deposited units and apparently lack tuff vesicles, accretionary lapilli, and impact sags indicative of subaerial emplacement. Based on this evidence, the lapilli-tuff and tuff were apparently emplaced subaqueously. The apparent

lack of tractional structures suggests that the lapilli-tuff and tuff were deposited below storm wave base.

11. The very fine grain size and low crystallinity of mafic fragments in the middle, mafic lapilli-tuff and tuff unit (2b) suggest that the fragments were completely chilled prior to alteration. The presence of mafic fragments showing variable degrees of post-depositional, heat-induced alteration indicates that most of the fragments were still hot when they were incorporated in the deposit.
12. The structural and grain size characteristics of the three lapilli-tuff and tuff units suggest that they were emplaced as tephra fall in a proximal setting. The laterally continuous, blanket-like character of the units imply that they were erupted from a flank fissure or fissures.
13. The component characteristics of tephra comprising lapilli-tuff and tuff of Member 2 are in agreement with the products of phreatomagmatic eruptions. The accessory felsic fragments were probably derived from the felsic volcanic substrate during initial phreatomagmatic eruptive phases.

## BIBLIOGRAPHY

- Ayres, L.D., 1982, Pyroclastic rocks in the geologic record: In Ayres, L.D. (ed.) Pyroclastic volcanism and deposits of Cenozoic intermediate to felsic volcanic islands with implications for Precambrian greenstone-belts volcanoes: Geol. Assoc. Canada, Short Course Notes, No. 2, p. 1-17.
- Ayres, L.D., 1983, Bimodal volcanism in Archean greenstone belts exemplified by greywacke composition, Lake Superior Park, Ontario: Can. Jour. Earth Sci., V. 20, p. 1168-1194.
- Ayres, L.D. and Thurston, P.C., 1985, Archean supracrustal sequences in the Canadian Shield: An overview: In Ayres, L.D., Thurston, P.C., Card, K.D. and Weber, W. (eds.) Evolution of Archean supracrustal sequences: Geol. Assoc. Canada, Sp. Pap. 28, p. 343-380.
- Baldwin, D.A., 1987, Physical volcanology of the northwest segment of the Karsakuwigamak block, Proterozoic Rusty Lake metavolcanic belt, northern Manitoba: Unpubl. Phd. thesis, Univ. of Manitoba, 438 p.
- Barberi, F., Cioni, R., Rosi, M., Santacroce, R., Sbrana, A., and Vecci, R., 1989, Magmatic and phreatomagmatic phases in explosive eruptions of Vesuvius as deduced by grain-size and component analysis of the pyroclastic deposits: Jour. Volc. Geotherm. Res., V. 38, p. 287-307.
- Barley, M.E., Dunlop, J.S.R., Glover, J.E. and Groves, D.I., 1979, Sedimentary evidence for an Archean shallow-water volcanic-sedimentary facies, eastern Pilbara Block, Western Australia: Earth Planet. Sci. Let., V. 43, p. 74-84.
- Blatt, H., Middleton, G. and Murray, R., 1980, Origin of Sedimentary Rocks: Prentice-Hall, Inc., Englewood Cliffs, N.J., 634 p.
- Bond, G.C., 1973, A late Paleozoic volcanic arc in the eastern Alaska Range: J. Geol., V. 81, p. 557-575.
- Bouma, A.H., 1962, Sedimentology of some flysch deposits. Elsevier., Amsterdam, 169 p.

- Brazier, S., Davis, A.N., Sigurdsson, H. and Sparks, R.S.J., 1982, Fall-out and deposition of volcanic ash during the 1979 explosive eruption of the Soufriere of St. Vincent: Jour. Volc. Geotherm. Res., V. 14, p. 335-359.
- Buck, P.S., 1978, A Caldera sequence in the early Precambrian Favourable Lake Volcanic Complex, Northwestern, Ontario: Unpubl. MSc thesis, Univ. of Manitoba, 140 p.
- Busby-Spera, C.J. and White, D.L., 1987, Variations in peperite textures associated with differing host-sediment properties: Bull. Volc., V. 49, p. 765-775.
- Campbell, F.H.A., 1971, Stratigraphy and sedimentation of part of the Rice Lake Group, Manitoba: In McRitchie, W.D. and Weber, W. (eds.) Geology and geophysics of the Rice Lake region, southeastern Manitoba (Project Pioneer): Man. Mines Branch, Publ. 71-1, p. 135-188.
- Car, D.P., 1980, A volcanoclastic sequence on the flank of an early Precambrian stratovolcano, Lake of the Woods, northwestern Ontario: Unpubl. MSc thesis, Univ. of Manitoba, 111 p.
- Carey, S.N. and Sigurdsson, H., 1980, The Roseau Ash: deep-sea tephra deposits from a major eruption on Dominica, Lesser Antilles arc: Jour. Volc. Geotherm. Res., V. 7, p. 67-86.
- Cas, R.A.F., 1979, Mass-flow arenites from a Paleozoic interarc basin, New South Wales, Australia: mode and environment of emplacement: Jour. Sed. Petrol., V. 49, p. 29-44.
- Cas, R.A.F., Landis, C.A. and Fordyce, R.E., 1989, A monogenetic, Surtla-type, Surtseyan volcano from the Eocene-Oligocene Waiareka-Deborah volcanics, Otago, New Zealand: a model: Bull. Volc., V. 51, p. 281-298.
- Cas, R.A.F. and Wright, J.V., 1987, Volcanic successions: modern and ancient: a geological approach to processes, products and successions: Allen & Unwin Ltd., North Sydney, 528 p.
- Church, N. and Wilson, H.D.B., 1971, Volcanology of the Wanipigow Lake-Beresford Lake Area: In McRitchie, W.D. and Weber, W. (eds.) Geology and geophysics of the Rice Lake region, southeastern Manitoba (Project Pioneer): Man. Mines Branch, Publ. 71-1, p. 127-134.
- Cooke, H.C., 1922, Geology and mineral resources of Rice Lake and Oiseau River areas, Manitoba: Geol. Surv. Can. Summary Report, 1921, Part C.

- Condie, K.C., Macke, J.F. and Reimer, T.O., 1970, Petrology and geochemistry of early Precambrian greywackes from the Fig Tree Group, South Africa: *Geol. Soc. Amer. Bull.*, V. 81, p. 2759-2776.
- DeLury, J.S., 1921, Mineral Prospects in southeastern Manitoba: *Manitoba Government Bulletin, Commissioner of Northern Manitoba*, 55 p.
- DeLury, J.S., 1937, Boundary area, southeastern Manitoba: *Manitoba Department of Mines and Natural Resources, Mines Branch, Geological Map 37-4*.
- Dimroth, E. and Demarke, J., 1978, Petrography and mechanism of eruption of the Archean Dalember Tuff, Rouyn-Noranda, Quebec, Canada: *Can. Jour. Earth Sci.*, V. 15, p. 1712-1723.
- Dimroth, E. and Rocheleau, M., 1979, Volcanology and sedimentology of the Rouyn-Noranda area: *Guidebook, Excursion A1, Quebec, 1979, Geol. Assoc. Can.*, 200 p.
- Donaldson, J.A. and Jackson, G.D., 1965, Archean sedimentary rocks of North Spirit Lake area, northwestern Ontario: *Can. Jour. Earth Sci.*, V. 2, p. 622-647.
- Druitt, T.H. and Sparks, R.S.J., 1982, A proximal ignimbrite breccia facies on Santorini, Greece: *Jour. Volc. Geotherm. Res.*, V. 13, p. 147-171.
- Dunlop, J.S.R. and Buick, R., 1981, Archean epiclastic sediments derived from mafic volcanics, North Pole, Pilbara Block, Western Australia: In Glover, J.E., and Groves, D.I. (eds.) *Archean Geology, second international symposium: Geol. Soc. Australia, Sp. Publ. 7*, p. 225-233.
- Eriksson, K.A., 1978, Alluvial and destructive beach facies from the Archean Moodies Group, Barberton Mountain Land, South Africa and Swaziland. In Miall, A.D. (ed.) *Fluvial Sedimentology. Can. Soc. Pet. Geol., Mem. 5*, p. 287-311.
- Fink, J.H., 1983, Structure and emplacement of a rhyolitic obsidian flow: Little Glass Mountain, Medicine Lake Highland, northern California: *Geol. Soc. Am. Bull.*, V. 94, p. 362-380.
- Fisher, R.V., 1961, Proposed classification of volcanoclastic sediments and rocks: *Geol. Soc. Am. Bull.*, V. 72, p. 973-982.
- Fisher, R.V., 1966, Rocks composed of volcanic fragments and their classification: *Earth Science Reviews*, V. 1, p. 287-298.

- Fisher, R.V., 1977, Geologic guide to subaqueous volcanic rocks in the Nipomo, Pismo Beach and Avila Beach areas: Geol. Soc. Am. Penrose Conf. on the geology of subaqueous volcanic rocks, Nov. 1977.
- Fisher, R.V., 1979, Models for pyroclastic surges and pyroclastic flows: Jour. Volc. Geotherm. Res., V. 6, p. 305-318
- Fisher, R.V., 1982, Debris flows and lahars: In Ayres, L.D. (ed.) Pyroclastic volcanism and deposits of Cenozoic intermediate to felsic volcanic islands with implications for Precambrian greenstone-belt volcanoes: Geol. Assoc. Can., Short Course Notes, V. 2, p. 136-190.
- Fisher, R.V., 1984, Submarine volcanoclastic rocks: In Kokelaar, B.P. and Howells, M.F. (eds) Marginal basin geology: volcanic and associated sedimentary and tectonic processes in modern and ancient marginal basins: Geol. Soc. Lond. Sp. Publ., no. 16, p. 5-27.
- Fisher, R.V. and Schmincke, H.U., 1984, Pyroclastic Rocks: Springer-Verlag, Berlin, Heidelberg, New York, Tokyo, 472 p.
- Fiske, R.S., 1963, Subaqueous pyroclastic flows in the Ohanapecoh Formation, Washington: Geol. Soc. Am. Bull., V. 74, p. 391-406.
- Fiske, R.S., 1969, Recognition and significance of pumice in marine pyroclastic rocks: Geol. Soc. Am. Bull., V. 80, p. 1-8.
- Fiske, R.S. and Matsuda, T., 1964, Submarine equivalents of ash flows in the Tokiwa Formation, Japan: Am. Jour. Sci., V. 262, p. 76-106.
- Fiske, R.S. and Sigurdsson, H., 1982, Soufriere Volcano, St. Vincent: Its 1979 eruption observed from the ground, aircraft and satellites: Science, V. 216, p. 1105-1106.
- Francis, E.H. and Howells, M.F., 1973, Transgressive welded ash-flow tuffs among the Ordovician sediments of N.E. Snowdonia: Jour. Geol. Soc. Lond., V. 129, p. 621-641.
- Glikson, A.Y., 1976, Stratigraphy and evolution of primary and secondary greenstones: significance of data from shields of the southern hemisphere: In Windley, B.F. (ed.) The early history of the earth: New York, John Wiley, p. 257-277.
- Goodwin, A.M. and Smith, I.E.M., 1980, Chemical discontinuities in Archean metavolcanic terranes and the development of the Archean crust: Prec. Res., V. 10, p. 301-311.

- Heiken, G.H., 1974, An atlas of volcanic ash. Smithsonian Contr. Earth Sci., No. 12. 101 p.
- Henderson, J.B., 1972, Sedimentology of Archean turbidites at Yellowknife, Northwest Territories: Can. Jour. Earth Sci., V. 9, p. 882-902.
- Hildreth, W., Grunder, R.L. and Drake, R.E., 1984, The Loma Seca Tuff and the Calabogogos caldera: A major ash-flow and caldera complex in the southern Andes of central Chile: Geol. Soc. Am. Bull., V. 95, p. 45-54.
- Houghton, B.F. and Hackett, W.R., 1984, Strombolian and phreatomagmatic deposits of Ohakune Craters, Ruapehu, New Zealand: A complex interaction between external water and rising basaltic magma: Jour. Volc. Geotherm. Res., V. 21, p. 207-231.
- Houghton, B.F. and Wilson, C.J.N., 1989, A vesicularity index for pyroclastic deposits: Bull. Volc., V. 51, p. 451-462.
- Howells, M.F., Campbell, S.D.G and Reedman, A.J., 1985, Isolated pods of subaqueous welded ash-flow tuff: a distal facies of the Capel Curig Volcanic Formation (Ordovician), North Wales: Geol. Mag., V. 122, p. 175-180.
- Kano, K., Nakano, S., and Mimura, K., 1988, Deformation structures in shale bed indicate flow direction of overlying Miocene subaqueous pyroclastic flow: Bull. Volc., V. 50, p. 380-385.
- Koch, A.J. and McLean, H., 1975, Pleistocene tephra and ash-flow deposits in the volcanic highlands of Guatemala: Geol. Soc. Am. Bull., V. 86, p. 529-541.
- Kokelaar, B.P., 1986, Magma-water interactions in subaqueous and emergent basaltic volcanism: Bull. Volc., V. 48, p. 275-289.
- Kuenzi, W.D., Horst, O.H. and McGhee, R.V., 1979, Effect of volcanic activity on fluvial-deltaic sedimentation in a modern arc-trench gap, southwestern Guatemala: Geol. Soc. Am. Bull., V. 90, p. 827-838.
- Lajoie, J., 1984, Volcaniclastic rocks: In Walker, R.G. (ed) Facies Models, 2nd edn: Geol. Assoc. Can., Geosci. Can. Repr. Ser. 1., p. 39-52.
- Lajoie, J. and Ludden, J.N., 1984, Petrology of the Archean Pontiac and Kewagama sediments and implications for the stratigraphy of the southern Abitibi belt: Can. Jour. Earth Sci., V. 21, p. 1305-1314.



- Leat, P.T., 1985, Facies variations in peralkaline ash-flow tuffs from the Kenya Rift Valley: *Geol. Mag.*, V. 122, p. 139-150.
- Lowe, D.R., 1982, Sediment gravity flows: II, depositional models with special reference to the deposits of high density turbidity currents: *Jour. Sed. Petrol.*, V. 52, p. 279-297.
- Lowman, R.D.W. and Bloxam, T.W., 1981, The petrology of the Lower Paleozoic Fishguard Volcanic Group and associated rocks E. of Fishguard, N. Pembrokeshire (Dyfed), South Wales: *Jour. Geol. Soc. Lond.*, V. 138, p. 47-68.
- McRitchie, W.D. and Weber, W. (eds), 1971, Geology and geophysics of the Rice Lake region, southeastern Manitoba (Project Pioneer): *Man. Mines Branch Publ.* 71-1, 430 p., 15 maps.
- Meyn, H.D. and Palonen, P.A., 1980, Stratigraphy of an Archean submarine fan: *Prec. Res.*, V. 12, p. 257-285.
- Moore, E.S., 1914, Region east of the south end of Lake Winnipeg: *Geol. Surv. Can.*, Summary Report, 1912.
- Moore, J.G., 1985, Structure and eruptive mechanisms at Surtsey volcano, Iceland: *Geol. Mag.*, V. 122, p. 649-661.
- Niem, A.R., 1977, Mississippian pyroclastic flow and ash-fall deposits in the deep-marine Ouachita flysch basin, Oklahoma and Arkansas: *Geol. Soc. Am. Bull.*, V. 88, p. 49-61.
- Nemec, W. and Steel, R.J., 1984, Alluvial and Coastal conglomerates: their significant features and some comments on gravelly mass-flow deposits: In Koster, E.H. and Steel, R.H. (eds.) *Sedimentology of Gravels and Conglomerates: Can. Soc. Petrol. Geol.*, Mem. 10, p. 1-31.
- Norin, E., 1958, The sediments of the central Tyrrhenian Sea: In Pettersson, H. (ed.) *Reports of the Swedish Deep-Sea expedition, 1947-1948, Sediment cores from the Mediterranean Sea and the Red Sea: Elanders Boktryckeri Aktiebolag, Goteborg*, p. 1-136.
- Ojakangas, R.W., 1985, Review of Archean clastic sedimentation, Canadian Shield: major felsic volcanic contributions to turbidite and alluvial fan-fluvial facies associations: In Ayres, L.D., Thurston, P.C., Card, K.D. and Weber, W. (eds.) *Evolution of Archean supracrustal sequences: Geol. Assoc. Canada, Sp. Pap.* 28, p. 23-47.

- Owens, D.J., 1986, Stratigraphy and structure of the Upper Stormy Lake Formation, Rice Lake greenstone belt: In Man. Energy and Mines, Report of Field Activities, p. 115-119.
- Padgham, W.A., 1980, An Archean ignimbrite at Yellowknife and its relationship to the Kam Formation basalts: Prec. Res., V. 12, p. 99-113.
- Parsons, W.H., 1969, Criteria for the recognition of volcanic breccias: A review: In Larsen, L., Manson, V. and Prinz, M. (eds.) Igneous and metamorphic geology: Geol. Soc. Am. Mem. 115, p. 263-304.
- Reedman, A.J., Howells, M.F., Orton, G. and Campbell, S.D.G., 1987, The Pitts Head Tuff Formation: a subaerial to submarine welded ash-flow tuff of Ordovician age, North Wales: Geol. Mag., V. 124, p. 427-439.
- Ross, G.M., 1986, Eruptive styles and construction of shallow marine mafic tuff cones in the Narakay Volcanic Complex, Proterozoic Hornby Bay Group, Northwest Territories, Canada: Jour. Volc. Geotherm. Res., V. 27, p. 265-297.
- Rowley, K., 1978, Late Pleistocene pyroclastic deposits of Soufriere Volcano, St. Vincent, West Indies: Geol. Soc. Am. Bull. V. 89, p. 825-835.
- Russel, G.A., 1952, Geology of the Lily Lake-Kickley Lake area: Man. Dept. Mines and Natural Resources, Mines Branch, Publ. 50-3, 16 p.
- Self, S. and Rampino, M.R., 1981, The 1883 eruption of Krakatau: Nature, V. 294, p. 699-704.
- Seneshen, D.M., 1986, Stratigraphy of the Manigotagan River Formation, Rice Lake Greenstone Belt: In Man. Energy and Mines, Report of Field Activities, p. 109-114.
- Seneshen, D.M. and Owens, D.J., 1985, Geological investigations in the Stormy Lake area: In Man. Energy and Mines, Report of Field Activities, p. 112-119.
- Shanmugam, G. and Moiola, R.J., 1988, Submarine fans: characteristics, models, classification, and reservoir potential: Earth Sci. Rev., V. 24, p. 383-428.
- Sheridan, M.F., 1979, Emplacement of pyroclastic flows: A review: In Chapin, C.E. and Elston, W.E. (eds.) Ash-flow tuffs: Geol. Soc. Am. Sp. Pap. 180, p. 125-136.
- Sheridan, M.F. and Wohletz, K.H., 1983, Hydrovolcanism: Basic considerations and review: Jour. Volc. Geotherm. Res., V. 17, p. 1-29.

- Sigurdsson, H., 1982, Volcanogenic sediments in island arcs: In Ayres, L.D. (ed.) Pyroclastic volcanism and deposits of Cenozoic intermediate to felsic volcanic islands with implications for Precambrian greenstone-belt volcanoes: Geol. Assoc. Canada, Short Course Notes, No. 2, p. 221-293.
- Sigurdsson, H., Sparks, R.S.J., Carey, S.N. and Huang, T.C., 1980, Volcanogenic sedimentation in the Lesser Antilles arc: Jour. Geology, V. 88, p. 523-540.
- Sparks, R.S.J., 1975, Stratigraphy and geology of the ignimbrites of Vulcini Volcano, central Italy: Geol. Rund., V. 64, p. 497-523.
- Smith, R.L., 1979, Ash-Flow magmatism: In Chapin, C.E. and Elston, W.E. (eds.) Ash-flow tuffs: Geol. Soc. Am. Sp. Pap. 180, p. 5-27.
- Sparks, R.S.J., 1976, Grain size variations in ignimbrites and implications for the transport of pyroclastic flows: Sedimentology, V. 23, p. 147-188.
- Sparks, R.S.J., Brazier, S., Huang, T.C. and Muerdter, D., 1983, Sedimentology of the deep-sea tephra layer in the Aegean and eastern Mediterranean: Marine Geology, V. 54, p. 131-167.
- Sparks, R.S.J., Sigurdsson, H. and Carey, S.N., 1980, The entrance of pyroclastic flows into the sea, I. Oceanographic and geologic evidence from Dominica, Lesser Antilles: Jour. Volc. Geotherm. Res., V. 7, p. 87-96.
- Sparks, R.S.J. and Walker, G.P.L., 1977, The significance of vitric-enriched air-fall ashes associated with crystal-enriched ignimbrites: Jour. Volc. Geotherm. Res., V. 2, p. 329-341.
- Stockwell, C.H., 1945a, Beresford Lake, Manitoba; Geol. Surv. Can., Map 809A.
- Stockwell, C.H., 1945b, Gem Lake, Manitoba; Geol. Surv. Can., Map 811A.
- Stockwell, C.H. and Lord, C.S., 1939, Halfway Lake-Beresford Lake, Manitoba: Geol. Surv. Canada, Mem. 219, p. 1-67.
- Tassé, N., Lajoie, J. and Dimroth, E., 1978, The anatomy and interpretation of an Archean volcanoclastic sequence, Noranda region, Quebec: Can. Jour. Earth Sci., V. 15, 874-888.

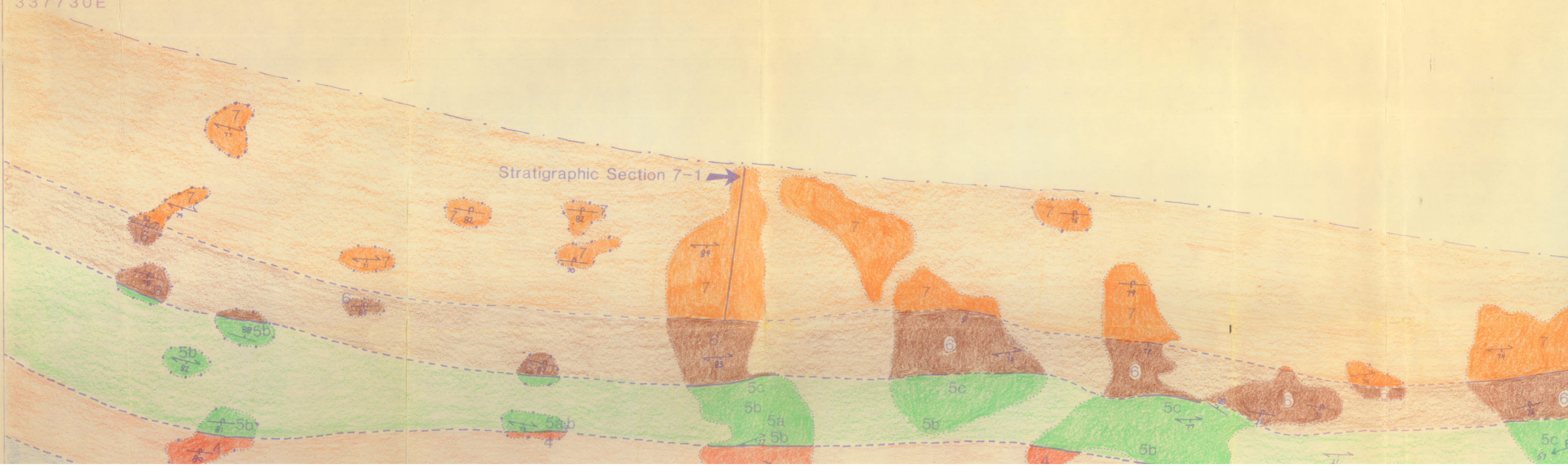
- Thurston, P.C., 1980, Subaerial volcanism in the Archean Uchi-Conederation Volcanic Belt: *Prec. Res.*, V. 12, p. 79-98.
- Turek, A., Weber, W. and Van Schmus, W.R., 1985, U-Pb zircon geochronology of the Rice Lake area: In *Man. Energy and Mines, Report of Field Activities*, p. 121.
- Vessel, R.K. and Davies, D.K., 1981, Nonmarine sedimentation in an active fore arc basin: In *Ethridge, F.G. and Flores, R.M. (eds.) Recent and ancient nonmarine depositional environments: models for exploration: Soc. Econ. Paleont. Mineral. Sp. Publ. 31*, p. 31-45.
- Walker, G.P.L., 1979, A volcanic ash generated by explosions where ignimbrite entered the sea: *Nature*, V. 281, p. 642-646.
- Walker, G.P.L., 1981, Generation and dispersal of fine ash and dust by volcanic eruptions: *Jour. Volc. Geotherm. Res.*, V. 11, p. 81-92.
- Walker, G.P.L., Self, S. and Wilson, L., 1984, Tarawera 1886, New Zealand—a basaltic plinian fissure eruption: *Jour. Volc. Geotherm. Res.*, V. 21, p. 61-78.
- Walker, G.P.L., Wilson, C.J.N. and Froggatt, P.C., 1980, Fines-depleted ignimbrite in New Zealand— The product of a turbulent pyroclastic flow: *Geology*, V. 8, p. 245-249.
- Walker, R.G., 1975, Generalized facies model for resedimented conglomerates of turbidite association: *Geol. Soc. Am. Bull.*, V. 86, p. 737-748.
- Walker, R.G., 1984, Turbidites and associated coarse clastic deposits: In *Walker, R.G. (ed) Facies Models, 2nd edn.*, *Geol. Assoc. Can., Geosci. Can. Repr. Ser. 1*, p. 171-188.
- Weber, W., 1971, Geology of the Long Lake-Gem Lake area: In *McRitchie, W.D. and Weber, W. (eds.) Geology and geophysics of the Rice Lake region, southeastern Manitoba (Project Pioneer): Man. Mines Branch, Publ. 71-1*, p. 63-106.
- Wood, J., 1980, Epiclastic sedimentation and stratigraphy in the North Spirit Lake and Rainy Lake area: a comparison: *Prec. Res.*, V. 12, p. 227-255.
- Wright, J.F., 1923, Preliminary map of a portion of the Rice Lake mining district, southeastern Manitoba: *Geol. Surv. Canada, Map 1992*.

- Wright, J.F., 1925, Beresford Lake area, Rice Lake mining district, southeast Manitoba: Geol. Surv. Canada, Map 2012.
- Wright, J.F., 1927, Beresford and Rice Lakes area: Geol. Surv. Canada, Map 195A.
- Wright, J.F., 1932, Geology and mineral deposits of a part of southeastern Manitoba (1st edition): Geol. Surv. Canada, Mem. 169, 150p.
- Wright, J.V., 1981, The Rio Caliente ignimbrite: analysis of a compound intraplinian ignimbrite from a major Late Quaternary Mexican eruption: Bull. Volc., V. 44, p. 189-212.
- Wright, J.V. and Coward, M.P., 1977, Rootless vents in welded ash flow tuffs from northern Snowdonia, Northern Wales, indicating deposition in a shallow water environment: Geol. Mag., V. 114, p. 133-140.
- Wright, J.V. and Mutti, E., 1981, The Dali Ash, Island of Rhodes, Greece: a problem in interpreting submarine volcanogenic sediments: Bull. Volc., V. 44, p. 153-167.
- Wright, J.V., Smith, A.L., and Self, S., 1980, A working terminology for pyroclastic rocks: Jour. Volc. Geotherm. Res., V. 8, p. 315-336.
- Yamada, E., 1973, Subaqueous pumice flow deposits in the Onikobe Caldera, Miyagi Prefecture, Japan: Jour. Geol. Soc. Japan, V. 79, p. 585-597.
- Yamazaki, T., Kato, I., Muroi, I., and Abe, M., 1973, Textural analysis and flow mechanism of the Donzurubo subaqueous pyroclastic flow deposits: Bull. Volc., V. 37, p. 231-244.
- Zwanzig, H.V., 1971, Structural geology at Long Lake, Manitoba: In McRitchie, W.D. and Weber, W. (eds.) Geology and geophysics of the Rice Lake region, southeastern Manitoba (Project Pioneer): Man. Mines Branch Publ. 71-1, p. 285-298.



5631700N  
337730E

Stratigraphic Section 7-1



# GEOLOGY OF THE MANIGOTAGAN RIVER FORMATION (PLATE 1)

Edmunds Lake Formation

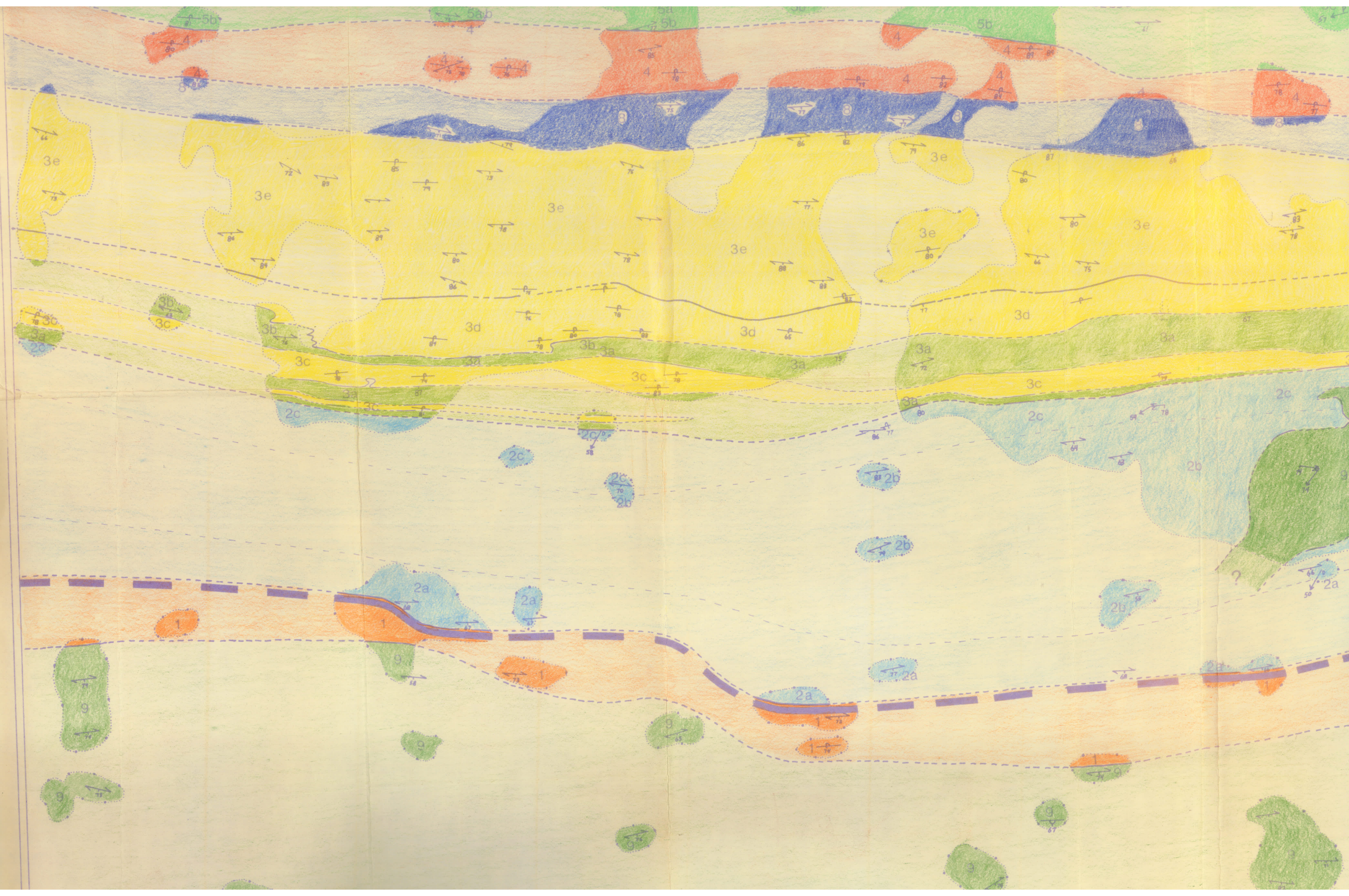


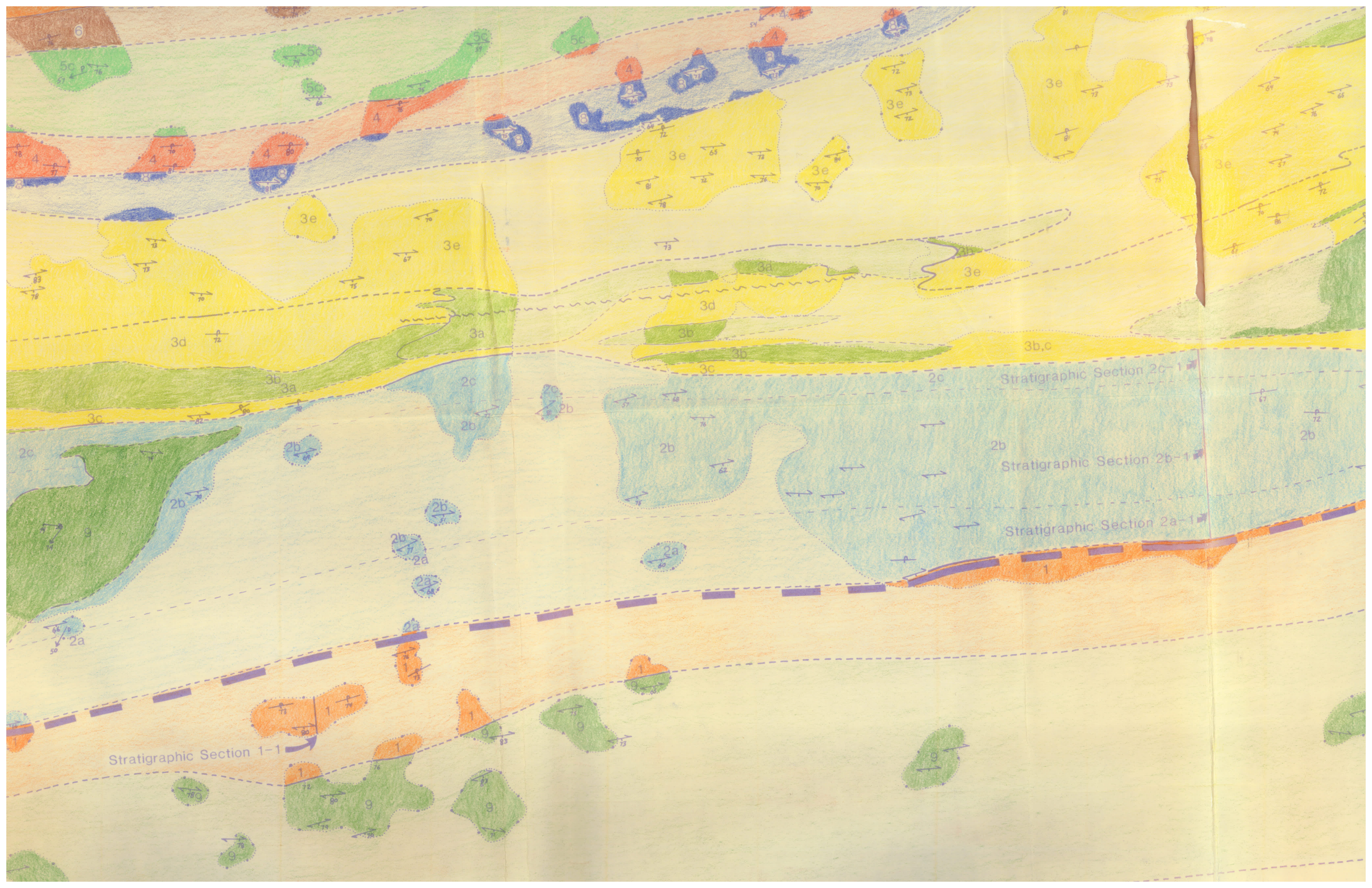
50 49 29 N  
95 18 52 W

Stratigraphic Section

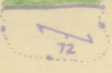
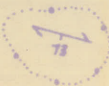














50 49 04 N  
95 18 01 W

## Legend





### Mafic Intrusions

-  (9) Gabbro
-  (8) Vesicular diabase



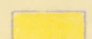


### Edmunds Lake Formation


Interbedded volcanic sandstone, siltstone, and mudstone with minor volcanic conglomerate and oxide-facies iron formation


### Manigotagan River Formation

-  (7) Ignimbrite  
Felsic lapilli-tuff and tuff
-  (6) Turbidites  
Interbedded volcanic sandstone and siltstone
-  (5) Mafic Lava Flows
  - (5a) Massive flows
  - (5b) Brecciated flows
  - (5c) Pillowed flows
-  (4) Peperite  
Volcanic sandstone, vesicular diabase lava pods and minor volcanic siltstone

### (3) Progradational Fan Succession

-  (3a) Massive, mafic lava flows
-  (3b) Pillowed, mafic lava flows
-  (3c) Volcanic mudstone and siltstone with minor volcanic sandstone (basin fill)
-  (3d) Volcanic sandstone with subordinate channel-fill volcanic conglomerate and minor volcanic siltstone and mudstone (interchannel)
-  (3e) Channel-fill volcanic conglomerate and sandstone (mid-fan)

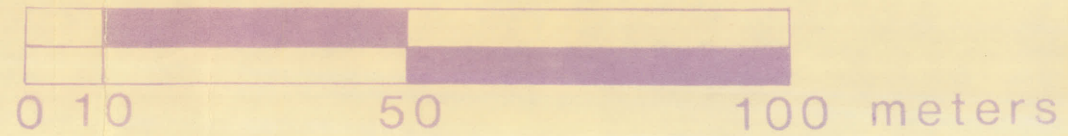
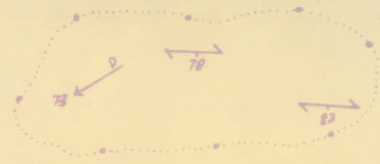
-  (2) Tephra-fall deposits with minor volcanic conglomerate and sandstone of uncertain origin
  - (2a) Mafic to intermediate lapilli-tuff with minor volcanic conglomerate and sandstone
  - (2b) Mafic lapilli-tuff and tuff
  - (2c) Mafic to intermediate lapilli-tuff and tuff

-  (1) Ignimbrite  
Felsic lapilli-tuff and tuff

### Narrows Formation

Felsic to intermediate tuff-breccia, lapilli

# Narrows Formation



SCALE 1:1000

## Symbols

Succession

lava flows

lava flows

one and siltstone with sandstone (basin plain)

one with subordinate volcanic conglomerate and siltstone and mudstone

volcanic conglomerate and (fan)

s with minor volcanic sandstone of uncertain genesis

mediate lapilli-tuff and tuff with conglomerate and sandstone

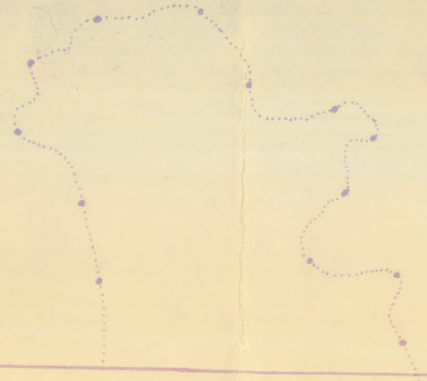
tuff and tuff

mediate lapilli-tuff and tuff

and tuff

tuff-breccia, lapilli-tuff and tuff

- Geological boundary (defined by shallow patches of overtopping)
- Outcrops
- Bedding (inclined)
- Bedding (inclined and overtopping facing direction)
- Foliation (inclined)
- Deformed clastic lineation
- Deformed pillow lineation
- Minor M-fold
- Shear zone (zone of intense deformation)



5632900N  
337570E

## Symbols

Boundary (defined, inferred, approximate)

o (defines a group of outcrops separated  
by benches of overburden)

ned)

ned and overturned; loop points towards  
n)

ned)

lineation

lineation

e of intense foliation)

defined, inferred)

*Doc. 961  
David Seneshen*

**Geology by David M. Seneshen, 1986**  
(base map was drawn from a 10x enlargement  
of a 1:10000 scale aerial photograph)